

Aus dem Institut für
Physiologie, Physiologische Chemie und Tierernährung
der Tierärztlichen Fakultät der
Ludwig-Maximilians-Universität München
Vorstand: Univ.-Prof. Dr. rer. nat. H.-J. Gabius

Angefertigt unter der Leitung von
Dr. Sabine André
Univ.-Prof. Dr. rer. nat. H.-J. Gabius

**COMPARATIVE CELL BIOLOGICAL ANALYSES OF
PROTO-TYPE GALECTINS IN COLON CANCER**

Inaugural-Dissertation

zur Erlangung der tiermedizinischen Doktorwürde
der Tierärztlichen Fakultät der
Ludwig-Maximilians-Universität München

von

Joachim Christian Manning
San Francisco, CA, U.S.A.

München 2006

Gedruckt mit Genehmigung der Tierärztlichen Fakultät der
Ludwig-Maximilians-Universität München

Dekan: Univ.-Prof. Dr. E. P. Märtlbauer

Referent: Univ.-Prof. Dr. H.-J. Gabius

Korreferent: Univ.-Prof. Dr. W. Hermanns

Tag der Promotion: 28. Juli 2006

To my mother,
who would have been proud.

TABLE OF CONTENTS

ABBREVIATIONS

1	INTRODUCTION	1
1.1	Glycans and Their Still Underappreciated Role as a Carrier of Information	1
1.2	Translation of the Sugar Code	4
1.3	Galectins	9
1.4	Proto-Type Galectins-1, -2 and -7	13
1.5	Galectins in Cancer	16
2	OBJECTIVES	18
3	MATERIALS, METHODS AND EQUIPMENT	19
3.1	Materials	19
3.2	Equipment	21
3.3	Cell Culture	22
3.3.1	Cell Lines	22
3.3.2	Cell Culture Conditions	22
3.3.3	Passaging of Cells	23
3.3.4	Generation of Stable Cell Transfectants	24
3.3.5	Origin of Cell Clones	25
3.3.6	Counting Cells	26
3.3.7	Freezing Cells	26
3.3.8	Thawing Cells	27
3.4	Biochemical Methods	27
3.4.1	Preparation of Cell Lysates for SDS-PAGE Analysis	27
3.4.2	SDS-PAGE	28
3.4.3	Electrophoretic Transfer of Protein to Nitrocellulose	31
3.4.4	Detection of Galectins on the Blot	32
3.4.5	Enzyme Linked Immunosorbent Assay	34
3.4.6	FACS Analysis	37
3.4.7	Cytochemical Analysis	39

3.5	Molecular Biology	39
3.5.1	Isolation of Genomic DNA	39
3.5.2	RNA Extraction, Reverse Transcription of RNA and PCR Analysis	40
3.5.3	Agarose Gel Electrophoresis	41
3.6	Video Microscopy	42
3.7	Assays with Cell Lines	43
3.7.1	Methylcellulose Assay	43
3.7.2	Doubling Time	44
3.7.3	MTT Assay	45
3.7.4	Statistical Analyses	48
4	RESULTS AND DISCUSSION	49
4.1	Characterization of Cell Clones	49
4.1.1	Generation and Selection of Stable Cell Clones	49
4.1.2	DNA and RNA Analysis	49
4.1.3	Analysis of Galectin Protein by ECL Blot	52
4.1.4	Enzyme Linked Immunosorbent Assay	55
4.1.5	FACS Analysis	56
4.1.6	Immunocytochemical Analysis	59
4.1.7	Morphology	66
4.2	Comparative Assays	68
4.2.1	Methylcellulose Assay	68
4.2.2	Doubling Time	71
4.2.3	MTT Assay	77
4.2.4	MTT Assay With Cytotoxic Drugs Added to the Medium	95
5	SUMMARY	103
6	BIBLIOGRAPHY	104
7	DANKSAGUNG	117
8	CURRICULUM VITAE	118

ABBREVIATIONS

°C	degree Celsius
Ab	antibody
approx.	approximately
APS	ammonium persulfate
Aqua dest.	aqua destillata
ASF	asialofetuin
BSA	bovine serum albumin
CD	cluster of differentiation
CRD	carbohydrate recognition domain
Cdk	cyclin-dependent kinase
DAPI	4'-6-diamidino-2-phenylindole
cDNA	complementary deoxyribonucleic acid
DEPC	diethylpyrocarbonate
DMSO	dimethyl sulfoxide
DPBS	Dulbecco's phosphate-buffered saline
DNA	deoxyribonucleic acid
dt	doubling time
DTT	dithiothreitol
E	extinction
EDTA	ethylenediaminetetraacetic acid
ELISA	enzyme-linked immunosorbent assay
ERK	extracellular signal-related kinase
EtOH	ethanol
FACS	fluorescence-activated cell sorting
FCS	fetal calf serum
FITC	fluorescein isothiocyanate
gal-1	galectin-1
gal-2	galectin-2
gal-7	galectin-7
h	hours

IC ₅₀	concentration of toxin required for 50 % inhibition of control value
IgG	immunoglobulin G
LAD II	leukocyte adhesion deficiency syndrome II
LB	Luria Bertani
MEK	mitogen-activated protein kinase/extracellular signal-regulated kinase kinase
min	minutes
mPa s	millipascal second
MTT	3-(4,5-dimethylthiazol-2-yl)-2,5-diphenyltetrazolium bromide
No.	number
OD	optical density
OPD	o-phenylenediamine dihydrochloride
p	p-value
PAGE	polyacrylamide gel electrophoresis
PBS	phosphate-buffered saline (20 mM, pH 7.2)
PCR	polymerase chain reaction
rpm	rounds per minute
sec	seconds
SD	standard deviation
SDS	sodium dodecyl sulphate
SN38	7-ethyl-10-hydroxy-20(S)-camptothecin
TAE	Tris-acetate-EDTA buffer
TE buffer	Tris(hydroxymethyl)aminomethane-ethylenediaminetetraacetic acid buffer
TEMED	N, N, N', N'-Tetramethylethylenediamine
TBS	Tris(hydroxymethyl)aminomethane-buffered saline
Tris	Tris(hydroxymethyl)aminomethane
T-TBS	Tris(hydroxymethyl)aminomethane-buffered saline with 0.05 % v/v Tween-20
V	Volt
x	“x” refers to the fold concentration of the stock solution
x g	times gravity (in context with centrifuge speed)
WT	wild-type

1 INTRODUCTION

Living organisms are made up of one or more cells, can grow, reproduce, process information, carry out chemical reactions, and respond to stimuli¹. Information transfer is a necessary precedent to responsiveness of cells to stimuli in their environment. The route of information transfer in living organisms cannot be a one-way street, though. Coordination in multicellular organisms requires feedback mechanisms between cells and to the environment. This must allow cells to respond to different challenges swiftly and accurately.

There is no doubt to the role of nucleic acids and amino acids in coding information in form of DNA, RNA and protein. However, it is becoming clearer that the whole story is not told, when describing the genome and proteome as the only hardware coding information of living organisms. In the concept of the genetic code, a new concept is emerging: the sugar code^{2,3}. This describes glycans as a third class of bio-informative macromolecules, next to nucleic acids and proteins. As a first step, the complexity of all glycans being produced by an organism, the glycome, is being identified⁴. In the past, the lack of possibilities to analyze glycan chains in detail was a main reason why scientists did not pay adequate attention to the potential information-encoding system hidden in sugar structures. Today, sophisticated analytical procedures are at hand and thus these problems have been elegantly mastered^{5,6,7}. Therefore in the next chapter, the view can be focused on saccharides as possible coding units.

1.1 GLYCANS AND THEIR STILL UNDERAPPRECIATED ROLE AS A CARRIER OF INFORMATION

Carbohydrates are well known as carriers of energy, such as starch and glycogen, and as main structural elements in plants and insects, such as cellulose and chitin. One noteworthy common characteristic of these four examples is, as very different as their form and function may be, that all are polysaccharides made up of repeating units of glucose, connected via the C1 and C4 carbon atoms. Differences between the anomeric linkage (α -D-glucose in starch and glycogen, or β -D-glucose in cellulose) or *N*-acetylation of C2 (β -D-*N*-acetylglucosamine in chitin) results in the diversity of the final structures.

Nucleic acids and amino acids encode information by being linked to each other in a specific order. Each single element has enough structural diversity from the other elements to be distinct. The question as to whether sugars also meet these requirements will now be addressed. The here presented reasoning to the importance of sugars follows the guidelines provided by Gabius et al.³. These authors emphasize the meaning and validity of the sugar code as an information carrier. The pyranose/furanose ring of monosaccharides presents many hydroxyl groups suitable for donor/acceptor bonds or for coordination bonds with cation such as Ca^{2+} . The sugar D-galactose has a set of weakly polarized C-H bonds, one side of C-H/ π -electron and *van der Waals* interactions. This makes stacking to aromatic ring systems possible, e.g. to the indolyl ring of tryptophan. The sugar D-galactose can also be used to exemplify the consequences of changes in positioning of a hydroxyl group in epimers. As in other monosaccharides, shifting the hydroxyl group to the other side of the ring will affect the potential for directional hydrogen bonds. An additional consequence will be a change in the areas of hydrophobicity specific for galactose. This shows that the positioning of the hydroxyl groups can clearly distinguish two monosaccharides from each other^{3, 8, 9, 10}. Introducing a substituent such as a sulfate group to a free hydroxyl group demonstrates an additional possibility to change one element of recognition. The activity of a heparan sulfate glucosaminyl 3-*O*-sulfotransferase is responsible for the generation of antithrombin-III binding sites¹¹. The glycosaminoglycan glycan chain is made up of repetitive units of $\text{GlcN}\alpha 1,4\text{GlcA}\beta 1,4$. At first sight, this is a monotonous structure, hardly capable of storing information or regulating coagulation. But by site specific epimerization and sulfation, regulated by enzymatic activity, the necessary complexity is achieved to specifically activate antithrombin-III upon binding. Thus, as nucleic acids and amino acids, monosaccharides fulfill the requirements to be clearly distinguished from another, comparable to separate letters of an alphabet.

Forming these letters to words, nucleic acids and amino acids are covalently linked to each other. The manner of connecting the units follows the same pattern along the chain. Sugars, however, can be connected with a larger amount of variation. The glycosidic bond connecting the C1 carbon atom can be linked to different hydroxyl groups of the next monosaccharide. Moreover, the binding is not sufficiently defined by the number of the two linked carbon atoms, but must also include the anomeric positioning of C1. A further deviation between the linkage of sugars compared with the linkage of amino acids or nucleic acids is the fact that saccharides can form branched chains. Taken together, the total of different combinations linking the building blocks together in monosaccharides surpasses the possibilities in amino

acids or nucleic acids by many orders of magnitude¹². This comparison clearly proves glycans to be potential carriers of information with the ability to form many words with only a few letters.

For information in sugars to be read, these must be spatially accessible. Indeed the glycan chains of membrane glycoconjugates reach out to the environment. They are therefore ideally located to serve as docking sites for sensors of other cells as well as of bacteria, viruses and protozoa. When proteins are glycosylated, glycan branches move away considerably (in the range of about 3 nm) from the peptide-sugar linkage point¹³. Their conformational behavior can often be considered as being essentially independent from the protein surface. Compared to phosphorylation as another well known form of post translational modification, glycosylation actually surpasses phosphorylation in terms of structural complexity, frequency of occurrence, and diversity of bond formation, with a total of at least 41 ways for connecting carbohydrates covalently to proteins^{14, 15, 16, 17, 18}. Reversible protein phosphorylation is a well known means of swiftly modulating protein activation and generating docking sites for other proteins. These attributes may also be conferred to the protein by glycosylation. An implication for the importance of protein glycosylation is given by the fact that many enzymes are responsible for glycan assembly and processing. Especially concerning enzymes with specificity for sugars that are located at the spatially accessible tips of the glycan chains. At least 13 separate enzymes can attach galactose in β 1,4- or β 1,3-position to an acceptor chain^{19, 20, 21}. Human sialyltransferases form a functional family of at least 18 different, Golgi-membrane-bound enzymes²². As discussed above, modification of monosaccharides by introducing a substituent to a free hydroxyl group is an excellent way to change the properties of a sugar into a new distinct unit with different characteristics. In a figurative sense, substitution increases the number of letters of the sugar alphabet and changes the meaning of the words spelled out. Also implying functionality, at least 23 mammalian sulfotransferases are characterized to introduce this group into different acceptors from *N*- and *O*-glycans and glycosaminoglycans^{23, 24, 25, 26}.

The pattern of distribution of glycans in cells and tissues appears to be tightly regulated^{27, 28, 29, 30, 31, 32, 33}. It is unlikely that this occurs without reason. Importantly, this is also true for malignant aberrations. Alterations in the glycosylation profile accompany disease onset and progression^{34, 35, 36, 37, 38, 39}. A major route to define the molecular basis of a disease is to correlate a lack of function with the syndrome. Impaired function of a distinct protein in glycan metabolism has indeed been associated with disease. For instance, leukocyte adhesion deficiency syndrome II (LAD II) is characterized by recurrent infections and marked

neutrophilia during infection⁴⁰. Severe mental and growth retardation demonstrates consequences of the defect beyond the immune system. The molecular cause of the symptoms was finally linked to a mutation in the GDP-fucose transporter⁴¹. The ensuing impairment of synthesis of sialylated/sulfated Lewis determinants has been a crucial factor to understand the role of fucose incorporation as the first step of leukocyte adhesion *in vivo*, i.e. to establish the initial contact between the leukocytes in the bloodstream and the activated endothelium^{42, 43}. An explanation for the development of mental and growth retardation has currently not been found. Further investigations are necessary to delineate the role of fucosylation in the development of these symptoms in LAD II. An additional example of a glycosylation defect being responsible for disease development is given in lysosomal storage disease (mucopolidoses)^{17, 44}. In type II (I-cell disease), type IIIA (pseudo-Hurler polydystrophy) and type IIIC (variant pseudo-Hurler polydystrophy) forms, a common mechanism in targeting lysosomal enzymes to their destination is affected: the decoration of *N*-glycans of enzymes destined to reach the lysosome with the mannose-6-phosphate signal, i.e. the reaction of the UDP-*N*-acetylglucosamine: lysosomal enzyme *N*-acetylglucosamine-1-phosphotransferase, either by abrogating (type II) or reducing its catalytic capacity (IIIA) or its target recognition (IIIC)^{44, 45}. Patients with I-cell disease suffer severe psychomotor retardation and skeletal deformities. Their lysosomes contain large inclusions of undigested glycosaminoglycans and glycolipids. At least eight acid hydrolases required for the degradation of the inclusions are missing from the affected lysosomes. In contrast, very high levels of the enzymes are present in blood and urine⁴⁶. Having thus shown the possibilities and the importance of glycosylation, the view will be focused on the next step of information processing. Obviously, the information encoded in sugars must be read for it to be of purpose. Taking nucleic acids as carriers of information as an example, there is a large array of DNA-binding proteins available helping to read the information encoded in the arrangement of nucleic acids. Therefore, it is pertinent to ask whether carbohydrate-binding proteins beyond those responsible for enzymatic processing exist, which recognize the distinct combinations and arrangements of glycans.

1.2 TRANSLATION OF THE SUGAR CODE

Carbohydrate-binding proteins were historically first identified as agglutinins by S. Weir Mitchell in venom of the tropical rattlesnake (*Crotalus durissus*) in 1860^{47, 48}. Their interaction with carbohydrates was first recognized in 1936 by J.B. Sumner and S.F.

Howell⁴⁹. The property of these proteins to select (Latin, *legere*) certain carbohydrate epitopes in binding helped to define the chemical nature of the ABH-blood group epitopes^{50, 51, 52, 53}. Because of this selecting ability, W.C. Boyd introduced the term *lectin* (the past participle of *legere*) in the year 1954 to describe these proteins⁵⁴. The above mentioned happenings and other key events in the history of lectins are shown in table 1.

Table 1. Brief historical account of lectinology

1860	Observation of blood "coagulation" by rattlesnake venom (S. W. Mitchell)
1888	Detection of erythrocyte agglutination by protein fractions from castor beans and other plant seeds (H. Stillmark)
1891	Toxic plant agglutinins applied as model antigens (P. Ehrlich)
1898	Introduction of the term "haemagglutinin" or phytohaemagglutinin for plant proteins that agglutinate red blood cells (M. Elfstrand)
1902	Detection of bacterial agglutinins (R. Kraus)
1902	Demonstration that blood "coagulation" by snake venom (later shown to depend on a C-type lectin) observed in 1860 was not due to blood clotting but to cell agglutination (S. Flexner, H. Noguchi)
1906	Detection of an agglutinin in bovine serum (later characterized as the C-type lectin conglutinin) acting on activated complement-coated erythrocytes (J. Bordet, F. P. Gay)
1907	Detection of non-toxic agglutinins in plants (K. Landsteiner, H. Raubitschek)
1913	Use of intact cells for the purification of lectins (R. Kobert)
1919	Crystallization of a lectin, concanavalin A (J. B. Sumner)
1936	Precipitation of starch, glycogen and mucins by concanavalin A and its interaction with stromata of erythrocytes define carbohydrate as ligand (J. B. Sumner, S. F. Howell)
1941	Detection of viral agglutinins (G. K. Hirst)
1947/48	Detection of lectins specific for human blood groups (W. C. Boyd, K. O. Renkonen)
1952	Carbohydrate nature of blood group determinants proven by lectin-mediated agglutination and its sugar-dependent inhibition (W. M. Watkins, W. T. J. Morgan)
1954	Introduction of the term "lectin" for plant agglutinins, primarily for those which are blood group-specific (W. C. Boyd)
1960	Detection of the mitogenic potency of lectins toward lymphocytes (P. C. Nowell)
1965	Application of affinity chromatography for the isolation of lectins (I. J. Goldstein, B. B. L. Agrawal)
1972	Determination of the amino acid sequence and the three-dimensional structure of a lectin, concanavalin A (G. M. Edelman, K. O. Hardman, C. F. Ainsworth et al.)

1972-1977	Detection of impaired synthesis of a marker for glycoprotein (lysosomal enzymes) routing as cause for a human disease (mucopolipidosis II) and its identification as Man-6-phosphate, the ligand for P-type lectins (E. F. Neufeld and colleagues; W. S. Sly and colleagues)
1974	Isolation of a mammalian Gal/GalNAc-specific lectin from the liver (G. Ashwell)
1978	First conference focusing on lectins and glycoconjugates, termed Interlec (T. C. Bøgg-Hansen)
1979	Detection of endogenous ligands for plant lectins (H. Rüdiger)
1983	Detection of the insecticidal action of a plant lectin (L. L. Murdock)
1984	Isolation of lectins from tumors (H.-J. Gabius; R. Lotan, A. Raz)
1985	Immobilized glycoproteins as pan-affinity adsorbents for lectins (H. Rüdiger)
1987	Introduction of neoglycoconjugates for localization of tissue lectins to tumor diagnosis (H.-J. Gabius and colleagues)
1989	Detection of the fungicidal action of a plant lectin (W. J. Peumans)
1992/93	Detection of impaired synthesis of lectin (selectin) ligands by defective fucosylation as cause for leukocyte adhesion deficiency type II (A. Etzioni and colleagues)
1995	Structural analysis of a lectin-ligand complex in solution by NMR spectroscopy (J. Jiménez-Barbero and colleagues)
1996-1998	Detection of differential conformer selection by plant and animal lectins (H.-J. Gabius and colleagues; L. Poppe and colleagues)
2001/02	Advances in lectinology and glycosciences honored by devoting special issues in <i>Biochim. Biophys. Acta</i> , <i>Biochimie</i> , <i>Biol. Chem.</i> , <i>Cells Tissues Organs</i> , <i>Chem. Rev.</i> , <i>Curr. Opin. Struct. Biol.</i> , <i>J. Agric. Food Chem.</i> (Liener symposium), and <i>Science</i> to the topics

from Gabius et al. (2004)⁵⁵

The definition of lectins has undergone some changes over time. Today, lectins are understood as carbohydrate-binding proteins, excluding carbohydrate-specific antibodies, enzymes modifying the structure of the carbohydrate ligand (substrate) and proteins accommodating free mono- or disaccharides (e.g. transport proteins or chemotaxis receptors)^{56, 57, 58}. The ability to distinguish blood group A from B with the agglutinin from *Dolichos biflorus*, the *N*-acetylation of the terminal D-galactose being the only difference between the two, gives us a first insight of the recognition capacity of lectins. Lagging behind the progress in plant lectins, research over the last decades have shown an enormous complexity in vertebrate lectins^{56, 59, 60}. The structural analysis of the folding pattern and architecture of the carbohydrate-recognition domain (CRD) has defined a classification system for animal lectins as shown in table 2.

Table 2. Current categories for classification of various animal lectins

Family	Structural Motif	Carbohydrate Ligand	Modular Arrangement
C-type	conserved CRD	variable (mannose, galactose, fucose, heparin tetrasaccharide)	Yes
I-type	immunoglobulin-like CRD	variable (Man6GlcNAc2, HNK-1 epitope, hyaluronic acid, α 2,3/ α 2,6-sialyllactose)	Yes
Galectins (S-type)	conserved CRD	β -galactosides	variable
Pentraxins	pentameric subunit arrangement	4,6-cyclic acetal of β -galactose, galactose sulfated and phosphorylated monosaccharides	Yes
P-type	homologous, not yet strictly defined CRD	mannose-6-phosphate-containing glycoproteins	Yes

from Gabius (2006)⁶¹

Having clarified structural aspects, it is pertinent to give a summary on current lectin functions. This is demonstrated in table 3, where numerous functions can be ascribed to a class of lectins. Animal lectins in general appear to have a wide variety of functions.

Table 3. Functions of animal lectins

Activity	Example of Lectin
Recognition of stem region of <i>N</i> -glycans, a signal for ubiquitin conjugation when accessible in incorrectly folded glycoproteins	F-box proteins Fbs1/2 (Fbx2/FBG1, Fbx6b/FBG2) as a ligand-specific part of SCF ubiquitin ligase complexes
Molecular chaperones with dual specificity for Glc ₁ Man ₉ GlcNAc ₂ and protein part of nascent glycoproteins in endoplasmic reticulum (ER)	Calnexin, calreticulin

Targeting of misfolded glycoproteins with Man ₈₋₅ GlcNAc ₂ as carbohydrate ligand to ER-associated degradation (ERAD)	EDEM1,2/Mnl1 (Htm1) Yos9 protein (MRH domain)
Intracellular routing of glycoproteins and vesicles and apical delivery	ERGIC-53 and VIP-36 (probably also ERGL and VIPL), P-type lectins, comitin, galectin-4
Intracellular transport and extracellular assembly	Non-integrin 67 kDa elastin/laminin-binding protein
Enamel formation and biomineralization	Amelogenin
Inducer of membrane superimposition and zippering (formation of Birbeck granules)	Langerin (CD207)
Cell type-specific endocytosis	Hepatic and macrophage asialoglycoprotein receptors, dendritic cell and macrophage C-type lectins (mannose receptor family members) (tandem-repeat type) and single CRD lectins such as trimeric langerin/CD207 or tetrameric DC-SIGN/CD209), cysteine-rich domain (β -trefoil) of the dimeric form of mannose receptor for GalNAc-4-SO ₄ -bearing glycoprotein hormones in hepatic endothelial cells, P-type lectins
Recognition of foreign glycans (β 1,3-glucans, LPS)	CR3 (CD11b/CD18, Mac-1 antigen), C-type lectins such as DC-SIGN and dectin-1, immulectins, intelectins, <i>Limulus</i> coagulation factors C and G, earthworm CCF
Recognition of foreign or aberrant glycosignatures on cells (incl. endocytosis or initiation of opsonization or complement activation)	Collectins, ficolins, C-type macrophage and dendritic cell lectins, CR3 (CD11b/CD18, Mac-1 antigen), α/θ -defensins, pentraxins (CRP, limulin), tachylectins
Targeting of enzymatic activity in multimodular proteins	Acrosin, <i>Limulus</i> coagulation factor C, laforin (frequent in microbial glycosylhydrolases for plant cell wall polysaccharides)
Bridging of molecules	Galectins, cytokines (e.g. IL-2:IL-2R and CD3 of TCR), cerebellar soluble lectin

Induction or suppression of effector release (H ₂ O ₂ , cytokines, etc.)	Galectins, selectins and other C-type lectins such as CD23, BDCA-2 and dectin-1, I-type lectins (CD33 (siglec-3), siglecs-7 and -9)
Cell growth control, induction of apoptosis/anoikis and axonal regeneration	Galectins, C-type lectins, amphoterin-like protein, hyaluronic-acid-binding proteins, cerebellar soluble lectin, CD22 (siglec-2), MAG (siglec-4)
Cell migration and routing	Galectins, selectins and other C-type lectins, I-type lectins, hyaluronic-acid-binding proteins (RHAMM, CD44, hyalectans/lecticans)
Cell-cell interactions	Selectins and other C-type lectins (e.g. DC-SIGN), galectins, I-type lectins (e.g. siglecs, N-CAM, P ₀ or L1), glilectin
Cell-matrix interactions	Galectins, heparin- and hyaluronic-acid-binding lectins including hyalectans/lecticans, calreticulin

from Gabius (2006)⁶¹

As mentioned above, spatial accessibility is a requirement for reading the sugar code. Units of β -galactose are located at the tips of glycan branches. Galectins are lectins with specificity for this sugar. They are often listed in table 3, showing that galectins influence numerous aspects of cell biology. This is seen in their contribution to cell adhesion, migration, growth control, effector release and immune regulation^{42, 56, 62, 63, 64, 65}.

1.3 GALECTINS

Galectins are a conserved family of β -galactosyl-binding lectins that occur in both vertebrates and invertebrates⁶⁶. They share binding activities towards β -galactosides and derivatives thereof and do not make use of any metal ion in their binding site⁶⁷. Structurally, the folding pattern is an antiparallel β -sandwich and named the legume-lectin-like β -sandwich, also known as the jelly-roll-like fold⁶⁸. The family of galectins have previously been known as the S-type (sulfhydryl-dependent) lectins, but the name of the family has changed, as a few family members are not sulfhydryl-dependent⁶⁹. The profiles of fine specificities of the individual galectins can differ to a certain extent, when testing a wide panel of synthetic and natural oligosaccharides, dendrimers or glycoproteins^{70, 71, 72, 73, 74}. To date, there are 14 known family members of galectins in mammals. They have been grouped into three subfamilies: the proto-type, tandem-repeat-type and chimera-type galectins⁷⁵. The growth

regulation on human neuroblastoma cells by proto-type galectin-1 and its competitive inhibition by chimera-type galectin-3 clearly shows that galectins cannot simply be regarded as functional homologues, even when their ligand selection is very similar^{76,77}. Here, functional divergence was seen between two galectins belonging to different subgroups. Is function related to subgroup classification? In a study by Sturm et al., the effects of three members of the proto-type family, galectins-1, -2 and -7, were determined on activated T cells⁷⁸. Intriguingly, the responses of the T cells differed with each of the tested galectins. This proves that despite the common specificity for β -galactosides, galectin functions can differ between subfamilies as well as within the same subfamily. The proto-type galectins are homodimers composed of subunits of approximately 130 amino acids. Each subunit folds as one compact jelly-roll-like globular domain^{67,79}. The tandem-repeat-type galectins contain two homologous CRDs connected by a peptide linker⁸⁰. Galectin-3 is presently the only member defined as a chimera-type galectin. In addition to the CRD, galectin-3 has a short *N*-terminal domain and an intervening proline, glycine and tyrosine-rich domain. Galectin-3 is isolated as a monomer but undergoes multimerization on binding to surfaces that contain multivalent glycoconjugate ligands, and the *N*-terminal half of the protein is required for this property^{81,82,83}. An important consequence of the galectin structures described above is that most are topologically multivalent, either by forming non-covalent dimers or higher oligomers, or by having two CRDs within one peptide chain. They are therefore able to cross-link β -galactoside containing glycoconjugate ligands at physiological concentrations, possibly resulting in modulation of cell adhesion and signaling^{62,84,85,86}. A list of mammalian galectins, their occurrence in cells and tissues, and their structural features is given in table 4.

Table 4. Members of the galectin family. From Gabius (2006)⁶¹.

Name	Occurrence	Structural Features
galectin-1 (galaptin, L-14)	many cell types	homodimer; one CRD per subunit (14-15 kDa): proto-type
galectin-2	predominantly epithelial presence in digestive, pulmonary and urogenital tracts	homodimer; one CRD per subunit (43% sequence identity to galectin-1; 14 kDa): proto-type
galectin-3 (CBP35, Mac-2 antigen, IgE-binding protein, L-29, L-34)	many cell types	monomer with one CRD (pentamer formation in solution and on surfaces); pro-, tyr-, and gly-rich repeats in <i>N</i> -terminal section (27-36 kDa): chimera-type
galectin-4	colon, small intestine, stomach, oral epithelium, esophagus, lung, testis, breast, liver and placenta by RT-PCR	monomer with two partially homologous but distinct CRDs, connected by a link peptide (36 kDa); proteolysis generates truncated proto-type-like products: tandem-repeat-type
galectin-5	Reticulocytes, erythrocytes (rat)	monomer with one CRD (17 kDa): proto-type
galectin-6	small intestine, colon (mouse)	tandem-repeat arrangement of two CRDs (33 kDa)
galectin-7	keratinocytes, stratified epithelia, carcinoma cells	homodimer; one CRD per subunit (15 kDa): proto-type
galectin-8	several tissues; frequent presence in tumor cell lines (link peptide extension possible)	homologous to galectins-4 and -6 (tandem-repeat arrangement of two CRDs with unique link peptide; 34 kDa)
galectin-9	small intestine, liver, lung, kidney, thymus (rat/mouse; small intestinal isoform with 31/32 amino acid extension of link peptide); lymphatic tissue and B cells, T cells and macrophages, pancreas, colon carcinoma cells (human)	homologous to galectins-4, -6 and -8 (tandem-repeat arrangement of two CRDs with unique link peptide; 36 kDa)
Charcot-Leyden crystal protein (galectin-10)	major autocrystallizing constituent of eosinophils and basophils	One CRD-like structure with specificity to D-Man (16.5 kDa)
galectin-11 (ovgal-11)	sheep gastrointestinal tract, induced upon nematode infection	One CRD resembling proto-type galectins (14 kDa)
galectin-12	several tissues (upregulation in cells synchronized at the G ₁ phase or G ₁ /S boundary of the cell cycle), adipocytes	homologous to galectins-4, -6, -8 and -9 (tandem-repeat arrangement of two CRDs with unique link peptide; 35.3 kDa)
galectin-13	identical to placental protein 13 (pp13); also expressed in spleen, kidney, bladder and in tumor cells	homodimer; one CRD per subunit (16.1 kDa); close similarity to galectin-7 and the Charcot-Leyden crystal protein
galectin-14	ovine eosinophils, secreted into bronchoalveolar lavage fluid	one CRD resembling proto-type galectins (18.2 kDa)

Many of the functions of galectins described above are sugar-dependent. It is interesting to note that galectins can also target peptide and lipid moieties^{87, 88}. This presents additional possibilities of interacting with binding partners and associated effects. Table 5 gives a summary of known physiologically relevant binding partners for galectins-1 and -3 grouped by the type of interaction.

Table 5. Binding Partners for Galectins-1 and -3.

Type of ligand	Galectin-1	Galectin-3
Glycan	CA125, CD2, CD3, CD4, CD7, CD43, CD45, CEA, fibronectin (tissue), GI mucin, hsp90-like glycoprotein, $\alpha_1/\alpha_5/\alpha_7/\beta_1$ -integrins, L1, laminin, lamp-1, Mac-2 binding protein, thrombospondin, Thy-1, chondroitin sulfate proteoglycan, distinct neutral glycolipids, ganglioside GM ₁	LI-cadherin, C4.4A (member of Ly6 family), IgE, CD7, CD11b of CD11b/CD18 (Mac-1 antigen, CR3), CD32, CD66a,b, CD95, CD98, CEA, colon cancer mucin, cubilin, haptoglobin β -subunit (after desialylation), hensin (DMBT-1), β_1 -integrin (CD29), laminin, lamp-1/-2, Mac-2 binding protein, Mac-3, MAG, MP20 (tetraspanin), NG2 proteoglycan, TCR complex, tenascin, ganglioside GM ₁
protein	Gemin4, oncogenic H-Ras, pre-B cell receptor (human, not murine system)	AGE products, Alix/AIP-1, axin, Bcl-2, β -catenin, Cys/His-rich protein, Gemin4, mSufu, nucling, oncogenic K-Ras, pCIP, PIAS1, synexin (annexin VII), TTF-1

from Gabius (2006)⁶¹

As shown in table 4, in which each galectin member is assigned to one of the three subgroups, proto-type galectins are well established with several members. It is an open question whether the close structural similarity (see below) will translate into functional overlap when overexpressed in cells.

1.4 PROTO-TYPE GALECTINS-1, -2 AND -7

These three galectins are of particular interest, because of their structural similarities, their reported growth inhibitory effects and also because of reported functional divergence seen after exogenous addition to activated T cells⁷⁸. In addition to the information given in table 4 on occurrence and basic structural features of the proto-type galectins-1, -2 and -7, comparative structural aspects will be discussed. Alignment of amino acid sequences of the human galectins-1, -2 and -7 is shown in figure 1. The identity scores between gal-1 and -2 are highest with 43 %. Comparison of gal-1 and gal-7 results in 31 % identity, and gal-2 and gal-7 show the least number of common amino acids among the three galectins with 26 % identity.

```

1                                     50
hGal-1  MACGLVASNL  ..NLKPG ECL  RVRGEVAPDA  KSFVLNL... GKDSNNLCLH
hGal-2  MTGELEVKNM  ..DMKPGSTL  KITGSIADGT  DGFVINL... GQGTDKLNLH
hGal-7  MSNVPHKSSL  PEGIRPGTVL  RIRGLVPPNA  SRFHVNLLCG  EEQGSDAALH
Consensus  M...l..sn$  ....kPG..L  r!rG.!ap.a  ..Fv.NL...  g.....l.LH

51                                     100
hGal-1  FNPRFNAHGD  ANTIVCNSKD  GGAWGTEQRE  AVFPFQPGSV  AEVCITFDQA
hGal-2  FNPRFSE...  .STIVCNSLD  GSNWGQEQRE  DHLCFSPGSE  VKFTVTFESD
hGal-7  FNPRLDT...  .SEVVFNSKE  QGSWGREERG  PGVPPFQRGQP  FEVLIIASDD
Consensus  FNPRf.....  .st!VcNSk#  gg.WG.E#Re  ...pFqpGs.  .ev.!tf..d

101                                     141
hGal-1  NLTVKLPDGY  EFKFPNRLNL  EAINYMAADG  DFKIKCVAFD  .
hGal-2  KFKVKLPDGH  ELTFPNRLGH  SHLSYLSVRG  GFNMSSFKLK  E
hGal-7  GFKAVVGDAQ  YHHFRHRLPL  ARVRLVEVGG  DVQLDSVRIF  .
Consensus  .fkvklpDg.  e..FpnRL.l  ....y..v.G  df...sv...  .

```

Figure 1. Sequence comparison of human galectins-1, -2 and -7. Amino acid sequences of human gal-1, -2, and -7 were aligned using the program Multalin version 5.4.1 (<http://prodes.toulouse.inra.fr/multalin/multalin.html>). A consensus sequence calculated from the three galectin sequences is added to the alignment; consensus symbols represent: ! is I or V; and # is N, D, Q, or E.

The structures of galectins-1, -2 and -7 have been determined by X-ray crystallography. These studies revealed that the CRD is folded tightly, with two anti-parallel β -pleated sheets forming a sandwich-like structure⁸⁹. Amino acid side chains on one of these sheets form the core carbohydrate-binding site. Pictures of the X-ray crystal structures are displayed in figures 2 to 4.

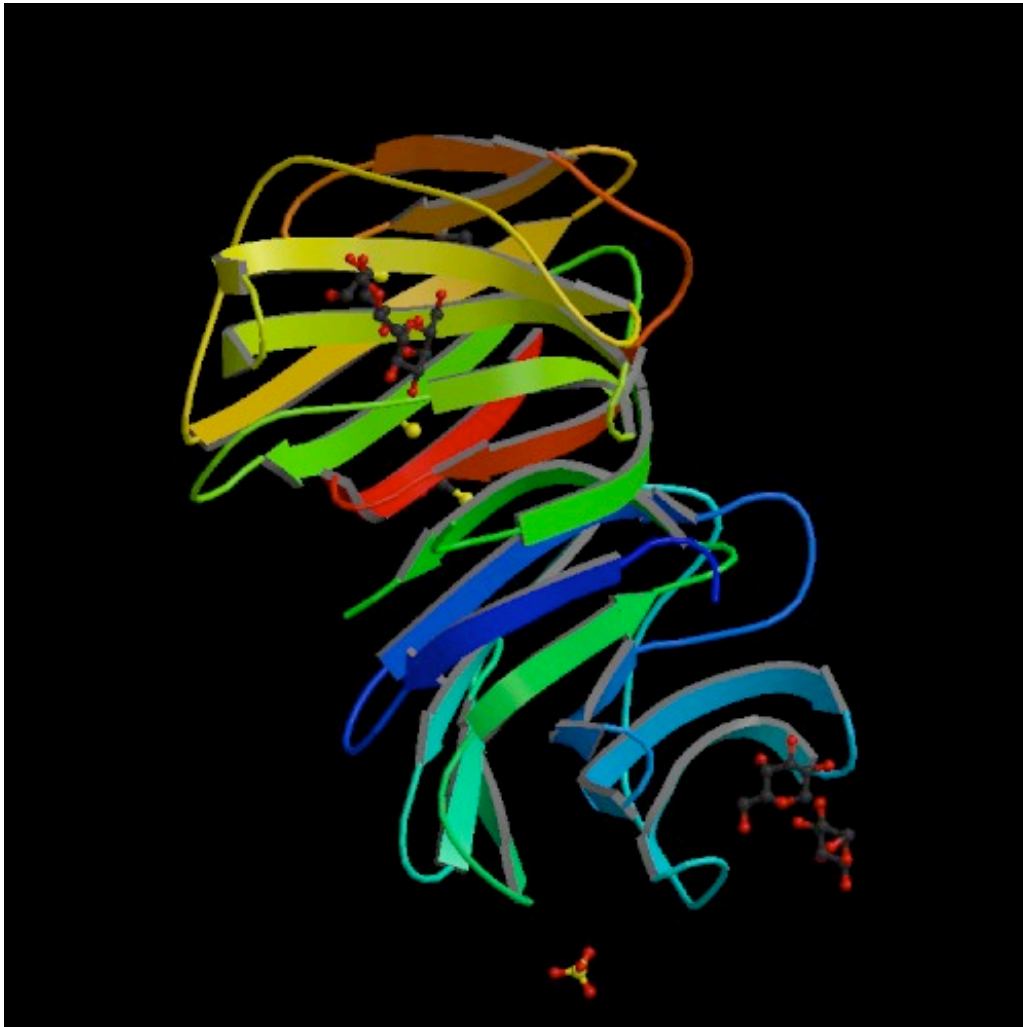


Figure 2. X-ray crystal structure of a galectin-1 homodimer complexed with Gal- β 1,4-Glc⁹⁰ (PDB code 1GZW).

Having illustrated the structural details of the three proto-type galectins-1, -2 and -7, their relation to clinical aspects, especially cancer, will be given in the next chapter.

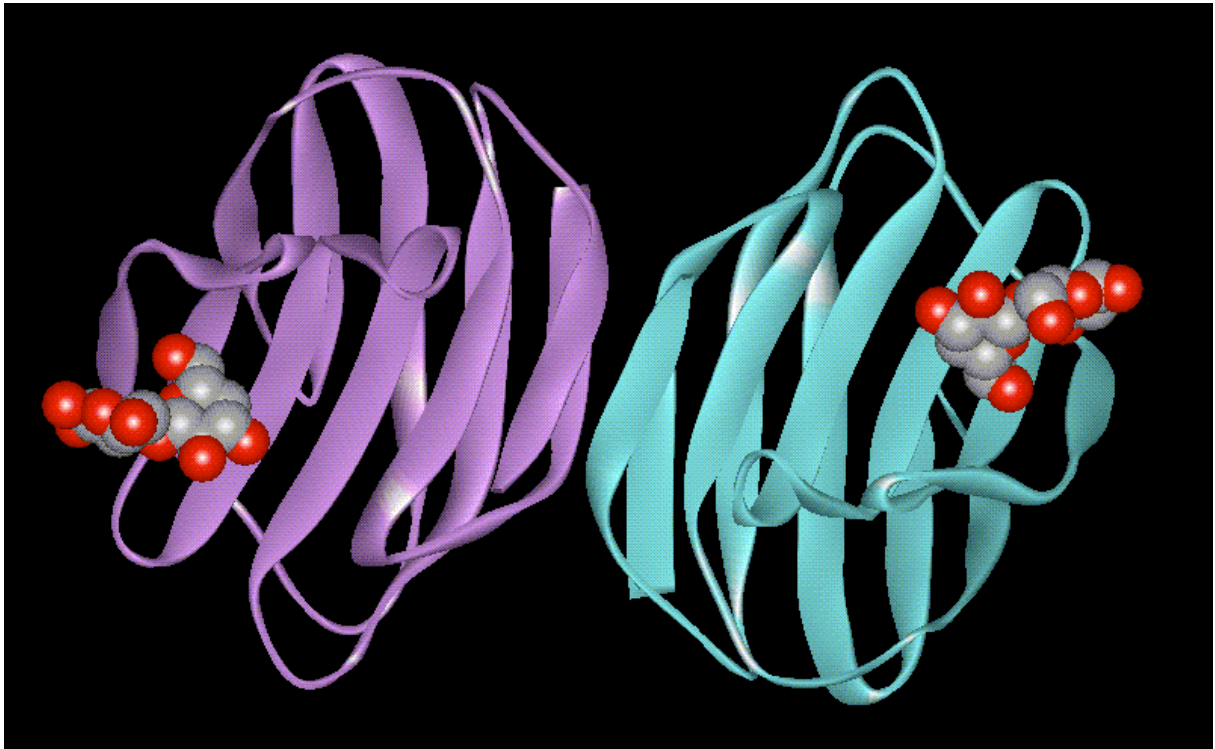


Figure 3. X-ray crystal structure of a galectin-2 homodimer complexed with Gal-β1,4-Glc⁶⁷ (PDB code 1HLC).

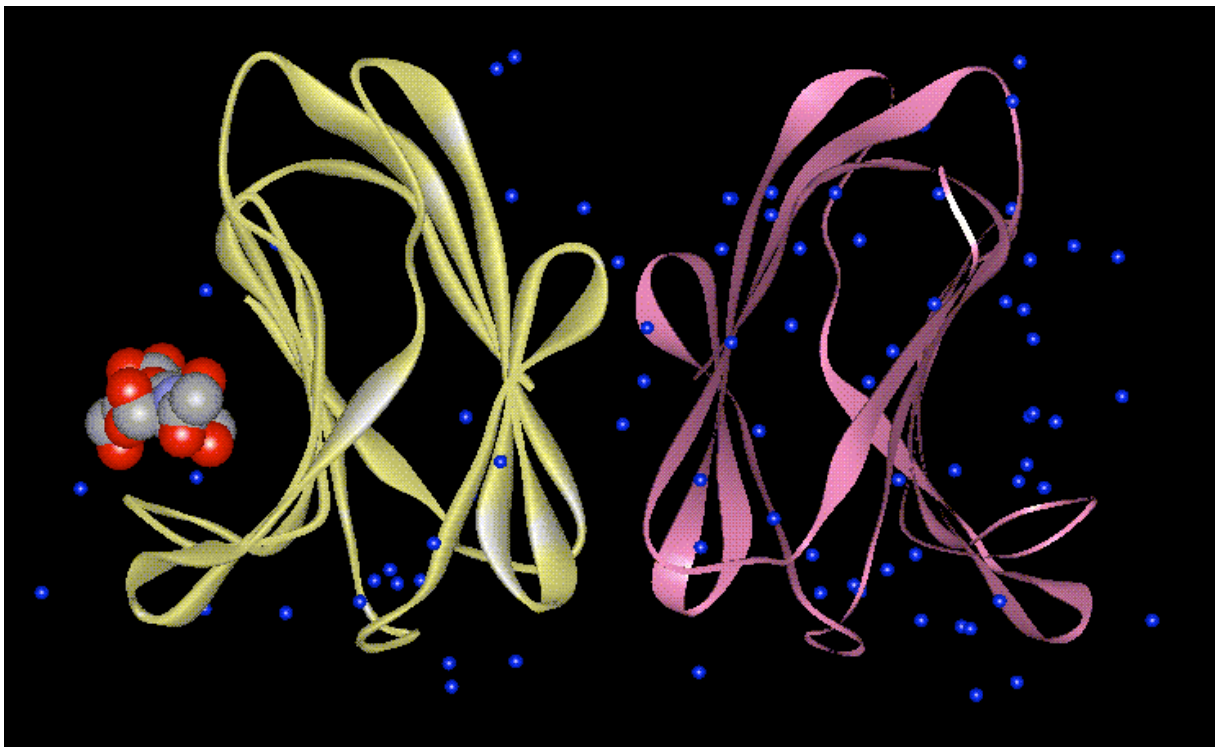


Figure 4. X-ray crystal structure of a galectin-7 homodimer complexed with Gal-β1,4-GlcNAc⁹¹ (PDB code 5GAL).

1.5 GALECTINS IN CANCER

Adenocarcinoma of the large bowel affects one person in 20 in most Westernized countries⁹². More than 155,000 new cases are diagnosed in the United States each year, representing 15 % of all cancers. This disease clearly constitutes a major public health problem, and improved disease management can be expected from advances in understanding of the malignant phenotype.

Malignant transformation of cells is often caused by molecular defects, which consist of mutations in key classes of genes governing cell growth⁶⁵. These mutations alter the amount or behavior of the proteins encoded by proliferation-regulating genes and thereby disrupt functions that control cell division. Members of the galectin family have been proposed to mediate cell adhesion, to regulate cell growth, and to trigger or inhibit programmed cell death. It has been demonstrated that the expression pattern of various galectins is altered in carcinomas. Summarizing the current status, it is fair to say that galectins are expressed in tumors heterogeneously, as also known from other markers⁹³. The clinical significance of heterogeneity is currently not defined and calls for rigorous examination in suitable cell biological models. This issue has given research a clear direction which will be discussed below, after providing details to the significance of galectin presence in malignancy.

Focusing on the proto-type family members, studies have shown galectins as key factors in malignancies of neoplasms including colon cancer⁹⁴. Studies have shown higher levels of galectin-1 in colon neoplasm in comparison to the normal mucosa, and have also correlated overexpression with advanced tumor stages and shorter survival⁹⁵. Nagy et al. have also recognized galectin-1 as a prognostic factor in colon tumors, which had been classified as Dukes A and B tumors⁹⁶. High levels of galectin-1 were inversely correlated with survival periods. Using Northern blotting and Western blotting analysis, *in situ* hybridization and immunohistochemistry, Berberat et al. have investigated the expression pattern of galectin-1 in primary pancreatic cancers and in metastases in comparison to normal pancreases⁹⁷. They observed a strong galectin-1 immunoreactivity in most fibroblasts in fibrotic tissue strains in and around the tumor mass. However, no labeling was found for galectin-1 in metastatic pancreatic cells.

Less data is available concerning the expression of other proto-type galectins such as galectins-2 and -7 in malignancy. In a study by Saal et al., galectin-2 and galectin-2 binding sites were visualized in histological tissue samples of various origin, including normal tissue and samples with benign/malignant neoplasms⁹⁸. A tendency of increased presentation of galectin-2-binding sites was seen in malignant tissue. Polyak et al. have identified the

transcription of the galectin-7 gene to be upregulated before the onset of p53-induced apoptosis in DLD-1 colon cancer cells⁹⁹. Apparently, galectin-7 functions as a proapoptotic factor, as has been recognized in studies by Kuwabara et al.¹⁰⁰. This makes recent findings of Saussez et al. particularly interesting, in which high levels of galectin-7 has been positively correlated to a high recurrence rate and poor prognosis of stage IV hypopharyngeal cancer¹⁰¹. Galectin-7 has therefore been related to effects beneficial for prognosis (proapoptotic activity) and unfavorable prognosis (clinical correlation).

Turning to cancer cell lines as an *in vitro* model to investigate characteristics of tumor cells, a study by Lahm et al. was conducted with a panel of 61 tumor cell lines of different origin¹⁰². The expression patterns for human galectins-1, -2, -3, -4, -7, -8, and -9 were defined by using the RT-PCR approach. This study was designed as fingerprinting, without detailed functional investigation. Its strength is the fact that it identified cancer cell lines, which lack expression of certain proto-type galectins. These data will thus provide a guideline to select colon cancer lines for a study on ectopic expression of proto-type galectins-1, -2 and -7. Explicitly, the lines HCT-15 and DLD-1 appeared to be suitable to examine the effects of overexpression of galectins-1, -2, and -7 on clinically relevant cell behavior. This reasoning guides to the objectives of the thesis.

2 OBJECTIVES

- to establish stable clones of cell transfectants with ectopic galectin overexpression in the cases of the three homodimeric proto-type galectins
- to select subclones with different extent of galectin expression on the basis of biochemically monitoring protein presence
- to determine cell surface expression by FACS analysis
- to monitor intracellular expression and nuclear presence by immunocytochemical analysis
- to monitor morphological aspects by videomicroscopy
- to determine the effect of lectin expression on anchorage-independent growth
- to determine the effect of lectin expression on anchorage-dependent growth
- to determine the effect of lectin expression on the doubling time
- to determine the effect of lectin expression on growth in medium with reduced content of nutrients
- to determine the effect of lectin expression on sensitivity to chemotherapeutics
- intergalectin comparison of the data sets obtained from the three different proto-type galectins

3 MATERIALS, METHODS AND EQUIPMENT

3.1 MATERIALS

Chemicals and other materials were purchased from Carl Roth GmbH & Co. KG, Karlsruhe, VWR International GmbH, Ismanning and from Sigma, Munich and were of analytical grade. It is indicated if chemicals or other materials were used from other sources.

Agarose SeaKem LE agarose (Product No. 50004)	BioWhittaker Molecular Applications, Rockland, Maine, U.S.A.
Bio-Rad protein assay dye reagent concentrate	Bio-Rad Laboratories GmbH, Munich, Germany
CL-Xposure film (Product No. 34090)	Perbio Science Deutschland GmbH, Bonn, Germany
Coverslips (sterile) Superfrost	Menzel GmbH & Co. KG, Braunschweig, Germany
Diethylpyrocarbonate (DEPC)	AppliChem GmbH, Darmstadt, Germany
D-lactose monohydrate (Product No. 61340)	Fluka Chemie, Buchs, Switzerland
DMEM/F-12 (1:1) powder (Product No. 42400-010)	Gibco BRL, Life Technologies, Invitrogen GmbH, Karlsruhe, Germany
DNA extraction kit	Wizard Genomic DNA Purification Kit, Promega GmbH, Mannheim, Germany
DNA loading dye solution, 6 x	Fermentas GmbH, St. Leon-Rot, Germany
ECL Western blotting detection reagents	Amersham Biosciences Europa GmbH, Freiburg, Germany
ELISA microplate, MICROLON 600, 96-well, high binding, U-bottom	Greiner Bio-One GmbH, Frickenhausen, Germany
Eukaryotic expression vector pCDNA3.1(+)	Invitrogen, Karlsruhe, Germany
Fetal calf serum (Product No. S0115)	Biochrom, Berlin, Germany
GeneRuler 100 bp DNA ladder plus	Fermentas GmbH, St. Leon-Rot, Germany
Methylcellulose (Product No. 64630)	Methocel MC, viscosity 4,000 mPa.s, Fluka Chemie, Buchs, Switzerland

Nunclon Δ 60 mm dishes, gridded 2 x 2 mm, for selection of clones	Nunc GmbH & Co. KG, Wiesbaden, Germany
o-Phenylenediamine dihydrochloride (OPD) (Product No. 78440)	Fluka Chemie, Buchs, Switzerland
PROTRAN nitrocellulose transfer membrane, pore size 0.2 μ m	Schleicher & Schuell GmbH, Dassel, Germany
Petri dish with vents, 35 mm	Greiner Bio-One GmbH, Frickenhausen, Germany
Plasmid isolation	Perfectprep Plasmid Midi (Eppendorf, Hamburg, Germany)
Poly-L-lysine hydrobromide 30,000-70,000 (Product No. 81338)	Fluka Chemie, Buchs, Switzerland
Reverse Transcriptase Superscript II RNase H-	Invitrogen/Life Technologies, Karlsruhe, Germany
RNA isolation, RNeasy Mini Kit	Qiagen, Hilden, Germany
G418 sulfate (Product No. 345810)	Calbiochem, EMD Biosciences, Inc, Darmstadt, Germany
Tetramethylethylenediamine (TEMED)	Serva, Heidelberg, Germany
Thiazolyl Blue Tetrazolium bromide (MTT) (Product No. 88415)	Fluka Chemie, Buchs, Switzerland
Tissue culture flask, 25 cm ² style, 50 ml	Falcon, Becton Dickinson U.K. LTD, Plymouth, England
Transfection Reagent SuperFect	Qiagen, Hilden, Germany
Tissue culture test plates 96-well, well \varnothing 6.7 mm; 24-well, \varnothing 16.2 mm; 12-well, \varnothing 22.2 mm; 6-well, \varnothing 34.5 mm, flat bottom	TPP AG, Trasadingen, Switzerland
Triton X-100	Serva, Heidelberg, Germany

3.2 EQUIPMENT

Autoclave steam sterilizer	Varioklav, H + P Labortechnik GmbH, Oberschleißheim
Biological safety cabinet	Microflow Class 2, Nunc GmbH & Co. KG, Wiesbaden, Germany
Centrifuge, Eppendorf	5415 C , Eppendorf AG, Hamburg, Germany
Centrifuge, Hettich EBA 3 S	Hettich, Tuttlingen, Germany
Centrifuge, Refrigerated	Z382K, Hermle Labortechnik GmbH, Wehingen, Germany
CO ₂ incubator	Cellstar, Nunc, Nalge Nunc International, Rochester, NY, U.S.A.
Dry heat sterilizer	Memmert model no. 500, Memmert GmbH & Co. KG, Schwabach, Germany
Flow cytometer	FACScan and CellQuest software, Becton Dickinson, BD Biosciences, San Jose, CA, U.S.A.
Gel documentation	Gel Doc 2000 Software: Quantity One 4.1.1, Bio-Rad Laboratories GmbH, Munich, Germany
Inverted optical microscope	Wilovert S, Wetzlar, Germany
Isopropanol freezing container	NALGENE Cryo 1 C Freezing Container, Nunc, Nalge Nunc International, Rochester, NY, U.S.A.
Mechanic tissue homogenizer	Ultra-Turrax T25 with dispersing tool S25N-8G, Janke & Kunkel, Staufen, Germany
Microcentrifuge	5415 D, Eppendorf AG, Hamburg, Germany
Microplate reader	Model 550, Bio-Rad Laboratories GmbH, Munich Germany
Microscope	Olympus BH-2, Olympus Deutschland GmbH, Hamburg, Germany
Microwave	Model M633, Samsung, Korea
Photometer	Hitachi U-2000 Spectrophotometer, Colora Messtechnik GmbH, Lorch, Germany
Power supply	Power Pac 3000, Bio-Rad Laboratories GmbH, Munich, Germany

Rotator	Roto-Torque, Model No. 7637-10, Cole-Parmer Instrument Company, Vernon Hills, Illinois, USA
Scanner	Coolscan 5000, Nikon GmbH, Düsseldorf, Germany
SDS-PAGE protein sequestration Equipment	Mini-PROTEAN II cell, Bio-Rad Laboratories GmbH, Munich, Germany
Shaker	Ika-Vibrax-VXR, IKA-Werke GmbH & Co. KG, Staufen, Germany
Ultrasonic homogenizer	Sonopuls GM 200, Sonotrode MS73, Bandelin electronic, Berlin, Germany
Water heater	Thermostat 2761, Eppendorf AG, Hamburg, Germany
Western blotting apparatus	Bio-Rad Mini Trans-Blot Electrophoretic Transfer Cell, Bio-Rad Laboratories GmbH, Munich, Germany

3.3 CELL CULTURE

3.3.1 CELL LINES

HCT-15 epithelial, colorectal adenocarcinoma, CCL-225, American Type Culture Collection

DLD-1 epithelial, colorectal adenocarcinoma, CCL-221, American Type Culture Collection

3.3.2 CELL CULTURE CONDITIONS

Both cell lines were grown in RPMI-1640 medium (Sigma, R-6504), supplemented with 2 mM L-glutamine (Sigma, G-8540), 100 U/ml penicillin G sodium salt (Sigma, P-3032) and 100 µg/ml streptomycin sulfate (Sigma, S-9137). In general, 10 % of FCS (v/v) that had been heat inactivated for 30 min at 56 °C was added. Content of FCS was only reduced for specific assays of growth characteristics with reduced content of FCS.

Cells were kept at constant conditions in an incubator, with a temperature of 37 °C and 5 % CO₂ in the humidified atmosphere. Unless specified, cells were grown in 25-cm²-style (50 ml) sterile tissue culture flasks with 5 to 7 ml culture medium, depending on cell density. To enable gas exchange, the cap was screwed on loosely. Culture medium was exchanged after 4 days or when the phenol red pH indicator in the medium turned to a yellowish bright orange, showing an increase in acids resulting from the cells metabolizing the nutrients in the medium.

3.3.3 PASSAGING OF CELLS

20 mM phosphate-buffered saline (PBS), pH 7.2:

Stock solution A (1 x: 1.54 M NaCl, 20 mM Na₂HPO₄ x 2 H₂O) 10 x:

90 g NaCl

35.6 g Na₂HPO₄ x 2 H₂O

aqua dest. *ad* 1,000 ml

Stock solution B (1 x: 1.5 M NaCl, 0.1 M KH₂PO₄) 10 x:

87.7 g NaCl

13.6 g KH₂PO₄

aqua dest. *ad* 1,000 ml

Eighty milliliters of stock solution A and 20 ml of stock solution B were mixed and then diluted with aqua dest. to a volume of 1,000 ml to obtain a 20 mM phosphate-buffered saline solution, pH 7.2.

PBS-EDTA-detaching solution: PBS was supplemented with 2 mM EDTA disodium dihydrate, 0.75 g/l, and the pH was set to 7.2. The solution was autoclaved and stored at 4 °C.

Before the cells grew to a confluent layer, which might then acquire different properties resulting from density dependent growth inhibition, the cell number in the flask was reduced by detaching the cells using 2 ml of 20 mM PBS pH 7.2 containing 2 mM EDTA. After 5 min of incubation, the loosely attached cells were brought into suspension first by gently pushing the flask against the palm of the left hand and then by repeatedly pipetting the cell suspension and washing off cells of the bottom of the flask. The cells were then first transferred to and later centrifuged in sterile centrifuge tubes at 2,000 rpm (Hettich centrifuge) for 3 min to form a cell pellet from which the supernatant could easily be removed. Afterward, cells were

resuspended in culture medium. A fraction of the volume was transferred back into the tissue culture flask, and additional medium was added as necessary.

3.3.4 GENERATION OF STABLE CELL TRANSFECTANTS

LB-Medium:

25 g Luria Bertani Broth base (Roth, Product No. X968.1)

ad 1,000 ml aqua dest., pH 7.2

autoclaved and stored at 4 °C

Plasmid preparation: Perfectprep Plasmid Midi (Eppendorf, Hamburg, Germany)

Stable cell transfectants were generated as previously described^{103, 104, 105}. The vectors for transfection of the cell lines were provided by our laboratory. In order to clone and amplify DNA sequences encoding human full-length galectin-1 cDNA (408 bp), galectin-2 cDNA (399 bp) or galectin-7 cDNA (411 bp) that were suitable for ligation into the *Kpn I* restriction site of the eukaryotic expression vector pcDNA3.1(+), a PCR reaction was performed with the following primer sets (the *Kpn I* restriction site is underlined):

Table 6. Primers used for PCR of human full-length galectin-1-, galectin-2- and galectin-7-cDNA suitable for ligation into the expression vector pcDNA3.1(+). The *Kpn I* restriction site is underlined.

gal-1 forward	5'-CGCTAGGGT <u>ACCAT</u> GGCTTGTGGTCTGGTCG-3'
gal-1 reverse	5'-CGTACGGG <u>TACCT</u> CAGTCAAAGGCCACACA-3'
gal-2 forward	5'-CGTACGGG <u>TACCAT</u> GACGGGGAACTTG-3'
gal-2 reverse	5'-CGCTAGGGT <u>TACCTT</u> ATTCTTTAACTTGAAAGAGGACATG-3'
gal-7 forward	5'-CGTACGGG <u>TACCAT</u> GTCCAACGTCCCC-3'
gal-7 reverse	5'-CGTTAGGGT <u>TACCT</u> CAGAAGATCCTCACG-3'

The cDNA preparations for galectins-1, -2 or -7 were then subcloned into the *Kpn I* restriction site of the eukaryotic expression vector pcDNA3.1(+), where the respective galectin-specific cDNA was under control of the CMV promoter and clones could be selected by neomycin resistance. The ATG start codon was positioned into a Kozak translation initiation sequence (...ANNATGG...) for proper initiation of translation. The three vectors pcDNA3.1Gal-1, pcDNA3.1Gal-2 and pcDNA3.1Gal-7 were transformed into the *E. coli* strain TOP10 (Invitrogen, Karlsruhe, Germany). Isolated plasmids obtained from propagated single colonies

were screened for sense/antisense orientation by PCR. *E.coli* TOP10 bacteria containing plasmids with the respective galectin-specific cDNA in sense orientation were grown in 50 ml LB medium overnight. The plasmids for the transfection experiments were prepared using Perfectprep Plasmid Midi (Eppendorf, Hamburg, Germany). Agreement with databank sequences and in frame cloning were ascertained by sequencing (GATC, Konstanz, Germany). For the transfection experiments, the vectors were linearized with the restriction enzyme *Bgl* II.

Transfections were done using SuperFect Transfection Reagent (Qiagen), which generated liposome complexes. For stable transfections, 2 µg plasmid DNA and 10 µl SuperFect reagent were incubated in 100 µl serum- and antibiotic-free medium for 10 min at room temperature to allow complex formation. Sixty thousand cells were seeded the day before transfection in a 35 mm dish (6-well plate) to lead to 60 to 80 % confluence on the day of transfection. While complex formation took place, the growth medium was aspirated from the dish and washed once with 4 ml 20 mM PBS, pH 7.2. One milliliter of growth medium (containing serum and antibiotics) was added to the reaction tube containing the transfection complexes. After mixing, the medium was transferred to the cells in 35 mm dishes. The cells were incubated with the complexes for 3 h at 37 °C and 5 % CO₂. The medium containing the remaining complexes from the cells was carefully aspirated, and the cells were washed four times with 4 ml of 20 mM PBS, pH 7.2. Fresh cell growth medium was added, and the cells were incubated for 48 h. After trypsinization, resuspended cells were seeded into three 6 cm dishes and selection was performed with G418 (750 µg/ml) for 2 weeks. As control, the vector pcDNA3.1(+) without insert (mock treatment) was used to generate controls of stably mock-transfected clones.

3.3.5 ORIGIN OF CELL CLONES

The next task was to pick clones based on expression levels. Stably transfected cells were trypsinized, then one tenth of the suspension of cells was transferred into each of three 60 mm gridded Petri dishes. After 24 hours the cell population in the Petri dishes were examined under an invertoscope. Single adherent cells with sufficient distance to other cells, which might otherwise grow together, were localized and marked by drawing a circle around them on the bottom side of the Petri dish with a permanent marker. The Petri dishes were then placed in the incubator for an additional four to seven days until small colonies were visible. Following a subsequent examination using the invertoscope, suitable colonies - originating from single cells - that had not grown together with other neighboring colonies and were also

sufficiently distant from other colonies to ensure accurate picking of cells solely from this colony, were marked with a different colored marker on the bottom side of the Petri dish.

A 96-well tissue culture test plate was prepared by adding 100 μ l of selection medium to each well. The colonies that had been selected in the previous step were carefully picked by aspirating 10 μ l with a pipette while pushing the tip of the pipette directly into the marked area against the bottom of the dish. The aspirated cells were put into the tissue culture test plate, one well for each of the picked colonies. Stable clones were cultivated in the presence of G418 (200 μ g/ml) to ensure continued presence of resistance.

Once the cells had nearly grown to confluence, they were detached with 20 μ l of 20 mM PBS (pH 7.2) containing 2 mM EDTA and transferred to the wells of a 24-well cell culture plate containing 1 ml of selecting growth medium. The cells were then placed in the incubator until there was a sufficient quantity of cell material to biochemically assay the expression levels of the respective galectin. This was done by means of SDS-PAGE and subsequent Western blotting, ELISA and FACS analyses.

3.3.6 COUNTING CELLS

Detaching solution: Trypsin-EDTA solution, 10 x (Sigma, T-4174)

Important exception: no trypsin was used to detach the cells for the cell count prior to FACS or cytochemical analyses. FACS and cytochemical analyses are used to determine the presence of distinct proteins on the cell surface. Treatment of cells with trypsin can degrade cell surface proteins, thereby altering the results of these assays.

Cells were washed once with 20 mM PBS, pH 7.2 and then incubated with the detaching solution for 5 min at 37 °C. The cells were suspended by repeatedly pipetting the solution against the bottom of the cell plate. A coverslip was placed onto an Improved Neubauer hemocytometer, and an aliquot of 10 μ l was transferred to the cell counting chamber after mixing the cell suspension by pipetting the volume up and down. Four 1 mm squares were counted, and the average cell number per 1 mm² was multiplied with the dilution factor and with 10⁴, resulting in an estimation of the cell count per ml cell suspension. An average of at least four cell counts was used for further calculations.

3.3.7 FREEZING CELLS

Freezing medium: 45 % RPMI-1640 medium (v/v), 45 % FCS (v/v), 10 % DMSO (v/v)

Cells were detached with 20 mM PBS, pH 7.2 containing 2 mM EDTA, centrifuged at 2,000 rpm (Hettich centrifuge), the supernatant was discarded, and the cells were washed once with 20 mM PBS, pH 7.2. After another round of centrifugation under the same conditions, the cells of the pellets were resuspended in freezing medium and filled in cryo-vials as 1 ml aliquots, then placed in a container for freezing cells (NALGENE) filled with isopropanol to reduce the cooling speed to approximately 1 °C per minute. The container was placed in a -80 °C freezer overnight after which the cryo-vials were transferred to a liquid nitrogen storage tank.

3.3.8 THAWING CELLS

Cryo-vials were placed in a water bath of 37 °C just until the ice in the vials melted. The cell suspension was then immediately transferred to a centrifuge tube with 4 ml of ice-cold RPMI-1640 medium. After centrifugation at 2,000 rpm (Hettich centrifuge) for 3 min, the supernatant was discarded and the cell pellet was resuspended in RPMI-1640 medium containing FCS, antibiotics and L-glutamine and then transferred to cell culture flasks.

3.4 BIOCHEMICAL METHODS

3.4.1 PREPARATION OF CELL LYSATES FOR SDS-PAGE ANALYSIS

Cell lysis buffer for SDS-PAGE of cellular extracts, pH 7.2:

2 mM EDTA disodium dihydrate	0.075 g
1 % Triton X-100 (v/v)	1 ml
0.1 % sodium deoxycholate (w/v)	0.1 g
50 mM D-lactose monohydrate	1.8 g
2 mM DTT	0.031 g
2 µg/ml aprotinin	200 µg
5 µg/ml leupeptin	500 µg
1 mM pefablock	0.024 g
20 mM PBS, pH 7.2	<i>ad</i> 100 ml

Protein assay dye:

Bio-Rad protein assay dye concentrate diluted 1:2.5 (40 % (v/v)) with aqua dest.

Cells were detached and centrifuged as described and washed with 1 ml of cold 20 mM PBS, pH 7.2. After an additional centrifugation for 3 min at 800 x g (3,000 rpm, eppendorf centrifuge), the supernatant was removed. The cells were resuspended in cell lysis buffer for SDS-PAGE of cellular extracts. 50 µl of cell lysis buffer were added to cells grown to subconfluency in one well of a 24-well cell culture test plate. Two hundred microliters were added to cells from a tissue culture flask. The cells were further lysed using a homogenizer emitting ultrasonic waves in cycles of 90 % for 20 sec. During this procedure the suspension was cooled on ice to prevent overheating. The solution was centrifuged at 25,000 x g (14,000 rpm, Hermle centrifuge) and 4 °C for 5 min. The supernatant was transferred to a fresh micro-test tube, whereas the pellet was discarded.

The protein content was determined using the method developed by Bradford¹⁰⁶ and adapted by Redinbaugh and Cambell for small volumes¹⁰⁷. A one microliter aliquot of cell extract was diluted with 20 mM PBS, pH 7.2 to 100 µl, and a series of concentrations was set up in a 96-well plate by stepwise 1:2 dilutions. One microliter of lysis buffer plus 99 µl 20 mM PBS, pH 7.2, was used as blank to monitor the response of the assay without protein. One hundred microliters of 40 % commercial solution with protein assay dye was added to the wells. After an incubation time of 5 min at room temperature the optical density was determined at the wavelength of 595 nm using an ELISA minireader. Optical densities in the linear range between 0.4 and 0.6 were used to calculate the protein concentration relative to a standard curve established with BSA.

3.4.2 SDS-PAGE

10 % SDS (w/v): 10 g SDS, aqua dest. *ad* 100 ml, stored at room temperature

Tris buffer, 0.5 M, pH 6.8: 6.06 g Tris-base, aqua dest. *ad* 100 ml, pH 6.8

SDS Sample buffer:

3.8 ml aqua dest.
1 ml 0.5 M Tris-HCl, pH 6.8
0.8 ml glycerol
1.6 ml SDS, 10 %
0.4 ml β -mercaptoethanol
0.4 ml 0.05 % bromophenol blue (w/v)
stored at -20 °C

Running Gel Tris Buffer (1.5 M Tris, 0.4 % SDS (w/v)), pH 8.8:

45.4 g Tris-base
1 g SDS
aqua dest. *ad* 250 ml, pH 8.8, stored at 4 °C

Stacking Gel Tris Buffer (0.5 M Tris, 0.4 % SDS (w/v)), pH 6.8:

6.06 g Tris-base
400 mg SDS
aqua dest. *ad* 100 ml, pH 6.8, stored at 4 °C

10 % ammonium persulphate (APS) (w/v):

100 mg APS
aqua dest. *ad* 1 ml, prepared just before use

Rotiphorese Gel 30 (Roth, 3029.1): water soluble 30 % acrylamide (w/v) stock solution with
0.8 % bis-acrylamide (w/v)

per Gel with a width of 1 mm:

Stacking gel: acrylamide concentration 4 % (w/v)

aqua dest.	1.55 ml
0.5 M Tris, 0.4 % SDS, pH 6.8	625 μ l
Rotiphorese Gel 30	325 μ l
TEMED	4.5 μ l
10 % APS (w/v)	20 μ l

mixed together just prior to use

Resolving gel: acrylamide concentration 15 %

aqua dest.	1.8 ml
0.5 M Tris, 0.4 % SDS, pH 6.8	1.7 ml
Rotiphorese Gel 30	3.5 ml
TEMED	6 μ l
10 % APS (w/v)	35 μ l

mixed together just prior to use

Tris-glycine 10 x stock solution (250 mM Tris, 2 M glycine):

30.3 g Tris

150 g glycine

aqua dest. *ad* 1,000 ml, stored at room temperature

Electrophoresis buffer, 1 x:

35 ml Tris-glycine 10 x stock solution

3.5 ml 10 % SDS

aqua dest. *ad* 350 ml, prepared just before use

Recombinant galectins-1, -2 and -7, purified by affinity chromatography were supplied by our laboratory.

One-dimensional discontinuous gel electrophoresis in the presence of SDS was essentially performed as first described by Laemmli¹⁰⁸. The samples were prepared by heating 50 μ g of total protein with an equivalent amount of SDS sample buffer to 95 °C for 5 min.

Two hundred nanograms of a galectin was added in one lane as a positive control for the subsequent Western blotting and the visualization of distinct proteins with the ECL system.

The proteins were separated using the Bio-Rad Mini-Protean II system. The gel was cast using two different layers of acrylamide concentrations, one on top of the other. First, the components of the resolving gel were mixed and poured into the space between two glass plates to a height of 5.5 cm. Isopropanol covered the surface of the resolving gel to avoid evaporation and contact to the air, and the gel was left for 45 min at room temperature until polymerization was complete. Isopropanol was then thoroughly washed away with aqua dest., and the stacking gel was poured over the resolving gel to the top of the glass plates. A Teflon comb was placed into the stacking gel to create ten slots for the samples while the gel was left to polymerize for an additional 30 min. The gel cassette sandwich was then placed into the Electrode Assembly, which was then lowered into the Mini Tank. Three hundred fifty milliliters electrophoresis buffer were filled into the tank, which surfaced just above the top of the gel, and the samples were carefully pipetted into the gel pockets. Electrophoresis was then started and kept at a constant current of 200 V for approximately 45 min until the bromophenol blue left the gel. The gel was finally removed from the electrophoresis chamber and after removing the stacking gel the resolving gel was prepared for transfer of the proteins to a nitrocellulose membrane.

3.4.3 ELECTROPHORETIC TRANSFER OF PROTEIN TO NITROCELLULOSE

Blotting buffer:

100 ml Tris-glycine 10 x stock solution

200 ml methanol

aqua dest. *ad* 1,000 ml, stored at 4 °C

0.1 % Ponceau S sodium salt (w/v) (Sigma, P-3504) in 1 % acetic acid (v/v):

1 ml acetic acid

100 mg Ponceau S

aqua dest. *ad* 100 ml

Blocking solution: 5 % skim milk powder (w/v) in T-TBS buffer

Protein transfer from an SDS gel to a nitrocellulose membrane was performed essentially as described by Towbin et al.¹⁰⁹. Electroblotting was carried out using a Bio-Rad Mini-Trans Blot Cell system according to the manufacturer's instructions. Briefly, the gel was equilibrated in ice-cold blotting buffer three times for 10 min. A piece of nitrocellulose membrane that had been cut according to the size of the resolving gel, two fiber pads and six pieces of blot absorbent filter paper (also cut to fit) were soaked in ice-cold blotting buffer for 30 min. In order to prevent air bubbles getting trapped in the system, a few millimeters of blotting buffer was poured between each layer of one fiber pad, three gel-sized pieces of filter papers, the nitrocellulose membrane, the gel, three filter papers and the other fiber pad. This was placed into the gel holder cassette and then closed. The cassette was placed into the electrode assembly, which itself was placed in the buffer tank. After positioning the frozen Bio-Ice cooling unit (basically a container with ice) into the buffer tank, it was filled with blotting buffer and a magnetic stirring bar was added. Placing the Blot Cell system onto a magnetic stirring device set at full speed helped maintain even buffer temperature and ion distribution in the tank. The blot was run at constant voltage of 100 V for 90 min. Upon completion of the run, the blotting sandwich was disassembled, and the membrane was air dried for 5 min. The positions of the lanes of protein and the quality of the blot were ascertained by staining the proteins with Ponceau S solution. After marking the size of the positive control and the positions of the lanes with a ballpoint pen, the nitrocellulose membrane was washed with T-TBS buffer.

3.4.4 DETECTION OF GALECTINS ON THE BLOT

Tris-buffered saline (TBS) 10 x (0.5 M Tris, 1.5 M NaCl), pH 7.5:

60.50 g Tris-base

87.66 g NaCl

aqua dest. *ad* 1,000 ml, pH 7.5, stored at 4 °C

Tris-buffered saline 1 x with 0.05 % Tween-20 (v/v) (T-TBS):

100 ml TBS, 10 x

500 µl Tween-20

aqua dest. *ad* 1,000 ml, prepared just before use

Blocking solution:

5 g skim milk powder, blotting grade
T-TBS *ad* 100 ml, prepared just before use

Primary antibodies:

polyclonal rabbit-anti-galectin-1 IgG, 1:500 (2 µg/ml)
polyclonal rabbit-anti-galectin-2 IgG, 1:2,000 (0.5 µg/ml)
polyclonal rabbit-anti-galectin-7 IgG, 1:1,000 (1 µg/ml)
All anti-galectin IgG antibodies were supplied by our laboratory.

Secondary antibody goat-anti-rabbit IgG-peroxidase conjugate (Sigma, A-6154), 1:2,000 (0.5 µg/ml)

Primary and secondary antibodies were diluted in blocking solution and a total volume of 5 ml was used for each of the incubation steps.

ECL Western Blotting Detection Reagents (Amersham Biosciences)

12.5 % acetic acid (v/v) in aqua dest.

Kodak Professional D19 Developer (Sigma, P-5670), 15.6 g/100 ml aqua dest.

Kodak Fixer solution (Sigma, P-6557), 18.4 g/100 ml aqua dest.

Immunodetection blotting was performed to detect the presence of distinct proteins with specific antibodies in order to determine the galectin content in the cells. To block any antigen-independent binding of proteins, the nitrocellulose membrane was exposed to blocking solution for 1 hour at room temperature. Incubation of the membrane with 5 ml of the antibody solutions was carried out in 50 ml conical centrifuge tubes on a rotator to guarantee even distribution of the reagents on the membrane, while minimizing the necessary quantities of reagents for the experiment. The nitrocellulose membrane was first incubated with the primary antibodies to bind the target galectins overnight at 4 °C. After washing the membrane with 30 ml of T-TBS buffer three times quickly, then three times for 10 min, the

blots were incubated with solution containing the secondary antibody goat anti-rabbit immunoglobulin-peroxidase conjugate for 1 hour at room temperature. The blots were washed in the same manner as after the incubation with the primary antibody. Finally, bound secondary antibodies were visualized using the ECL Western blotting detection kit (Amersham Biosciences) following the manufacturers instructions. The substrate solution was prepared briefly before use and pipetted onto the blot, allowing coincubation to proceed for 1 min. After carefully removing excess liquid with a paper towel, the blot was placed into a film cassette and covered with plastic foil. The detection was based on a chemoluminescence reaction in which the luminol in the substrate solution is oxidized in the presence of H₂O₂ by the peroxidase conjugated to the secondary antibody. Light was hereby emitted, which was detected by exposing the membrane to an x-ray film. The film was then incubated in developer solution for approximately 90 sec until bands began to appear. Transferring the film to 12.5 % acetic acid (v/v) solution stopped the reaction and the film was then placed in fixer solution until the background was clear. Finally, the film was washed thoroughly in aqua dest. and air-dried.

To ascertain the resistance to possible interfering factors in cell extracts, SDS-PAGE and subsequent Western blot were carried out with different amounts of recombinant galectin (50 - 400 ng) with and without HCT-15 WT cell extract.

3.4.5 ENZYME LINKED IMMUNOSORBENT ASSAY

Cell lysis buffer for ELISA of cellular extracts, pH 7.2:

2 mM EDTA disodium dihydrate	0.075 g
0.25 % Triton X-100 (v/v)	0.25 ml
2 mM DTT	0.031 g
2 µg/ml aprotinin	200 µg
5 µg/ml leupeptin	500 µg
1 mM pefablock	0.024 g
20 mM PBS <i>ad</i> 100 ml	

Coating buffer (0.1 M sodium hydrocarbonate, 0.1 M disodium carbonate), pH 9.6:

2 components:

0.1 M NaHCO₃, 0.84 g *ad* 100 ml aqua dest. and

0.1 M Na₂CO₃, 1.06 g *ad* 100 ml aqua dest.

were mixed to reach a pH of 9.6

Lyophilized asialofetuin (ASF) and lactose-bovine serum albumin conjugate (Lac-BSA) were supplied by our workgroup.

ASF and Lac-BSA were redissolved in coating buffer to a concentration of 10 µg/ml each.

ELISA blocking solution: 1 g BSA dissolved in 100 ml 20 mM PBS, pH 7.2

The primary and secondary antibodies were used in the same concentration as for the detection on the nitrocellulose membrane (see 3.4.4).

Primary and secondary antibodies were diluted in ELISA blocking solution and a total volume of 100 µl per well was used for each of the incubation steps.

After coating and between each incubation step, the wells were washed four times with 200 µl of 20 mM PBS, pH 7.2.

Cell lysates and positive controls were diluted in ELISA blocking solution to a volume of 100 µl per well.

OPD buffer (50 mM disodium hydrophosphate, 20 mM citric acid), pH 5.0:

1.78 g Na₂HPO₄ x 2 H₂O

0.84 g citric acid monohydrate

aqua dest. *ad* 200 ml

OPD solution:

10 mg o-phenylenediamine dihydrochloride (OPD)

10 µl 30 % H₂O₂

OPD buffer *ad* 10 ml, prepared just before use

Stopping solution: 0.1 M H₂SO₄

An ELISA was developed to gain additional information of the actual active lectin activity of galectins-1, -2 or -7 in the transfected and control cells. A known ligand for the galectins served as a matrix to assess binding activity. This was either asialofetuin (ASF) or lactose-bovine serum albumin-conjugate (Lac-BSA), a chemically prepared glycoprotein¹¹⁰. Preparation of cells was identical as for SDS-PAGE analysis (see 3.4.1) except the lysis buffer had to be modified reducing Triton X-100 and excluding sodium deoxycholate and lactose, which could otherwise disturb the lectin binding to the matrix.

Adsorption of the (neo)glycoprotein to the ELISA microplate surface was performed after diluting ASF or Lac-BSA in coating buffer to a concentration of 10 µg per ml, then pipetting 100 µl (1 µg matrix protein) of this solution into each well and finally placing the microplate (without a lid or other covering) in an incubator at 37 °C for 12 hours - during which the liquid completely evaporated. After this step and between each of the incubation steps, the wells of the ELISA microplate were washed four times with 200 µl per well. To inhibit any residual binding of proteins to the microplate well surface, the wells were incubated with 200 µl 1 % BSA in PBS (ELISA blocking solution) at 37 °C. During this and the following incubation steps at 37 °C the microplate was covered to minimize evaporation. After the blocking procedure saturating the well surface, the cell lysates were added to the wells. Cell extract protein was diluted in ELISA blocking solution and 100 µl containing 1,000 µg to 62.5 µg of cell extract protein (depending on the response in the assay) per 100 µl was added to the first well. A concentration row was established diluting each next sample 1:2 with ELISA blocking solution and 100 µl of these solutions was added to the ELISA microplate. As a positive control and to set a relationship between known galectin content and respective response, a concentration row of samples with recombinant galectins-1, -2 or -7 diluted with ELISA blocking solution to a concentration between 800 ng and 50 ng (again depending on the intensity of the response) per 100 µl in the first sample was made. This was continuously further diluted 1:2 with ELISA blocking solution and 100 µl of these samples were added to the ELISA microplate. To evaluate the response without galectin (negative control to determine background values), 100 µl of ELISA blocking solution was pipetted into each of four wells.

The solutions in the microplate were incubated for 3 hours at 37 °C. To detect the respective bound galectin, the ELISA microplate was incubated with the non-cross-reactive primary antibody rabbit polyclonal IgG fractions specific for galectin-1, galectin-2 or galectin-7 for 2 hours at 37 °C. The secondary antibody goat anti-rabbit-IgG-peroxidase conjugate was then added to the wells and incubated at 37 °C for 1 hour. Afterwards, 100 µl OPD solution was

added to each of the wells and the microplate was incubated at 37 °C for 15 min, during which the OPD was processed, dependent on the amount of bound peroxidase, to a more or less intensive yellow color. This reaction was stopped by adding 100 µl of 0.1 M H₂SO₄ to each of the wells. The optical density at a wavelength of 490 nm was measured in an ELISA minireader. The OD was interpreted as nanogram of bound galectin per µg of cell extract by comparing the optical densities with those of the positive control while considering the blank. To ascertain the validity of the assay and its lack of impairment by any interfering compounds in cell extracts, the reactivity of recombinant galectin was measured with and without tissue extracts from bovine heart muscle. Approximately 1 g of frozen adult bovine heart muscle tissue was homogenized in 4 ml ice-cold 20 mM PBS, pH 7.2 with an Ultra-Turrax homogenizer set to full speed in impulses of ten times 5 sec during which the tissue sample was cooled with ice. The homogenate was transferred to 1.5 ml mini test tubes and centrifuged at 23,000 x g (13,000 rpm) at 4 °C for 5 min. The supernatant was pipetted into new mini test tubes, and the protein concentration was measured as described above. An ELISA was performed with 1 µg of ASF coated to each of the wells. Fifteen ng of recombinant galectin in 20 mM PBS, pH 7.2 was added to each of the wells with or without different quantities (100 µg to 1,000 µg protein) of bovine tissue extract. The response of the applied amounts of bovine tissue extract without recombinant galectin was also measured.

3.4.6 FACS ANALYSIS

Dulbecco's phosphate-buffered saline (DPBS) Mg²⁺ and Ca²⁺ free, 10 x (27 mM KCl, 14.7 mM KH₂PO₄, 1.38 M NaCl, 80.9 mM Na₂HPO₄ x 2 H₂O), pH 7.2:

2.0 g KCl

2.0 g KH₂PO₄

80.6 g NaCl

14.4 g Na₂HPO₄ x 2 H₂O

ad 1,000 ml aqua dest., stored at room temperature

DPBS 1 x, pH 7.2:

100 ml DPBS 10 x

ad 1,000 ml aqua dest., stored at 4 °C

Washing buffer: 0.1 % BSA (w/v) in DPBS

Primary antibodies: polyclonal rabbit-anti-galectins-1, -2, or -7 IgG diluted to 1 µg/100 µl

Secondary antibody: anti-rabbit-IgG-FITC conjugate (Sigma, F-0382) diluted to 1 µg/100 µl

Antibodies were diluted in 0.1 % BSA (w/v) washing buffer

Centrifugation was always at 800 x g (3,000 rpm, eppendorf centrifuge) for 3 min.

Flow cytometry allows the counting and analysis of physical and molecular attributes of cells in a liquid medium. With the fluorescence activated cell-sorting analysis (FACS-analysis) one can quantify the presence of surface receptors as well as intracellular proteins. The analysis is based on the specific interaction of antigens with antibodies, which are conjugated to fluorescent dyes. During the analysis the suspended cells are hydrodynamically focused and pass a laser beam of appropriate wavelength, leading to fluorescence activation and emission. The intensity of fluorescent signals is correlated to antigen presence. Additional information is given through the scatter signals of the laser itself, such as the cell size. The most often used application in flow cytometry, also the aim of these studies, is the analysis of expression levels of surface or intracellular determinants based on specific staining of these antigens with labeled antibodies on a single-cell level.

Cells were detached with 20 mM PBS, pH 7.2 containing 2 mM EDTA, counted and 4×10^5 cells were pipetted into micro-test tubes. No trypsin was added to the detaching solution, as this would have changed protein structures on the cell surfaces. After centrifugation, the supernatant was removed and the cells were washed with 500 µl ice-cold DPBS.

Extracellular staining

First, the cells were incubated with 50 µl of the primary antibody diluted in washing buffer for 30 min on ice. Then 500 µl washing buffer was added, the cells were centrifuged and after discarding the supernatant the cells were washed again in 500 µl washing buffer. The cells were incubated with 50 µl of the FITC-labeled antibody diluted in washing buffer for 30 min on ice in the dark. As before, the cells were carefully washed twice with washing buffer. Pellets were finally resuspended in 300 µl 1 % paraformaldehyde (w/v) and stored at 4 °C for at least 1 hour for fixation.

As negative controls, two samples of the cell clone were treated in parallel under identical conditions as described above, except that the primary antibody or both the primary and the secondary antibodies were excluded from the diluting solutions.

FACS analysis was finally performed using a FACScan flow cytometer with CellQuest software (Becton Dickinson).

3.4.7 CYTOCHEMICAL ANALYSIS

Poly-L-lysine solution: 0.2 mg/ml in sterile PBS (20 mM, pH 7.2)

2 % paraformaldehyde (w/v) in 20 mM PBS, pH 7.2

Sterile coverslips were incubated with 100 µl of the poly-L-lysine solution for 30 min at 37 °C. They were washed with sterile PBS and left to dry. HCT-15 cells were detached with 20 mM PBS, pH 7.2 containing 2 mM EDTA. No trypsin was added to the detaching solution, as this would have changed protein structures on the cell surfaces. Ten thousand cells in 100 µl medium were plated onto the poly-L-lysine coated area of the coverslip and incubated for 2 hours at 37 °C. The coverslips were carefully washed with 20 mM PBS, pH 7.2 and fixed in 2 % paraformaldehyde (w/v) for 5 min at room temperature. They were then washed three times for 5 min in PBS. Immunocytochemical and cytomorphological processing of the cells was performed in the lab of Prof. Dr. Smetana (Charles University, Prague) as previously described ¹¹¹.

3.5 MOLECULAR BIOLOGY

3.5.1 ISOLATION OF GENOMIC DNA

Wizard Genomic DNA purification kit (Promega, Mannheim, Germany)

DNA rehydration solution (Promega) 10 mM Tris-HCl, 1 mM EDTA, pH 7.4

Isolation of genomic DNA was done using the Promega Wizard Genomic DNA purification Kit according to the manufacturer's instructions. Two million cells were trypsinized, harvested and transferred to a 1.5 ml micro-test tube. They were centrifuged at 10,000 x g for

10 sec to pellet the cells. The supernatant was removed and after a washing step with 20 mM PBS, pH 7.2, 600 μ l nuclear lysis solution was added. This was carefully pipetted up and down until the solution was homogeneous. Three microliters of RNase solution was added to the nuclear lysate and manually inverting the tube a few times mixed the sample. After incubation for 30 min at 37 °C the sample was cooled to room temperature. Subsequently, 200 μ l of protein precipitation solution was added, vortexed vigorously and chilled on ice for 5 min. After centrifugation for 4 min at 13,000 x g the supernatant containing the DNA was transferred to a micro-test tube with 600 μ l of room-temperated isopropanol and was gently mixed by inversion until the white thread-like strands of DNA formed a visible mass. Following a centrifugation step (1 min at 13,000 x g) the DNA pellet was washed with 600 μ l 70 % ethanol (v/v) at room temperature. After centrifugation (1 min at 13,000 x g) the supernatant was carefully discarded, the DNA pellet air dried for 15 min and dissolved in 100 μ l DNA rehydration solution at 65 °C for 1 hour. The DNA concentration of the solution was then measured photometrically at a wavelength of 260 nm ($E = 1$ at 50 μ g/ml DNA), and 0.5 μ g genomic DNA was used in the PCR assay described below.

3.5.2 RNA EXTRACTION, REVERSE TRANSCRIPTION OF RNA AND PCR ANALYSIS

RNeasy Mini Kit (Qiagen, Hilden, Germany)

First strand buffer (50 mM Tris-HCl, pH 8.3, 75 mM KCl, 15 mM MgCl₂)

Total RNA from 2×10^6 cells was isolated using an RNeasy Mini Kit (Qiagen) according to the manufacturer's directions. The integrity of the RNA was verified by separating an aliquot of 1 μ g of total RNA by agarose gel electrophoresis. Intact RNA was separated into compact bands of distinct sizes. The following procedures were performed as previously described¹⁰². Briefly, an aliquot of 1 μ g of total RNA was used as a template for first strand synthesis of cDNA. Reverse transcription was performed for 50 min at 42 °C in a 20 μ l reaction volume containing first strand buffer, dNTPs (1 mM each), oligo(dT)₁₂₋₁₈ primer (0.5 μ g), 200 units Superscript II RNase H⁻ Reverse Transcriptase and DEPC-treated water. The reaction was terminated by incubation at 70 °C for 15 min. An aliquot of 2 μ l of the probe were then used in the following PCR amplification. The primer pairs used for RT-PCR amplification of cDNAs specific for galectins-1, -2, -7 and actin are shown in table 7.

Table 7. Primer pairs used for RT-PCR amplification of galectins-1, -2, -7 and actin.

Primer	Sequence	Location ^a	Size ^b
Galectin-1#1	5'-AAC CTG GAG AGT GCC TTC GA-3'	45 - 64	323
Galectin-1#2	5'-GTA GTT GAT GGC CTC CAG GT-3'	367 - 348	
Galectin-2#1	5'-ATG ACG GGG GAA CTT GAG GTT-3'	27 - 47	358
Galectin-2#2	5'-TTA CGC TCA GGT AGC TCA GGT-3'	384 - 364	
Galectin-7#1	5'-ATG TCC AAC GTC CCC CAC AAG-3'	19 - 39	282
Galectin-7#2	5'-TGA CGC GAT GAT GAG CAC CTC-3'	300 - 280	
β-Actin#1	5'-GGC ATC GTG ATG GAC TCC G-3'	521 - 539	612
β-Actin#2	5'-GCT GGA AGG TGG ACA GCG A-3'	1133 - 1115	

^a Numbers designate the base pair positions according to published cDNA sequences

^b Predicted size of the correct fragment

PCR was performed after an initial denaturation step at 95 °C for 5 min for 30 cycles (denaturation at 95 °C for 35 sec, annealing at 58 °C for 55 sec, extension at 72 °C for 40 sec). The final extension step was performed at 72 °C for 5 min.

3.5.3 AGAROSE GEL ELECTROPHORESIS

EDTA solution, 0.5 M, pH 8.0:

186.12 g EDTA disodium dihydrate

ad 1,000 ml aqua dest.

TAE buffer, 50 x (2 M Tris-Acetate, 50 mM EDTA) buffer:

242 g Tris-base

57.1 ml glacial acetic acid (acetic acid ≥ 99.7 %)

0.5 M EDTA (pH 8) 100 ml

ad 1,000 ml aqua dest., autoclaved and stored at room temperature

TAE buffer, 1 x (0.04 M Tris-Acetate, 1 mM EDTA):

20 ml TAE buffer, 50 x

ad 1,000 ml aqua dest., stored at room temperature

SeaKem LE Agarose (BioWhittaker Molecular Applications)

Ethidium bromide stock solution: 10 mg/ml (Sigma), stored at 4 °C and protected from light

Loading Dye solution, 6 x (Fermentas)

GeneRuler 100 bp DNA Ladder plus (Fermentas)

Amplified Products were separated by means of electrophoresis in 2 % agarose (w/v) gels. Specifically, SeaKem agarose was heated in the microwave in TAE buffer (1 x) until the agarose was completely dissolved and the solution was then left to cool to approx. 60 °C. To visualize the DNA bands, 5 µl of the DNA intercalating agent ethidium bromide per 100 ml agarose solution was added and mixed evenly in the solution by swirling the container. The solution was then poured into a gel chamber into which a comb had been inserted to generate pockets in the gel for the samples, and allowed to cool down and harden. The gel was then transferred to a gel chamber, which was filled with 1 x TAE buffer. DNA or standard size marker was dissolved in 6 x loading dye solution and was transferred into the slots of the gel. The DNA products were subjected to electrophoresis at a constant voltage until the samples had sufficiently been separated in the gel, which was visible by the dye in the loading buffer. The DNA was finally visualized by ultraviolet light and photographed.

3.6 VIDEO MICROSCOPY

Monitoring of cell populations by video microscopy and recording of snapshots after constant intervals was performed by a SAMBA 2005 computer-assisted microscope system (Samba Technologies, Grenoble, France) with a x 20 (aperture 0.50) magnification lens. Video microscopic analysis of the cells was performed in the lab of Prof. Dr. R. Kiss (Université Libre de Bruxelles, Brussels) as previously described¹¹².

3.7 ASSAYS WITH CELL LINES

3.7.1 METHYLCELLULOSE ASSAY

DMEF/F-12 doubly-concentrated:

15.57 g DMEM/F-12 (1:1) powder (Gibco BRL)

ad 500 ml (instead of 1,000 ml for cell culture medium) autoclaved Millipore water
sterile filtered

Methylcellulose solution:

8.8 g methylcellulose (Fluka Chemie)

188 ml DMEM/F-12 double-concentrated medium

1.125 g NaHCO₃

ad 500 ml autoclaved Millipore water

Methylcellulose solution was autoclaved with a stir bar in a 1,000 ml bottle. Two hundred eight milliliters of autoclaved Millipore water were then added. The solution was boiled and left to cool to room temperature in three cycles while being stirred. One hundred eighty-eight milliliters of double-concentrated DMEM/F-12 and 1.125 g NaHCO₃ were added after which the pH value was adjusted to 7.2. The volume was then set to 500 ml with autoclaved Millipore water, the solution was filtered to establish sterility and stirred for 48 hours at 4 °C, before it was finally aliquoted and stored at -20 °C.

Suspension of cells in methylcellulose:

4.7 ml methylcellulose solution

4.3 ml cell suspension with a total of 10⁴ cells in RPMI-1640 medium

1 ml FCS

In this assay setting, cells were grown in tissue culture medium containing highly viscous methylcellulose. This kept the cells from adhering directly to the cell culture flask. The ability of cells to proliferate in the absence of adhesion, termed anchorage-independent growth, is a main characteristic of transformed cells and is an important feature of tumorigenicity¹¹³.

A cell suspension was prepared in RPMI medium, FCS and methylcellulose. After vortexing at maximum speed for 10 sec an aliquot of 2 ml was pipetted into each of three 35 mm Petri

dishes. These were then incubated at 37 °C for 10 days. Decisive criterion was the ability of the non-adherent cells to grow into cell clones that were identified as single colonies. These were counted by monitoring cells through an invertoscope while placing the Petri dishes onto a gridded glass plate.

3.7.2 DOUBLING TIME

Cells were detached, and a cell suspension was made containing 5×10^4 cells per ml in culture medium. A total of 12 wells per cell clone (three per day, 4 days) of a 24-well plate already containing 1 ml of cell growth medium were filled with a 1 ml aliquot of the cell suspension. The cells were incubated for 72 hours (until day 3) during which the cells were allowed to “recover” from the previous handling, leave the quiescent phase and enter exponential growth. Then cells were detached with 300 μ l Trypsin-EDTA solution per well. Depending on cell density a 100 μ l to 200 μ l aliquot of the cell suspension was transferred to a micro-test tube and diluted with PBS-EDTA as necessary. The cell number was determined, while taking the total volume of the cell suspension, the aliquot taken and the dilution factor into consideration. The mean cell number of three wells represented the cell count for that day. This procedure was repeated on days 4, 5 and 6.

Assessment of the doubling time was performed by first setting the cell numbers into relation to the hours that had passed after seeding. To ascertain that the cells were in the exponential phase of growth, that they had left the quiescent phase and that cell growth was later not attenuated, i.e. by density-dependent inhibition, a graph was plotted setting the hours into relation to the logarithm of the according cell numbers. Exponential cell growth should reach a linear relationship at this point. If a cell count at the beginning or end of the assay did not meet these terms, it was not included in the equation of the doubling time.

An exponential function $f(x) = b * m^x$ that best fit the obtained data was computed by regression analysis using the computer program Microsoft Excel.

$f(x)$ cell numbers

x hours after seeding

b a constant defining the cell number at $x = 0$

m the base of the exponential function

b and m were computed by the program Excel

The calculation was transformed expressing the doubling time (dt) through m :

if $x = dt$ then

$$f(dt) = b * m^{dt} = 2 * b \quad | /b$$

$$m^{dt} = 2 \quad | \ln \text{ (natural logarithm)}$$

$$\ln(m^{dt}) = \ln(2)$$

$$dt * \ln(m) = \ln(2) \quad | / \ln(m)$$

$$dt = \ln(2) / \ln(m)$$

$$\text{doubling time} = \ln(2) / \ln(m)$$

3.7.3 MTT ASSAY

96-well F-Plate

RPMI-1640 medium with 1 %, 2 %, 3 % or 10 % FCS (v/v)

MTT stock solution (0.5 % MTT (w/v)) 10 x:

50 mg MTT dissolved in 10 ml 20 mM PBS, pH 7.2, sterile filtered and stored at 4 °C

MTT medium:

MTT stock solution was diluted 1:10 in RPMI-1640 medium, prepared just before use

Chemotherapeutical agents:

Irinotecan hydrochloride trihydrate (CPT-11) and SN38 (7-ethyl-10-hydroxycamptothecin) were kindly supplied by Prof. Dr. R. Kiss (Brussels, Belgium).

Oxaliplatin stock solution: 5 mg of oxaliplatin (Sigma, Product No. O-9512) were dissolved in 2 ml of 20 mM PBS, pH 7.2.

Irinotecan stock solution: 1.5 mg irinotecan were dissolved in 20 μ l of a solvent consisting of 80 % ethanol (v/v) and 20 % DMSO (v/v) (EtOH:DMSO 80:20).

SN38 stock solution: 1 mg SN38 was dissolved in 637.4 μ l EtOH:DMSO 80:20.

The stock solutions of the chemotherapeutical agents were diluted in cell growth medium shortly before addition to the cells to the following concentrations:

oxaliplatin: 10^{-4} M, 10^{-5} M, 10^{-6} M, 10^{-7} M

irinotecan: 10^{-4} M, 10^{-5} M, 10^{-6} M, 10^{-7} M

SN38: 10^{-6} M, 10^{-7} M, 10^{-8} M, 10^{-9} M

MTT [3-(4,5-dimethylthiazol-2-yl)-2,5-diphenyltetrazolium bromide] assay, first described by Mosmann¹¹⁴, is based on the ability of a mitochondrial dehydrogenase from viable cells to cleave the tetrazolium rings of the pale yellow MTT and form dark blue formazan crystals which are largely impermeable to cell membranes, thus resulting in their accumulation in viable cells. Solubilization of the cells by the addition of a detergent results in the liberation of the crystals, which are dissolved. The number of viable cells is directly proportional to the level of the formazan product created. The intensity of the developed colored product can then easily be quantified with an ELISA reader.

Because sterile conditions could not be kept during the final evaluation of the assay, i.e. when placing the microplate in the ELISA reader, one microplate was used for each day that the MTT cleavage was to be measured. After detaching and counting the cells, a cell suspension was made with 2×10^4 cells per ml of medium made up of RPMI-1640 medium, supplemented with the usual amount of penicillin, streptomycin, L-glutamine (see 3.3.2) and 10 % of FCS (v/v). To assess cell viability under stress conditions with reduced FCS content, cells were resuspended in medium with 1 %, 2 %, 3 % FCS (v/v).

Five wells were each filled with 100 μ l of cell suspension (2,000 cells) for every cell line and day that was to be assessed. The wells on each side were not used for the assay but were filled with 20 mM PBS, pH 7.2 instead, as these were more subject to evaporation than the other wells. The microplates were then placed in the incubator. Unless declared otherwise, the medium was not exchanged until the date of evaluation. This prevented the unwanted detachment of cells, which might occur during the removal or addition of medium.

When examining susceptibility to stress by the cytotoxic agents oxaliplatin, irinotecan and SN38, the cells were first plated in medium without the chemotherapeutical agents. After 24 hours, the medium was exchanged with medium containing the cytostatics in four concentrations (oxaliplatin and irinotecan: 10^{-4} to 10^{-7} M; SN38: 10^{-6} to 10^{-9} M). Each concentration was diluted to the next lower concentration 1:10. For comparison, cells were plated in parallel with medium or in cases where a solvent had to be used, with medium and the applied amounts of solvent. The cells were then incubated for 72 hours.

The protocol started by exchanging the medium with 100 μ l of the MTT medium per well. The cells were then placed back into the incubator for 2 (assessment of cell growth in different FCS concentrations) or 4 hours (measurement of susceptibility to cytotoxic agents). The MTT solution was subsequently removed and 100 μ l of DMSO was pipetted to each well. The cells were lysed, and the dark blue formazan reaction product was evenly distributed in the solution by repeatedly pipetting DMSO up and down and also by stirring the pipette in the well. One hundred microliters of DMSO in previously empty wells served as the negative value. The microplate was finally placed in an ELISA reader and the optical density of the wells was measured at a wavelength of 595 nm.

3.7.3.1 DETERMINATION OF THE IC₅₀ VALUE OF CYTOTOXIC AGENTS

The percentage of the optical density compared to that of the control was displayed in a diagram in relation to the concentrations of the cytotoxic agent on a logarithmic scale. The effect of the agent was described as the concentration responsible for 50 % inhibition of the control value (IC₅₀). This was evaluated by first describing a linear function $f(x) = k * x + d$ with the values closest to the 50 % mark (x_1, y_1 and x_2, y_2).

$f(x)$ percent of the measured optical density in relation to the control value

x log(concentration of the cytotoxic agent)

k constant defining the inclination of the linear curve

d constant defining $f(x)$ at $x = 0$

x_1 logarithmic value of the applied concentration of the cytotoxic agent responsible for a response just below 50 %

y_1 response of x_1

x_2 logarithmic value of the applied concentration of the cytotoxic agent responsible for a response just above 50 %

y_2 response of x_2

$$k = (y_2 - y_1) / (x_2 - x_1)$$

$$d = y_1 - k * x_1$$

Evaluation of IC_{50} :

$$C = \log(IC_{50})$$

$$50 = k * C + d$$

$$C = (50 - d)/k$$

$$IC_{50} = 10^C$$

3.7.4 STATISTICAL ANALYSES

The paired two-tailed Student's t-test was used to analyze the differences between data determined for the analyzed cells and the mock-transfected cells treated under identical conditions. Determined p-values ≤ 0.05 were defined as significant.

4 RESULTS AND DISCUSSION

4.1 CHARACTERIZATION OF CELL CLONES

4.1.1 GENERATION AND SELECTION OF STABLE CELL CLONES

Neomycin-kanamycin aminoglycoside antibiotics such as G418 block protein synthesis in mammalian cells by interfering with ribosomal function¹¹⁵. HCT-15 and DLD-1 cells were transfected with a galectin-cDNA-carrying vector. The vector also contained an aminoglycoside phosphotransferase gene, resulting in detoxification of neomycin-kanamycin antibiotics¹¹⁵. This conferred resistance of the cells to otherwise lethal concentrations of antibiotic in the medium. Therefore, the presence of G418 in the medium enabled selection of vector-positive cells from the population. Having acquired stable transfectants by this selection procedure, the next step was to analyze the genomic DNA of each cell clone.

4.1.2 DNA AND RNA ANALYSIS

G418 resistance over a period of 2 weeks makes it likely that plasmid DNA of the remaining viable cells is stably associated with high molecular weight cellular DNA¹¹⁵. This was verified by examining the genomic DNA of the HCT-15 cells for the encoded galectins. After the genomic DNA of the cells was extracted, the presence of the galectin-specific DNA was confirmed by using suitable primers. If successful, DNA of predicted size would be amplified by the polymerase chain reaction. To detect transcription of galectin-specific DNA to RNA, the RNA of the cells was extracted and rewritten as cDNA by reverse transcription. The cDNA encoding the galectins was then similarly searched for by PCR. The DNA mixture was finally separated by agarose gel electrophoresis and the bands were visualized by ethidium bromide in ultraviolet light.

Figures 5 and 6 show agarose gels with the amplified products generated by this assay. The size of the resulting products was determined by comparison to a 100 bp DNA ladder added as calibration of length next to the samples.

RNA can easily be degraded by RNase activity. This would lead to false negative results when analyzing transcription levels. The integrity of the RNA was therefore confirmed by

evaluating an aliquot of 1 μ g of total RNA by agarose gel electrophoresis. Intact RNA would be separated into compact bands of distinct sizes. This is shown in figure 7.

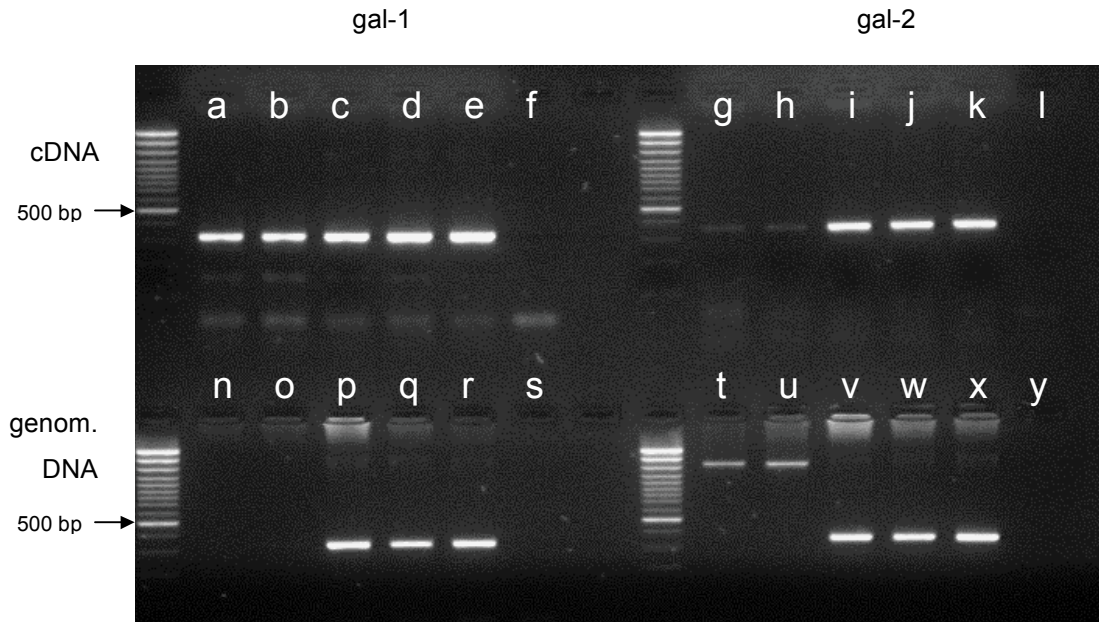


Figure 5: PCR and RT-PCR analysis. Amplified products from cDNA (a - e, g - k) or from genomic DNA (n - r, t - x). Searching for galectin-1 (323 bp) a - f and n - s; galectin-2 (358 bp) g - l and t - y. Negative controls without template: f, l, s, and y. Extracts from WT (a, g, n, t) and mock-transfected cells (b, h, o, u). Cells transfected with galectin-1-specific cDNA: clone 17w (c, p), 35m (d, q) and 72s (e, r). Cells transfected with galectin-2-specific cDNA: clone 27w (i, v), 21m (j, w) and 18s (k, x). The size was determined by comparison to a 100 bp DNA ladder added next to the samples.

The results substantiated the successful vector transfection of the selected cell clones, leading to incorporation of the respective sequences into the genomic DNA. The vector DNA was distinguishable from naturally present genomic DNA, encoding the respective galectins independent of vector transfection. Primer pairs were selected that would include intron sequences incorporated in naturally present genomic DNA. Only sequences amplified from vector DNA yielded PCR products of the expected size.

Amplification of cDNA confirmed presence of galectin-1-, galectin-2- or galectin-7-specific mRNA in clones transfected with the respective galectin-cDNA. A sign of the presence of galectin-1-specific cDNA was seen in wild-type (WT) and mock-transfected cells. No signal indicative of galectin-2- or galectin-7- specific mRNA was found encoded in WT or mock cDNA. As internal loading control, β -actin DNA was amplified in the same manner. To

exclude erroneous signal appearance in the absence of total cDNA, a parallel sample was run without a template but was otherwise treated identically.

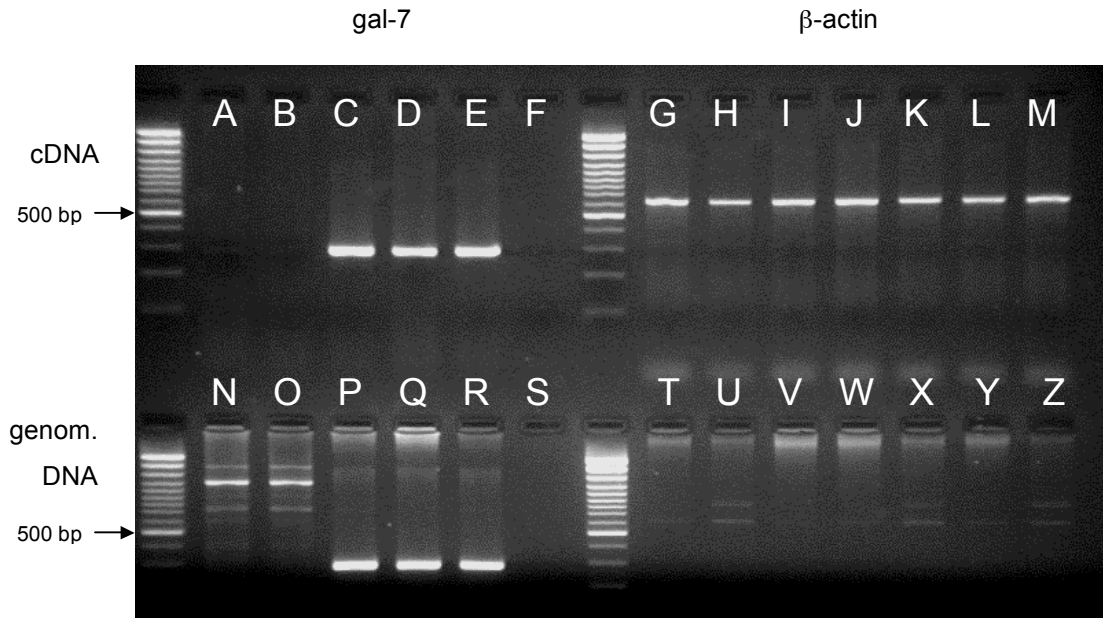


Figure 6: PCR and RT-PCR analysis. Amplified products from cDNA (**A - E**, **G - M**) or from genomic DNA (**N - R**, **T - Z**). Searching for galectin-7 (282 bp) **A - F** and **N - S**; or for β -actin (612 bp) **G - M** and **T - Z**. Negative controls without template: **F** and **S**. Extracts from WT (**A**, **N**) and mock-transfected cells (**B**, **O**). Cells transfected with galectin-7-specific cDNA: clone 19w (**C**, **P**), 13m (**D**, **Q**) and 2s (**E**, **R**). The size was determined by comparison to a 100 bp DNA ladder added next to the samples.

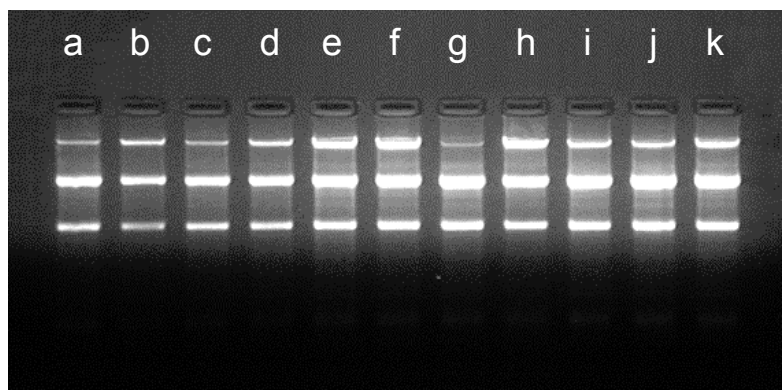


Figure 7: Illustration of the integrity of RNA. In agarose gel electrophoresis, intact RNA separated into compact bands of distinct sizes. One microgram of total RNA extract of HCT-15 WT, mock-transfected and the galectin-1- (clone 17w, 35m, 72s), -2- (clone 27w, 21m, 18s) and -7- (clone 19w, 13m, 2s) cDNA-transfected-cells was inspected for signs of RNA degradation. RNA extracts from clones 2s (**a**); 13w (**b**); 17w (**c**); 18s (**d**); 19m (**e**); 21m (**f**); 27w (**g**); 35m (**h**); 72s (**i**); and from WT (**j**); and mock-transfected cells (**k**).

After analyzing the HCT-15 cells on the level of DNA/RNA, the next question was addressed. This dealt with the consequences of the verified galectin-specific DNA/RNA content in the cells. The resulting quantity of the respective galectin protein was evaluated in each of the cell clones.

4.1.3 ANALYSIS OF GALECTIN PROTEIN BY ECL BLOT

The aim of analyzing the galectin protein content of the HCT-15 cells was to find cell clones overexpressing the respective galectin. This would enable the confirmation of a galectin-specific effect with more than one cell clone. Additionally, by using clones with a low, medium and high content of galectin, information on whether and how an effect might be quantity-dependent could also be collected.

As a first step in assessing the quantity of galectins-1, -2, or -7 proteins, the cells were lysed and the extracts were analyzed by means of SDS-PAGE and subsequent Western blotting, after which the presence of galectin was monitored by the ECL system.

To ensure that components of the cell extract did not influence the reactivity of the galectin in this assay, resulting in false-negative results, a control was run in parallel. This control consisted of recombinant galectin-2 concentrations in the range from 400 ng down to 50 ng - without or with addition of 50 µg protein of HCT-15 WT cell extract. As shown in figure 8, no differences that could be attributed to the presence of cell extract could be seen. This result confirms the experimental conditions of the cell lysates preparation, SDS-PAGE and ECL blot to be appropriate.

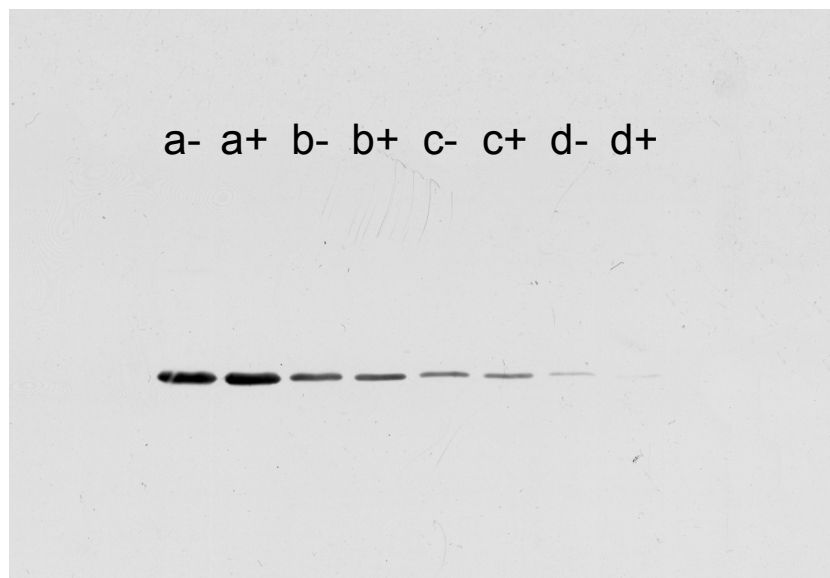


Figure 8. Influence of cell extract on ECL reactivity. Recombinant galectin-2 without (-) or with (+) 50 μ g protein of HCT-15 WT cell extract. **a:** 400 ng; **b:** 200 ng; **c:** 100 ng; or **d:** 50 ng of galectin-2. Film was exposed for 1 min.

When systematically screening the selected cultures, transfectants were found with very different levels of galectin content in the cell lysates. Protein levels ranged from a barely visible response in the ECL system to high quantities, relative to the positive control of 0.2 μ g galectin. Also, some clones were found that did not contain the respective galectin.

During evaluation of HCT-15 cells on their galectin-1 content, blots sporadically showed a slight reactivity in WT and mock cells, indicating a low baseline production of galectin-1 in these cells. Galectin-2 or galectin-7 were never seen in the HCT-15 WT or mock cell lysates.

After testing each clone in at least five independent blotting experiments, three cell clones of the galectin-1-cDNA-transfected cells, three cell clones of the galectin-2-cDNA-transfected cells and three cell clones of the galectin-7-cDNA-transfected cells were chosen. Their response in the ECL system were weak, medium or strong compared to the positive control of the respective galectin. The name of the clone was extended by the clone number with "w" for weak, "m" for medium or "s" for strong to define these clones. Figures 9 - 11 illustrate the different intensity levels for each series of transfectants after ECL processing.

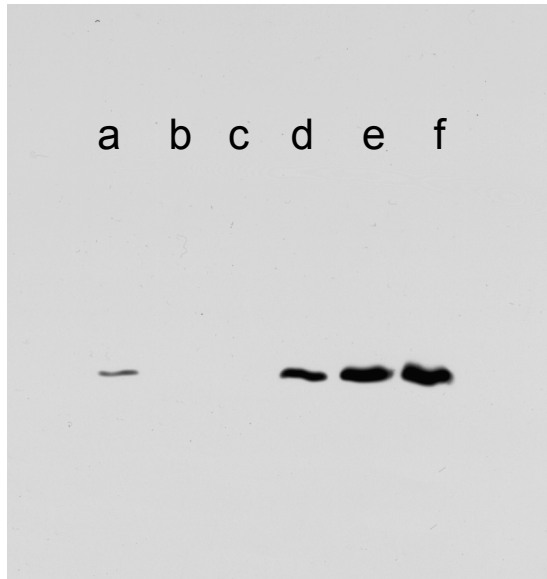


Figure 9. Galectin-1 in HCT-15 Cells. ECL blot using anti-gal-1 IgG as primary reagent. **a:** 0.2 μ g recombinant human galectin-1 as positive control; **b - f:** 50 μ g cell extract protein from **b:** WT, **c:** mock-transfected, and galectin-1-cDNA-transfected cells: **d:** clone 17w, **e:** clone 35m, **f:** clone 72s. Film was exposed for 1 min.

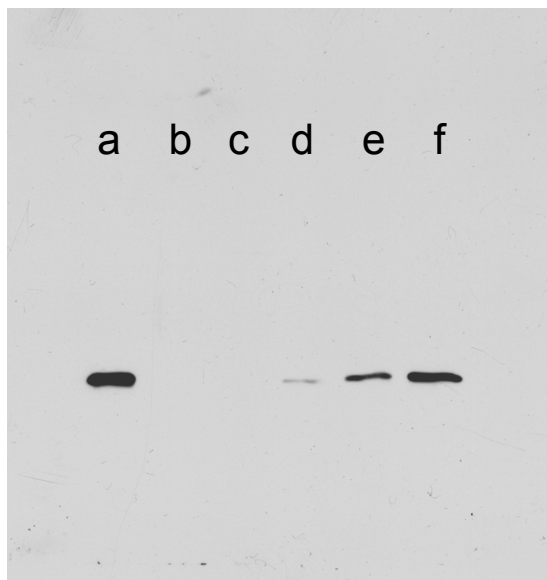


Figure 10. Galectin-2 in HCT-15 Cells. ECL blot using anti-gal-2 IgG as primary reagent. **a:** 0.2 μ g recombinant human galectin-2 as positive control; **b - f:** 50 μ g cell extract protein from **b:** WT, **c:** mock-transfected, and galectin-2-cDNA-transfected cells: **d:** clone 27w, **e:** clone 21m, **f:** clone 18s. Film was exposed for 5 min.

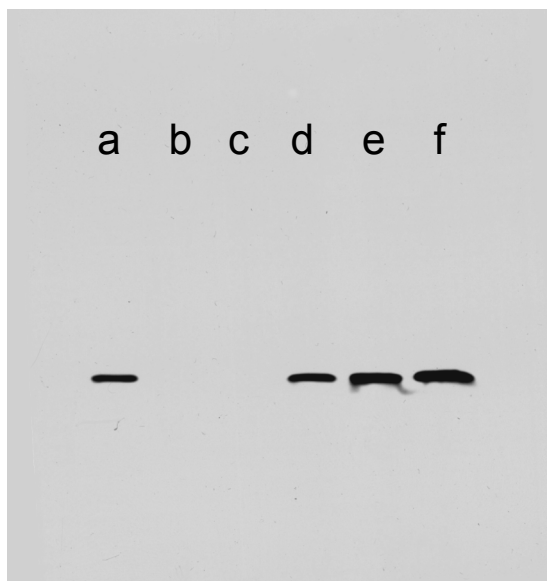


Figure 11. Galectin-7 in HCT-15 Cells. ECL blot using anti-gal-7 IgG as primary reagent. **a:** 0.2 μ g recombinant human galectin-7 as positive control; **b - f:** 50 μ g cell extract protein from **b:** WT, **c:** mock-transfected, and galectin-7-cDNA-transfected cells: **d:** clone 19w, **e:** clone 13m, **f:** clone 2s. Film was exposed for 1 min.

After a first quantification of the galectin protein in the cells by the ECL blot processing, further characterization of the overexpressed galectin was necessary. The most well known feature of galectins is their ability to bind β -galactosides. The binding capacity of the overexpressed galectins to known ligands was investigated in the next procedure.

4.1.4 ENZYME LINKED IMMUNOSORBENT ASSAY

The conditions of an ELISA were adapted to quantify the binding of galectins to a matrix presenting suitable ligands of these lectins. HCT-15 cell extracts of WT, mock-transfected cells and cells transfected with cDNA specific for galectins-1, -2, and -7 were subjected to this assay. ELISA plates were prepared with a matrix (asialofetuin or lactose-conjugated BSA), known to present suitable ligands for galectins¹¹⁶. Cell extracts were incubated in these plates, and the binding of the galectins was assessed by staining them with peroxidase-conjugated antibodies specific for the respective galectins. This ultimately led to an enzymatic reaction causing an increase of concentration of photometrically active substance. The optical density was then measured in a minireader.

When measuring the response of the galectin-1-cDNA-transfected cells, intensities of the reaction were very different between independent experiments. Results of galectin-2 and galectin-7 activity in this assay was contradictory, as the response was often inversely proportional to the added amount of cell extract protein. The determined quantity of bound recombinant galectin to the matrix was conclusive, though. It was assumed that substances in the lysis buffer interfered with binding of galectin to the matrix. However, experiments with recombinant galectin and different compositions of the lysis buffer could not unambiguously solve the problem. Next, the influence of the cell extract itself was examined. The response of recombinant galectin was measured in the presence or absence of HCT-15 cell extracts, which had been homogenized in 20 mM PBS, pH 7.2 instead of lysis buffer. The results showed a marked reduction of the signal by the cell extracts. To determine whether this was a unique characteristic of extracts of HCT-15 cells, the assay was repeated with adult bovine heart muscle extracts, which had also been homogenized in 20 mM PBS, pH 7.2. While the extract itself was not reactive, it effectively reduced the response in assays with recombinant galectin. The evaluation of the carbohydrate-binding activity of the overexpressed galectins was not possible because of the inherent inhibiting properties of cellular extracts in this assay, leading to inherently ambiguous data. Therefore, further characterization of the HCT-15 galectin-overexpressing cells was pursued.

It has been demonstrated that members of the galectin family such as galectin-1 are not confined to the intracellular space, despite the absence of a typical secretion signal peptide¹¹⁷. Hughes describes the secretion and cell surface presentation of galectins as a common event¹¹⁸. In a study presented by Kopitz et al., the interaction of galectin-1 with the ganglioside GM₁, which are both present on the surface of neuroblastoma cells, is described. The data are indicative that the *trans* binding action of these two binding partners on neighboring cells is responsible for cell density dependent differentiation and growth arrest⁷⁶. In order to assay comparable functions in the present study, information had to be gained on the HCT-15 cell surface presentation of the overexpressed galectins. To address this question, cells were processed by FACScan analysis.

4.1.5 FACS ANALYSIS

FACS analysis quantifies the amount of bound FITC-conjugated antibody in each cell of a population. This enabled a conclusion to be made on the distribution of fluorescence intensity among the cells analyzed. If nearly all cells had a certain amount of bound antibody, then a sharp peak was the result in the readout. A more even distribution resulted in a wider peak. The confined accessibility of the antibodies to the cell surface enabled data to be gained on a possible transport of the galectin to the extracellular area of the cell membrane. Figures 12 - 14 illustrate representative results of the FACS analyses.

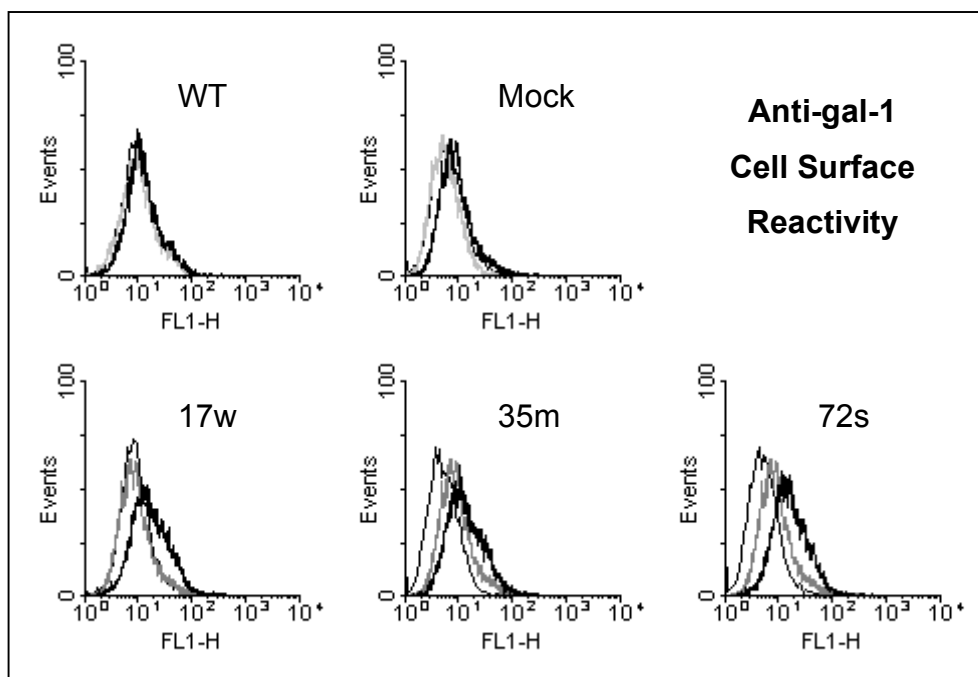


Figure 12: FACS analysis. Reactivity using anti-gal-1 IgG as primary reagent. **Light gray line** (WT and Mock): response without anti-gal-1 IgG or IgG-FITC conjugate; **thin black line**: response without anti-gal-1 IgG; **thick black line**: response with anti-gal-1 and IgG-FITC-conjugate; **dark gray line** (gal-1-cDNA-transfected cell lines): response of mock-treated clone for comparison.

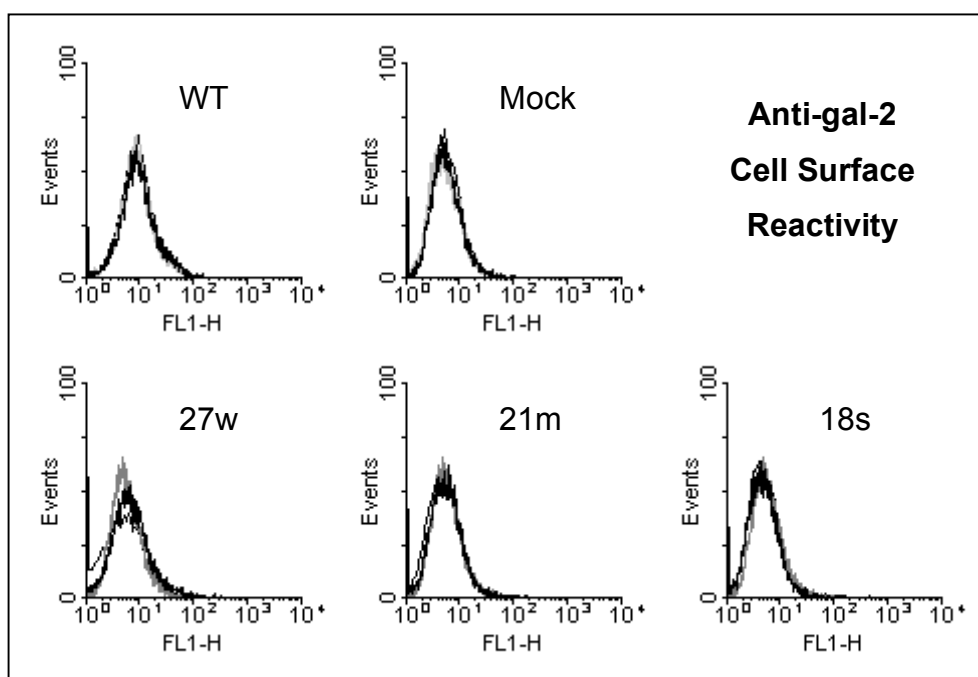


Figure 13: FACS analysis. Reactivity using anti-gal-2 IgG as primary reagent. **Light gray line** (WT and Mock): response without anti-gal-2 IgG or IgG-FITC-conjugate; **thin black line**: response without anti-gal-2 IgG; **thick black line**: response with anti-gal-2 and IgG-FITC conjugate; **dark gray line** (gal-2- cDNA-transfected cell lines): response of mock-treated clone for comparison.

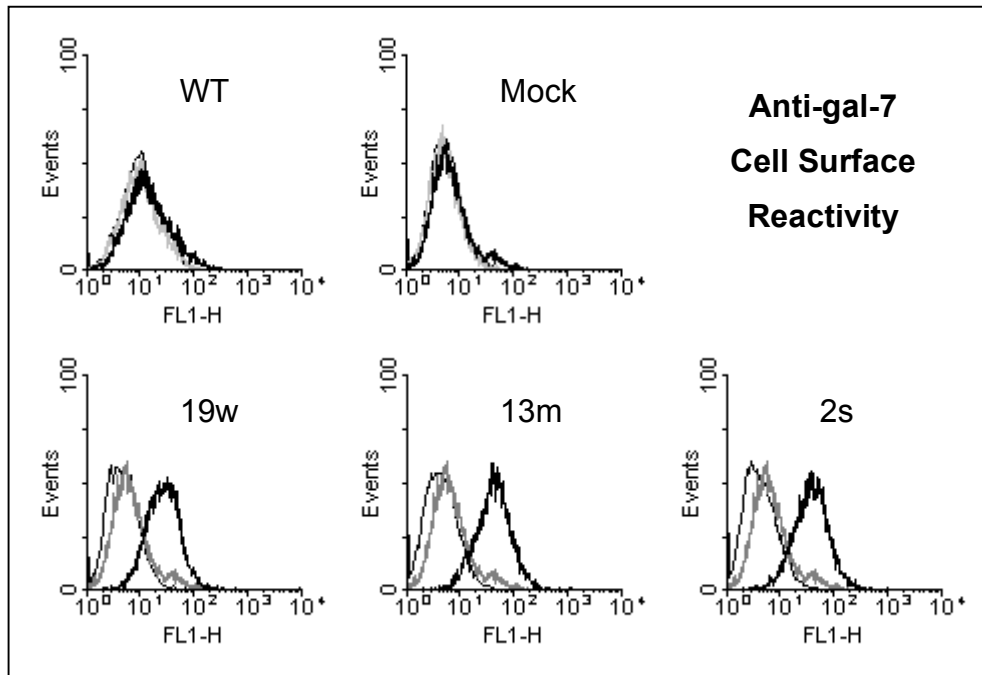


Figure 14: FACS analysis. Reactivity using anti-gal-7 IgG as primary reagent. **Light gray line** (WT and Mock): response without anti-gal-7 IgG or IgG-FITC conjugate; **thin black line**: response without anti-gal-7 IgG; **thick black line**: response with anti-gal-7 and IgG-FITC conjugate; **dark gray line** (gal-7-cDNA-transfected cell lines): response of mock-treated clone for comparison.

Table 8 expresses representative data obtained by FACS analysis in numerical values. Anti-gal-1, anti-gal-2 and anti-gal-7 IgG reactivity is given in the top, middle and bottom groups, respectively. The first number in each field represents the mean fluorescence assayed after incubating the samples with primary and secondary antibodies. The reactivity profile is illustrated in figures 12 to 14. The response was also evaluated after incubating the samples without the primary antibody against the respective galectin protein, but with the IgG-FITC-conjugate (negative control). The percentage of the area beneath the peak reflecting the amount of galectin, without the overlapping portion beneath the peak of the negative control, is added in parentheses as the second value in each field. This value represents the percentage of positive cells in the sample.

Table 8: FACSscan analysis. Anti-gal-1, -2 and -7 reactivity of HCT-15 WT, mock-treated and gal-1-, gal-2- and gal-7-cDNA-transfected cells.

	WT	Mock	G1 17w	G1 35m	G1 72s
Anti-gal-1	20 (15 %)	17 (22 %)	27 (39 %)	22 (50 %)	28 (63 %)
	WT	Mock	G2 27w	G2 21m	G2 18s
Anti-gal-2	14 (13 %)	9 (13 %)	15 (29 %)	10 (13 %)	8 (13 %)
	WT	Mock	G7 19w	G7 13m	G7 2s
Anti-gal-7	29 (18 %)	15 (14 %)	44 (80 %)	61 (87 %)	57 (86 %)

Cell surface staining of the HCT-15 cells using anti-gal-1 IgG was analyzed. The response of the WT and mock-transfected cells was indistinguishable from the negative controls. All of the galectin-overexpressing clones had an increased level of reactivity compared to the mock-transfected cells. This was highest in the clone 72s, followed by the clone 17w and 35m.

Anti-gal-2 IgG was then used as primary reagent for cell surface staining. The obtained data showed no sign of cell surface expression of galectin-2. When assessing anti-gal-7-reactivity, WT and mock-control cells showed no extracellular staining. The galectin-7-overexpressing cells, however, demonstrated a clearly increased intensity of fluorescence. The antigen-independent signal of cells was very low in all cell types. The fluorescence profile of the transfectants revealed sharp and nearly symmetric peaks with a mean average of fluorescence around three to four times that of mock. This indicated transport of galectin-7 to the extracellular surface of the cell membrane.

FACS analysis revealed clear variations in the distribution profiles of the three overexpressed galectins in the HCT-15 cells. This result prompted further analysis to address the following aspects: a.) the relative number of cells with detectable amounts of the respective galectin protein; b.) associations between galectin overexpression and cell size or c.) associations between galectin overexpression and signs of proliferation; and d.) the cellular localization of galectins-1, -2 or -7. The method of choice to provide the answers was immunocytochemical analysis. This procedure was combined with cytomorphological assessment of the cells.

4.1.6 IMMUNOCYTOCHEMICAL ANALYSIS

In this study part galectin-cDNA-transfected cells were not only assessed immunocytochemically, but also cytomorphologically. HCT-15 WT, mock-transfected, galectin-1-cDNA-transfected clone 72 s, galectin-2-cDNA-transfected clone 18s and galectin-7-cDNA clone 2s were subjected to this processing. First, fixed cell populations of

clones were stained with antibodies reactive with the respective overexpressed galectin protein and then counterstained with the DNA fluorochrome DAPI. In the preceding evaluation of DNA/RNA and galectin protein in ECL blots and FACScan, HCT-15 WT and mock-transfected cells showed basal amounts of galectin-1. However, there were no signs of galectin-2 or galectin-7 presence in these cell types. Therefore, WT and mock-transfected cells were included in the assays of galectin-1 detection. As expected, only very few of the WT and mock-transfected cells showed a slight reactivity towards the anti-gal-1 antibody. Cells transfected with cDNA specific for galectins-1, -2 or -7, respectively, showed significant levels of staining when incubated with antibodies directed to the respective overexpressed galectin. Comparison of the reactive cells of the three clones revealed clearly visible differences. Anti-gal-1- and anti-gal-7-positive areas were larger but less intense than those stained by the anti-gal-2 antibody. Representative results are shown in figure 15. The cells displayed the column A1 - E1 were stained with anti-gal-antibodies. The first label in the upper right corner of these images written in capital letters describes the cells analyzed. The specificity of the used antibody is then described in small letters. The microphotographs in the column A2 - E2 show the respective cells, their nuclei being counterstained with DAPI.

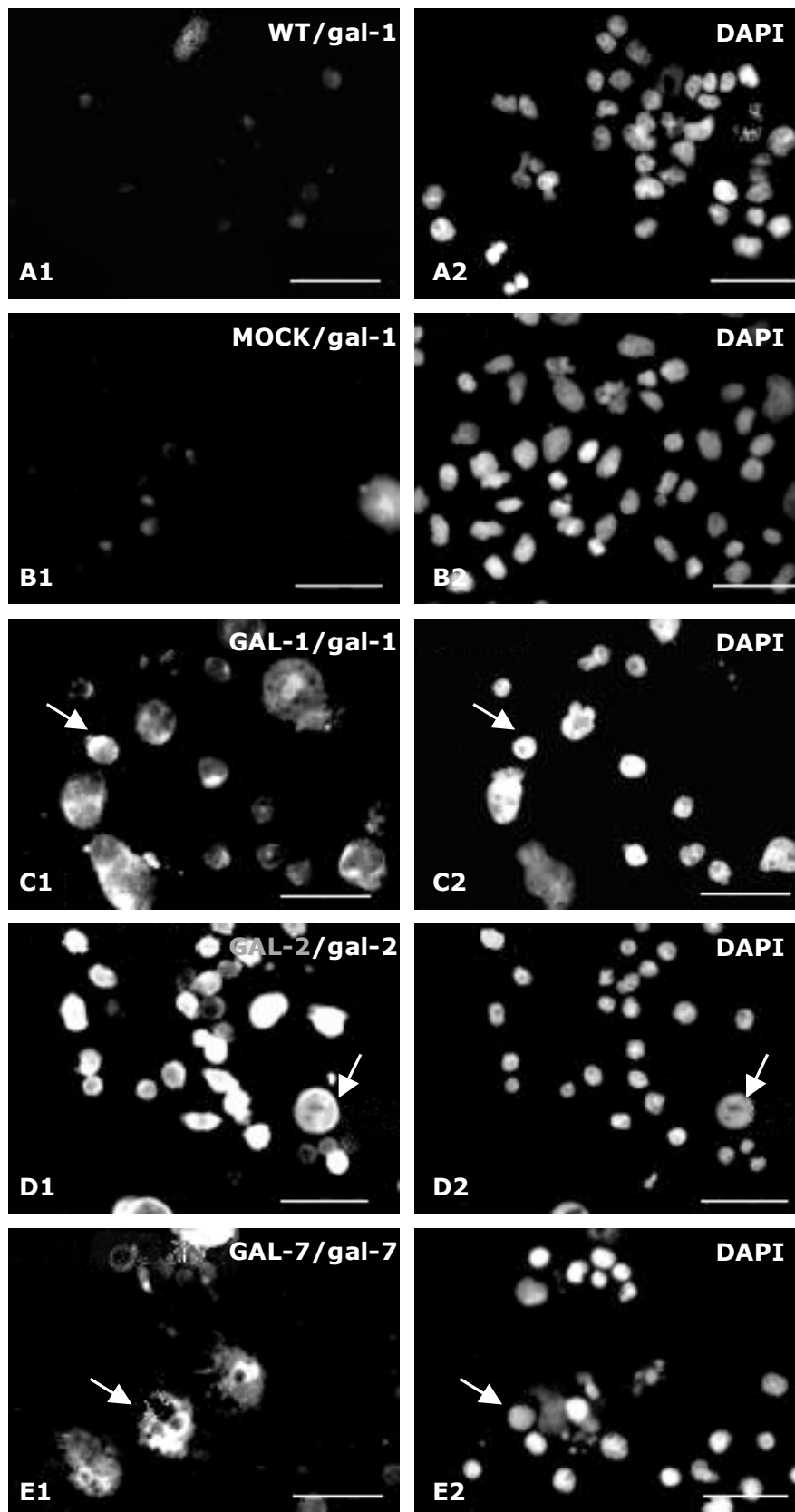


Figure 15. Detection of gal-1 (A1-C1), gal-2 (D1) and gal-7 (E1) in WT (WT) HCT-15 cells (A1), Mock-treated cells (B1), and cells transfected with cDNA specific for gal-1 (C1), gal-2 (D1) or gal-7 (E1). The nuclei of the same cells were counterstained with DAPI (A2-E2). An example of a cell after detection of galectin and staining with DAPI is marked with arrow. Bar is 50 μ m.

Next, cells were counted and stained with an antibody against the respective overexpressed galectin. By this method, the percentage of galectin-positive cells in clones resulting from each transfection was determined. Five hundred of the fixed cells on the slides were randomly chosen and their staining was evaluated. Results showed that the frequency of positivity was highest in galectin-2-cDNA transfectants with 79 %, followed by galectin-7-cDNA transfectants with 67 % positivity. The lowest fraction of positivity was 53 % assayed in the galectin-1-cDNA transfectant. These results are illustrated in figure 16.

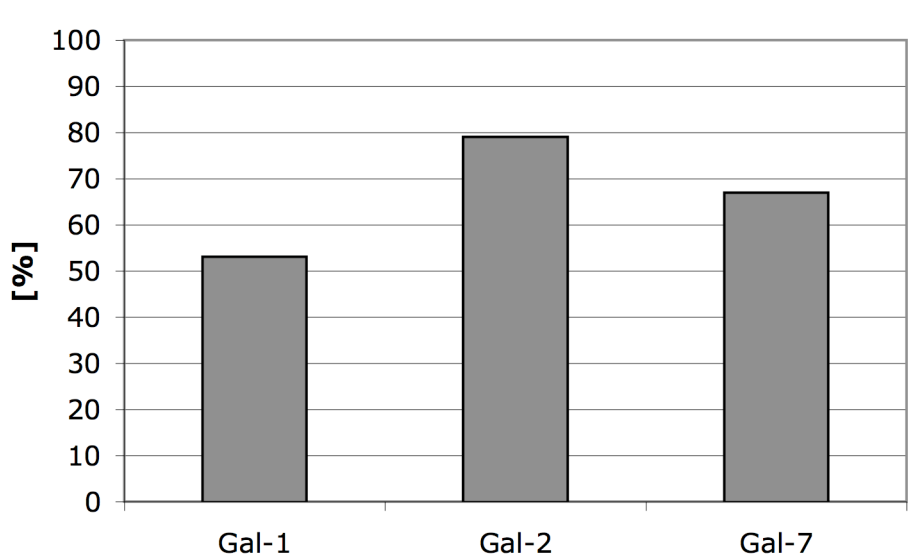


Figure 16. Proportion of HCT-15 cells positive for distinct galectins-1, -2, or -7 after transfection with their cDNA.

In this assay, the number of galectin positive and negative cells was determined. A question to be answered was whether these two cell pools had distinct characteristics. This question was addressed in the following procedure. Cells were not only divided into the two groups of positive and negative in respect to anti-gal-1, -2, or -7 staining, but these two groups were also divided into subgroups regarding the size of the cells. The data are set into relation to delineate, if possible, any association of the two parameters. The results of this assay are shown in figure 17. Cells are grouped according to staining and cell diameter. The number of cells negative for the galectin encoded in the transfected gene is shown in white columns and the number of positive cells in grey columns. Transfection of cDNA specific for galectin-1 and -7 induced formation of positive large-sized cells. Transfection of cDNA coding galectin-2 led to large cells negative for galectin-2, whereas the positive cells were predominantly rather small in cell diameter.

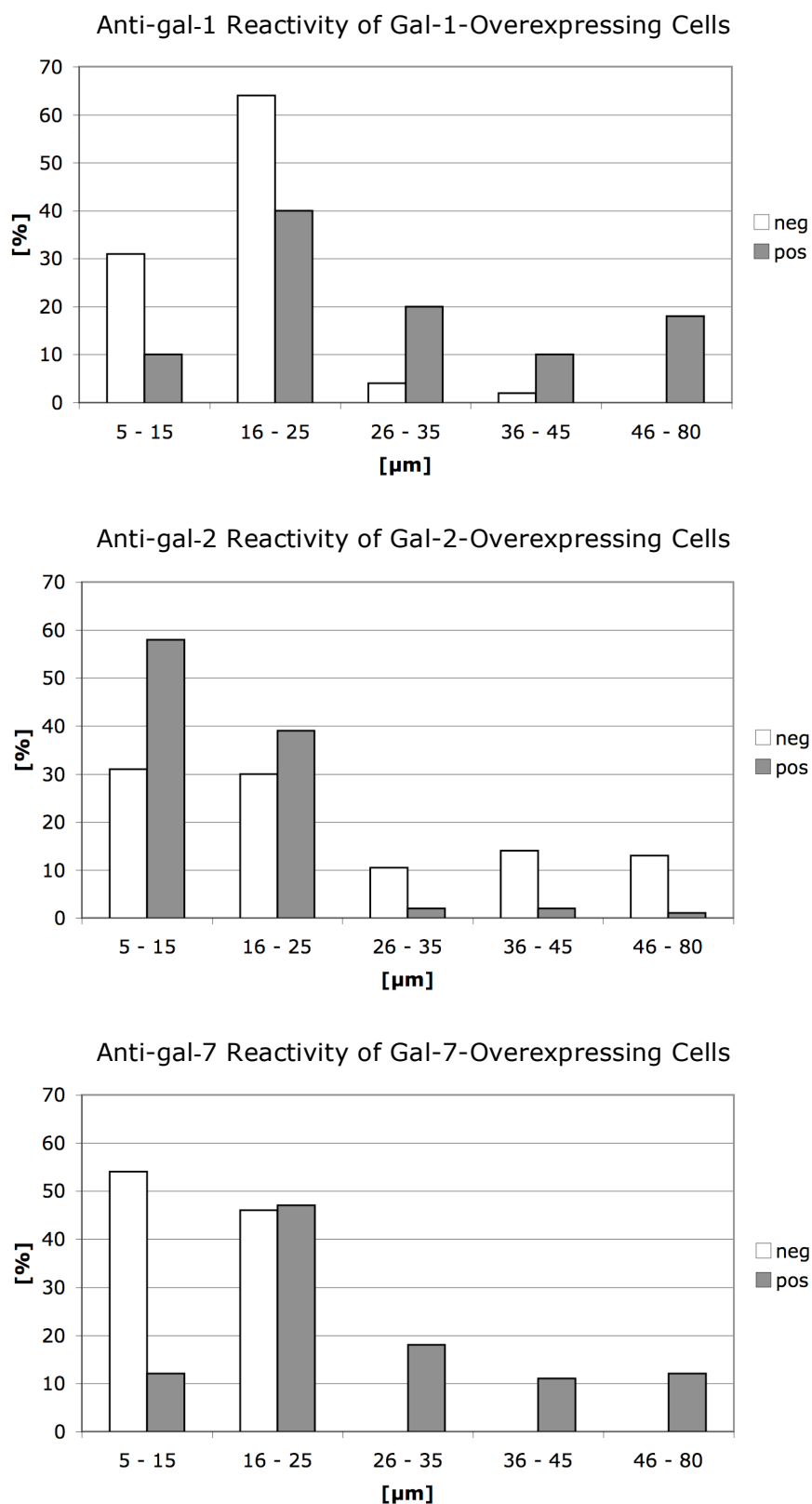


Figure 17. Size distribution and antibody reactivity of cells overexpressing galectins. The x-axis denotes cell diameter in [μm] and the y-axis cell number in [%] among positive and negative cells. **Top:** HCT-15 gal-1-cDNA-transfected clone 72s; **middle:** HCT-15 gal-2-cDNA transfected clone 18s; **bottom:** HCT-15 gal-7-cDNA transfected clone 2s.

Large cells were seen among the galectin-7-overexpressing cells, which showed staining patterns with obvious reactivity around the nucleus. These cells were subjected to further analysis. A representative image of a large cell positive for galectin-7 as frequently seen on slides is shown in figure 18. Cells were stained with an anti-gal-7 antibody, and the same cells were counterstained with DAPI. The diameters of the areas with the highest reactivity in both images were then compared with each other.

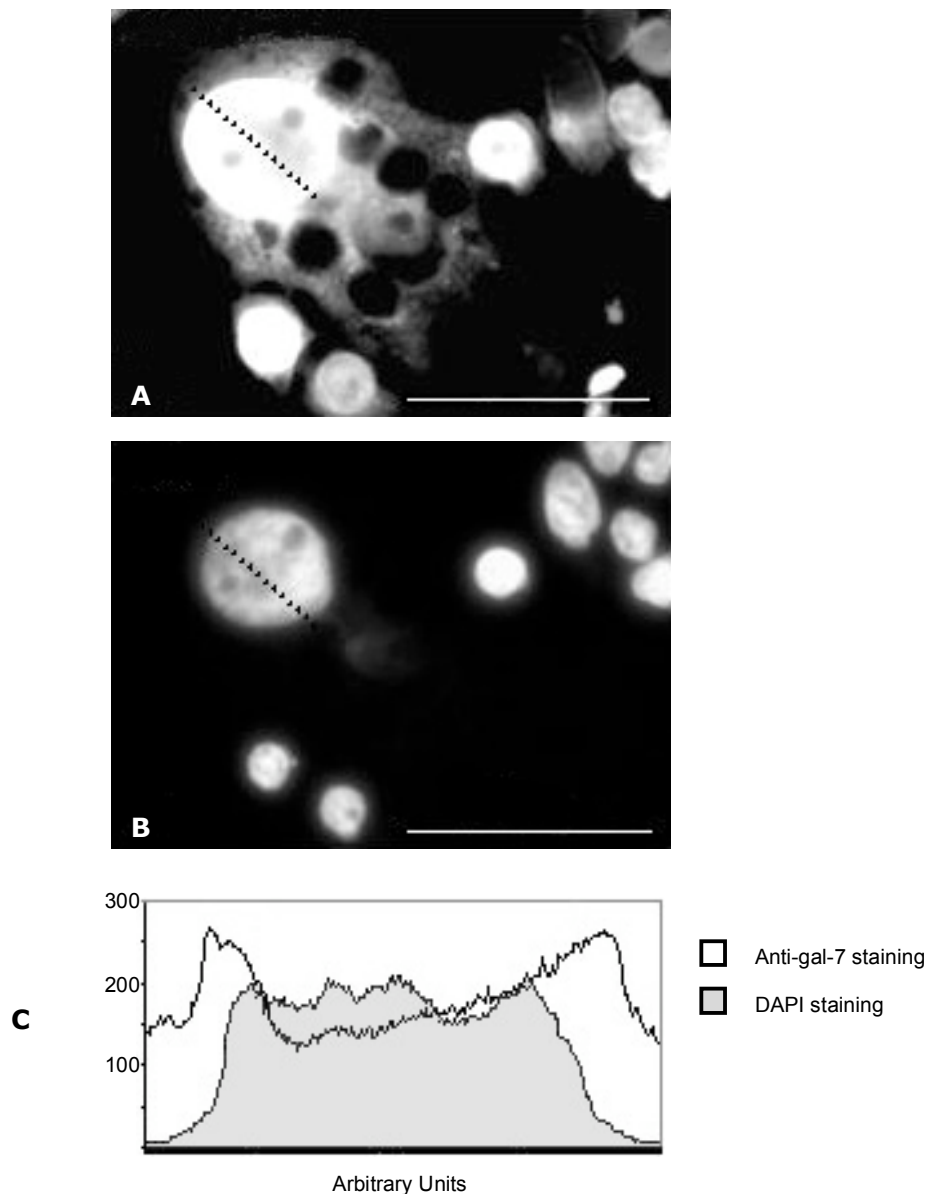


Figure 18. Typical example of a large cell positive for galectin-7 after the transfection of cDNA specific for this galectin. Interestingly, the nuclear area positive for galectin-7 (**A**) is larger than the area where DNA was stained with DAPI (**B**), which was verified by the measurements of fluorescence profiles (**C**). Bar is 50 μ m.

After processing with anti-gal-7, both cytoplasm and nucleus of the cells were positive. Following subsequent counterstaining with DAPI, there were differences regarding the diameter of the stained area around the nucleus. The anti-gal-7-reactive area was significantly larger in diameter than the DAPI reactive area. The size difference of DAPI and anti-gal-7 staining around the nucleus was also determined by measurements of the fluorescence profiles. No sign of nuclear shrinkage was seen that could otherwise explain this observation. The Ki-67 nuclear antigen is present in the S, G₁, G₂, and M phase of the cell cycle, but is absent in the G₀ phase. Immunostaining with a monoclonal antibody directed against the Ki-67 antigen therefore provides a means of rapidly estimating the proliferative active fraction of normal and neoplastic human cell populations¹¹⁹. By double-staining the cell clones in this assay with distinct antibodies directed towards Ki-67 and the respective overexpressed galectin, one could see a sign of correlation between galectin positivity and proliferation. Microphotographs of HCT-15 cells treated by this protocol are displayed in figure 19.

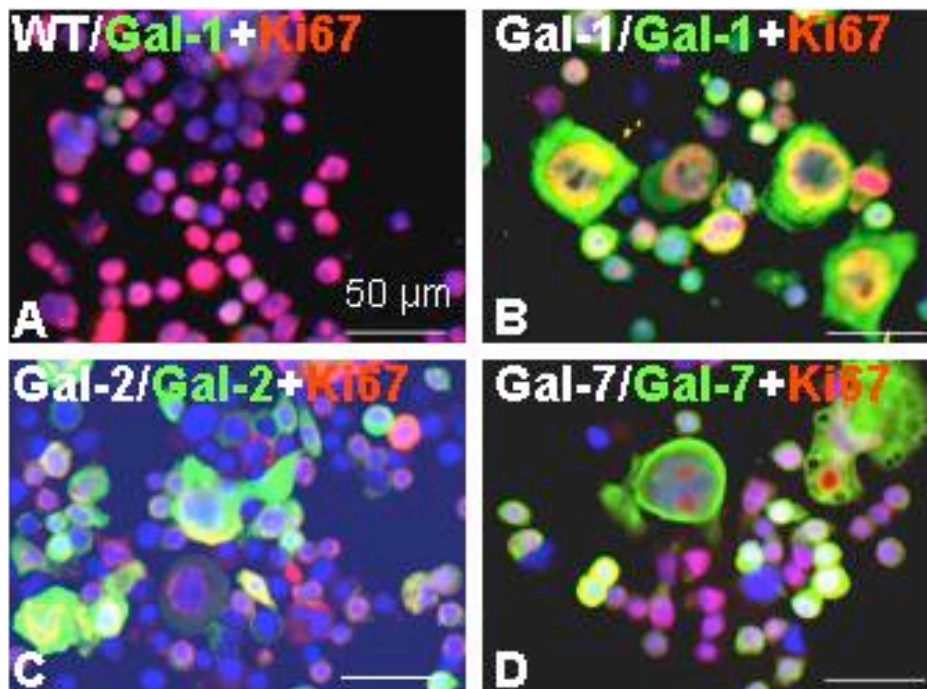


Figure 19. Comparison of expression of galectin-1 (A, B, green signal), -2 (C, green signal) and -7 (D, green signal) and proliferation marker Ki67 (A-D, red signal) in WT (A) HCT-15 cells and the same type cells transfected with gene encoding galectin-1 (B), galectin-2 (C) and galectin-7 (D). Bar is 50 µm.

The proportion of Ki-67-positive cells was higher in WT cells than in transfected cells. Small and galectin-negative cells were more frequently positive for Ki-67 than large galectin

positive cells. This is an implication of galectins-specific effects, influencing both morphology and proliferation activity. In this assay, galectin-expressing cells were larger than negative cells of the same clone. Furthermore, positive cells seemed to have a lower rate of cell cycle progression than cells in which no galectin staining occurred. In the following assay, a further aspect of the consequences of galectin overexpression was dealt with by regarding the morphology of the HCT-15 cells.

4.1.7 MORPHOLOGY

After evaluation of the transfected cell lines with RT-PCR, ECL blot processing, cytohistochemical and FACS analyses, the key question of the consequences of ectopic proto-type galectin expression was addressed.

Figure 20 documents representative images of the HCT-15 WT, mock-transfected cells and the galectin-1-, galectin-2- and galectin-7-cDNA-transfected cell clones, respectively, that showed the highest galectin content in the ECL reaction (see 4.1.3). As seen in these microphotographs, mock- and all galectin-cDNA-transfected cells had a distinctive appearance compared to the WT cells. It was not possible to spot obvious differences between the mock, galectin-2 or galectin-7 transfectants. When observing the galectin-1 transfectants, cells which had lost contact to the substratum and large cells with prominent vacuoles were seen more often than in the other cell phenotypes.

After assessing morphological parameters, the question was addressed as to whether galectin overexpression can lead to an alteration of growth characteristics. For this purpose, the culture conditions can be adjusted to focus on different facets of cell growth. Basically, culture conditions for cell growth can be divided into two main categories: anchorage-independent growth, where cells proliferate while suspended in semisolid medium, and anchorage-dependent growth, where cells grow with contact to a substratum. In the following step, anchorage-independent growth was analyzed in the methylcellulose assay.

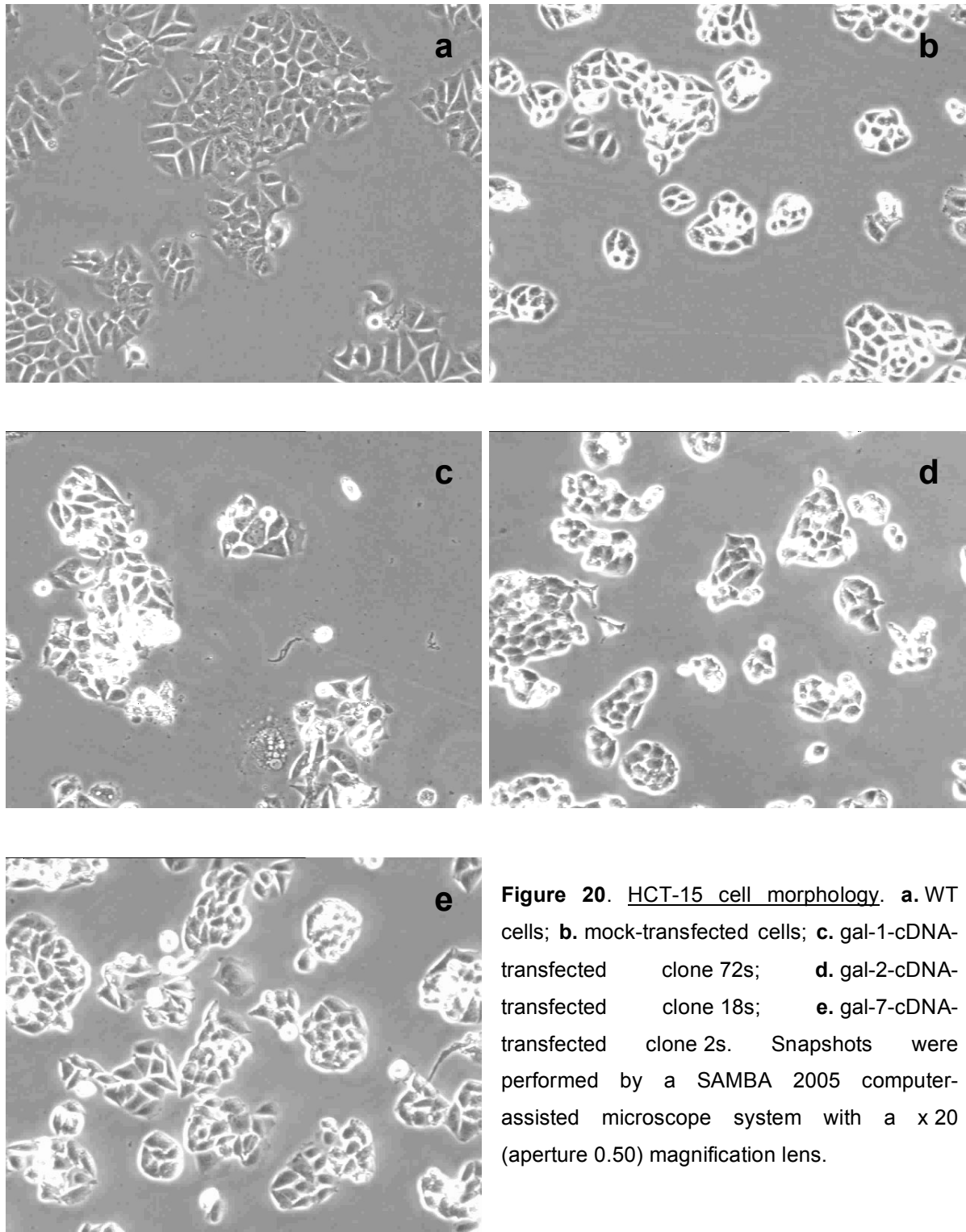


Figure 20. HCT-15 cell morphology. **a.** WT cells; **b.** mock-transfected cells; **c.** gal-1-cDNA-transfected clone 72s; **d.** gal-2-cDNA-transfected clone 18s; **e.** gal-7-cDNA-transfected clone 2s. Snapshots were performed by a SAMBA 2005 computer-assisted microscope system with a x 20 (aperture 0.50) magnification lens.

4.2 COMPARATIVE ASSAYS

4.2.1 METHYLCELLULOSE ASSAY

Anchorage-independent growth is one of the most important features correlated to tumorigenicity¹¹³. To assess growth characteristics of HCT-15 transfectants under anchorage-independent conditions, the cells were grown in semisolid medium. The gel-like state of the medium was achieved by addition of methylcellulose. After culturing the cells for 10 days, the number of colonies that had developed were determined. Figure 21 shows the obtained data as a bar diagram with the average values of three independent experiments and the standard deviations.

The behavior of the mock-transfected cells was compared to that of the WT cells, gal-1-cDNA-transfected clone 72s, gal-2-cDNA-transfected clone 18s and gal-7-cDNA-transfected clone 2s. In average, cell populations overexpressing galectins-1, -2 and -7 developed less colonies under anchorage-independent conditions than the mock-transfected control cells. The p-values resulting from the comparison between mock and galectin-1- ($p = 0.357$), galectin-2- ($p = 0.243$) and galectin-7- ($p = 0.279$) overexpressing cells showed that the differences were not significant.

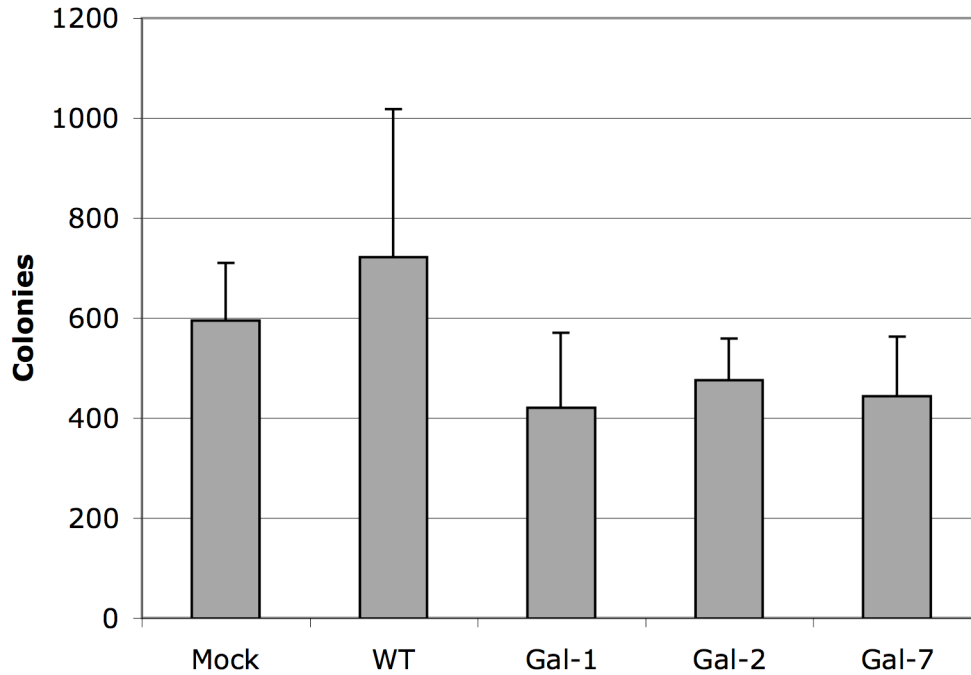


Figure 21. Colony formation assay in methylcellulose supplemented medium. Number of colonies of mock-transfected cells (**Mock**) was compared with those of WT cells (**WT**), gal-1-overexpressing clone 72s (**Gal-1**), gal-2-overexpressing clone 18s (**Gal-2**) and gal-7-overexpressing clone 2s (**Gal-7**). Values represent means \pm SD of three independent experiments.

Setting these data into relation to evidence in literature, it is noteworthy that the gene encoding galectin-7 belonged to one of only 14 out of 7202 genes, of which transcription was upregulated before the onset of p53-induced apoptosis⁹⁹. This was evaluated in studies by Polyak et al. with the colorectal cancer line DLD-1, containing an inactive endogenous p53 gene. These cells were infected with a replication-defective adenovirus encoding p53, resulting in induction of apoptosis. The property of p53 reaching highest levels of reproducibility is its ability to activate transcription of genes. The transcripts induced by p53-expression before the onset of apoptosis were examined in detail. The upregulation of transcription of the galectin-7-encoding gene was recognized by referring to it as p53-induced gene 1.

Galectin-7 was originally identified after systematic analysis of keratinocyte proteins using two-dimensional gel electrophoresis¹²⁰. The feature of it being a protein highly down-regulated in SV40-transformed keratinocytes attracted the attention of the researchers, whose aim was to spot respective markers. Of special interest here, Ueda et al. performed a study with cells of the colon carcinoma line DLD-1 stably transfected with galectin-7-cDNA¹²¹. Their aim was to examine the influence of galectin-7 overexpression on tumor growth.

Anchorage-independent growth was assessed by culturing the cells in soft agar for 21 days. Thereafter, the cells were stained and the colonies were counted. They report that a significantly lower number of colonies formed from the galectin-7 transfectants than the mock-transfected control cells. However, these results should not be extrapolated because the following influences may have a bearing on the outcome of the assay: type of cell line, experimental parameters and the extent of galectin-7 overexpression. Combining knowledge on signaling routes and corresponding galectin effects may provide clues for further experiments.

Growth under anchorage-independent conditions has been demonstrated to be under the influence of the phosphatidylinositol 3-kinase pathway^{122, 123, 124}. There is a direct connection between a galectin and this pathway. Of particular relevance for our context, Elad-Sfadia et al. have described the intriguing ability of intracellular galectin-1 to bind to and activate the oncogenic small GTPase H-Ras, which plays a pivotal role in the development of malignancy¹²⁵. This interplay was independent of the extracellular sugar binding functions of galectin-1. The obtained data point to an activating interaction, which involves insertion of the farnesyl moiety of Ras into a hydrophobic pocket of galectin-1. This explains the disruption of the bond between the constitutively active H-Ras(G12V) with galectin-1 by the farnesylcysteine mimetic farnesylthiosalicylic acid⁸⁸. This hypothesis was tested by a rationally designed galectin-1 (L11A) mutant¹²⁶. In this study, a hydrophobic pocket in galectin-1 was identified, sharing sequence and secondary structural motifs with the Cdc42 geranylgeranyl-binding cavity in RhoGDI. The mutation was set on L11 of galectin-1 because of the importance of its L77 homologue in RhoGDI in isoprenoid-binding. The galectin-1 (L11A) mutant possessed normal carbohydrate-binding capacity and homodimerization properties but selectively inhibited Ras-GTP. The interaction of galectin-1 with H-Ras has been shown to not only augment the activation of H-Ras but also to confer specificity to H-Ras by diverting its signals to Raf-1 at the expense of phosphoinositide 3-kinase.

Diverting signals away from the phosphoinositide 3-kinase pathway through galectin-1 influence could lead to inhibition of anchorage-independent growth. In the present study, the average number of colonies was lowest in galectin-1-overexpressing cells, though the p-value comparing the differences to mock-control went beyond the standard level defining significance. Further experiments are necessary to determine the influence of the phosphoinositide 3-kinase pathway in galectin-overexpressing HCT-15 cells. After closely examining anchorage-independent growth characteristics, the next step was to analyze growth under anchorage-dependent conditions.

4.2.2 DOUBLING TIME

A hallmark of cancer cells is their accelerated growth rate. To date, correlations have been identified between the influence of nuclear (Lin et al.) and exogenous (Sharma et al.) galectin-3, the early cell cycle regulator cyclin D1, and enhanced cellular proliferation^{127, 128}. Beyond galectin-3, though, very little was known of influences other members of the galectin family can have on cell cycle progression. While this work was in progress, a novel growth-regulatory mechanism of galectin-1 was described by Fischer et al.¹²⁹. Therefore, the possible effect of the overexpression of galectins-1, -2, or -7 in HCT-15 cells on the rate of cell division was analyzed in the present study. This was carried out by plating 5×10^4 cells in each well of a 24-well plate. The cell numbers that emerged from this initial seeding were determined on days 3 through 6 in 24 hour intervals. The average values of the cell counts from three independent experiments are displayed in figure 22.

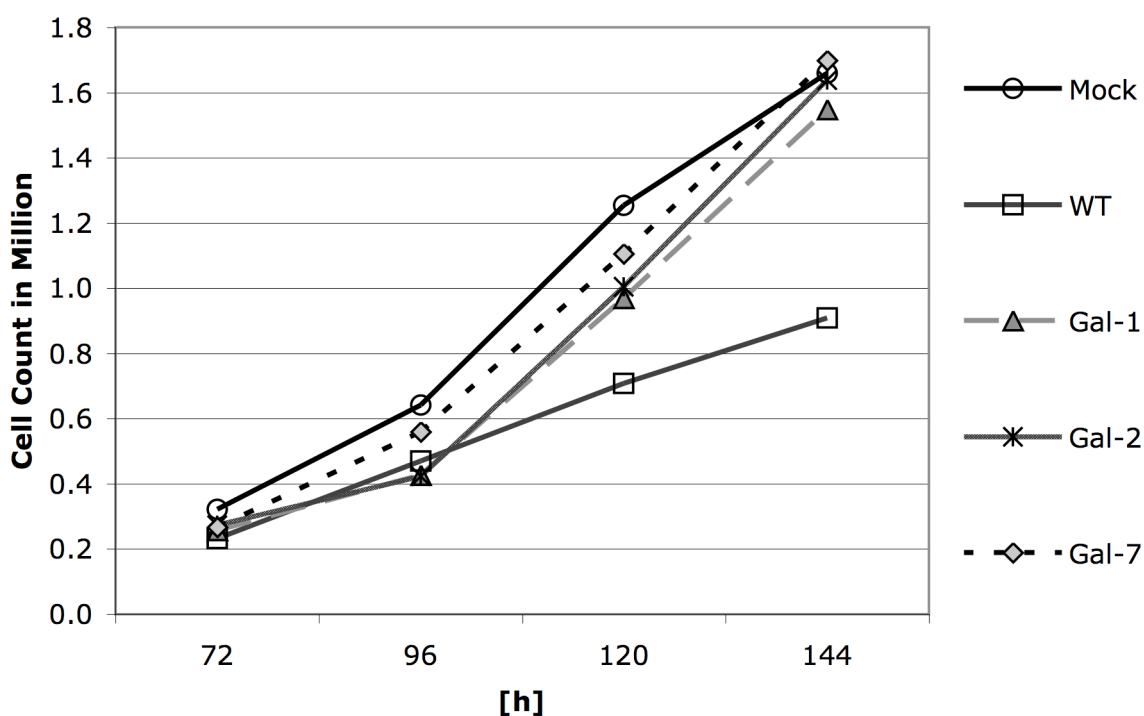


Figure 22. Evaluation of the cell number on days 3 through 6. HCT-15 cells were counted in 24 h intervals, 72 to 144 h after initial seeding. The results of WT (**WT**), mock (**Mock**), gal-1-cDNA-transfected clone-72s (**Gal-1**), gal-2-cDNA-transfected clone-18s (**Gal-2**) and gal-7-cDNA-transfected clone 2s (**Gal-7**) are displayed as mean growth curves. Data was gained in three independent experiments.

After careful evaluation of the gained data, the growth statistics were interpreted as the doubling time of the cells. The doubling time of the mock-transfected cells was compared

with that of the WT cells, and the cells overexpressing galectins-1-, -2- and -7, which is displayed in figure 23.

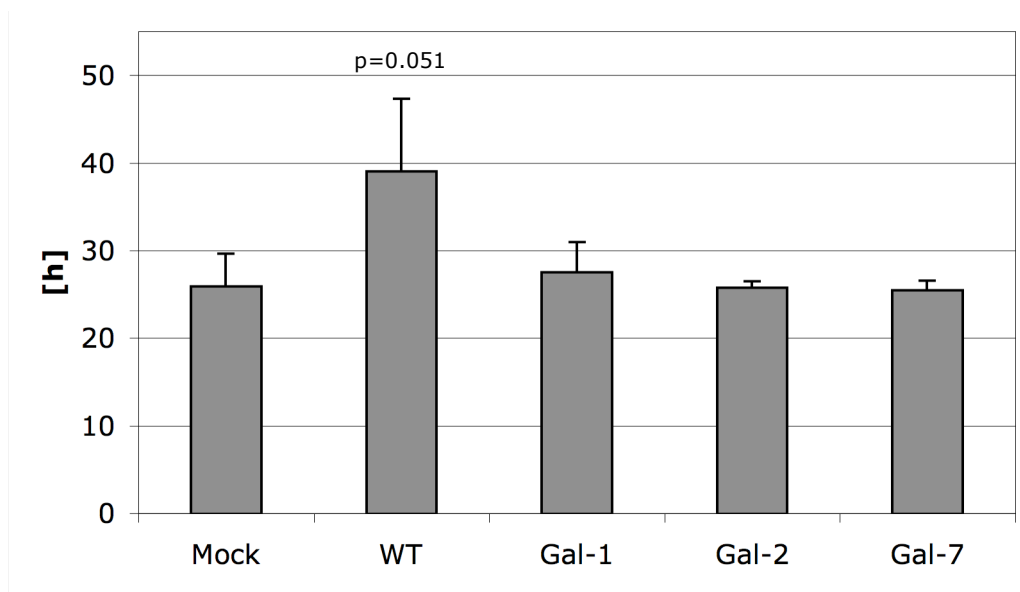


Figure 23. Doubling time. Doubling time of HCT-15 mock-transfected cells (**Mock**) was compared with that of WT cells (**WT**), gal-1-cDNA-transfected clone 72s (**Gal-1**), gal-2-cDNA-transfected clone 18s (**Gal-2**) and gal-7-cDNA-transfected clone 2s (**Gal-7**). Results represent means \pm SD of three independent experiments.

Whereas the individual values of the mean doubling time of the transfected cell clones all ranged closely around 26 hours, the WT cells showed a doubling time of 39 hours. After statistically processing the data, the p-value of the comparison of this parameter gained from the WT cells compared to the mock-transfected cells was just above the limit of being significant ($p = 0.051$). In this experimental model and under the given conditions, overexpression of galectins-1, -2 or -7 showed no impact on the doubling time of the cells compared to the mock control. There are studies described in the literature, however, that show unambiguous evidence of growth-regulatory effects caused by galectin-specific interactions.

Of note in respect to the present study, Fischer et al. addressed the question as to whether colon carcinoma and other carcinoma cells are susceptible to growth regulation by galectin-1¹²⁹. Experiments were performed on a panel of eight human epithelial cell lines including hepatoma, melanoma as well as colonic, breast, pancreas and ovarian carcinoma cell lines. Exogenous treatment of the cells with galectin-1 resulted in growth inhibition of six of the eight cell lines, as recorded by counting the number of cells that had proliferated after

4 days. The two cell lines that did not show this sensitivity were the colonic carcinoma cell lines HT-29 and Caco-2. Sugar-dependency of the growth inhibitory effect was indicative of the involvement of glycosylated regulators of cell growth, which were accessible to the galectin-1 added in the medium. Integrins as glycosylated membrane proteins, which act as salient translators of both inside-out and outside-in signaling, have these attributes¹³⁰. Therefore, the integrin expression profiles of cell lines responsive and of those resistant to the exogenous galectin-1 treatment were evaluated by flow cytometry and compared to one another. Indeed, the presence of a distinct integrin was found that correlated with galectin-1 responsiveness. This was the α_5 integrin, which associates with β_1 integrin to the $\alpha_5\beta_1$ fibronectin receptor. Further experiments with integrin ligands and neutralizing antibodies directed towards different integrins proved a specific functional relationship between the $\alpha_5\beta_1$ fibronectin receptor and the growth inhibitory effect of exogenous galectin-1. This was substantiated by stably transfecting both α_5 -deficient colon cancer cell lines with a cDNA encoding the α_5 integrin subunit. This conferred galectin-1 responsiveness, resulting in growth inhibition. The molecular mechanisms of the growth inhibitory effect were delineated in a stepwise manner in galectin-1-responsive HT-29 α_5 cells expressing α_5 integrin. Flow cytometric analysis of DNA content demonstrated that galectin-1 treated cells were retained in the G₁ phase, notably without signs of an increased rate of apoptosis. This was a consequence of the inhibition of cyclin-dependent kinase Cdk2 activity, which was shown to follow galectin-1 treatment. An explanation for Cdk inhibition was searched for by assessment of Cdk2 regulatory proteins. This monitoring revealed that the quantity of p21 and p27, which bind to and inhibit Cdk2/cyclin complexes, was higher in cells when galectin-1 was added to the medium. On the one hand, this was a result of enhanced protein stability of p27. The protein half-life was selectively prolonged in cells incubated with galectin-1. To address the next possibility of increasing protein content, transcription levels of luciferase reporter constructs with the promoter regions of p21 and p27 were determined. Transcription of the p21 and p27 reporter constructs were both upregulated by galectin-1 treatment.

To analyze transcriptional activation of p27 in detail, promoter elements that convey galectin-1 responsiveness were made out by deletion analysis of the p27 promoter. This revealed two GC-rich boxes as putative binding sites for Sp-like transcription factors. Further mutational analysis confirmed these to be accountable for galectin-1-specific upregulation of transcription. Ongoing analysis demonstrated galectin-1 to specifically and selectively stimulate the binding of Sp1 and Sp3 to the identified galectin-1 responsive element of the p27 promoter. While the cellular and nuclear content of Sp1 or Sp3 on blots was not altered

by galectin-1 treatment, the enhanced binding of Sp1 was found to be a result of posttranslational modifications, regulating its transactivating properties. Phospho-specific antibodies revealed that the relative amount of phosphothreonine was substantially reduced by galectin-1, which was then responsible for increased binding of Sp1 to the p27 promoter.

As the extracellular signal-related kinase (ERK) is a potential modulator of Sp1 phosphorylation, its activity was assessed using a phospho-specific ERK antibody in relation to galectin-1 treatment. The activity, but not the expression levels, of ERK was suppressed by galectin-1 in HT-29 α_5 cells. Importantly, this was not the case in α_5 -deficient HT-29 cells. This indicated that the modulation of ERK activity was due to interaction of galectin-1 with glycans of the $\alpha_5\beta_1$ fibronectin receptor. As expected, the activity of the immediate upstream ERK1/2 kinase MEK was inhibited, as determined by reduced binding of phospho-MEK-specific antibodies. A connection still had to be made between the interaction of galectin-1 with $\alpha_5\beta_1$ integrin and the activation of MEK. The small GTPase Ras was the potential missing link because of its role as an upstream regulator of ERK and regulation by $\alpha_5\beta_1$ integrin. The Ras-binding domain of Raf selectively precipitates GTP-bound active Ras. It can therefore be used as a tool to separate the active Ras fraction from the inactive GDP-bound fraction. By subsequent quantification of the bound Ras protein in immunoblots, the activity level can be determined. This was performed in the described study and Ras activation was indeed shown to be virtually abolished in galectin-1-treated cells. The scheme of galectin-1-mediated growth inhibition is depicted in figure 24. The indicated method of action of galectin-1 was tested at different checkpoints. As briefly mentioned above lactose, fibronectin and specific $\alpha_5\beta_1$ -blocking antibodies interfered with galectin-1/ $\alpha_5\beta_1$ interactions extracellularly and blocked the growth inhibitory effect. At the intracellular level, constitutively active Ras and MEK were no longer inhibitable by galectin-1 and the transcriptional induction of the p27 reporter gene construct was no longer observed. The specific MEK inhibitor PD 98059 on the other hand, mimicked galectin-1 effects as demonstrated by reduced threonine phosphorylation on Sp1, increased binding of Sp1 and Sp3 binding to the p27 promoter, increased cellular p27 content and G₁ cell cycle inhibition. Transfection of a dominant negative MEK variant (MEK S222A) as well as the presence of PD-98059 resulted in p27 promoter induction, similar to the effect of galectin-1.

In summary, evidence was found that galectin-1 binding to $\alpha_5\beta_1$ integrin inhibited the Ras-MEK-ERK signaling cascade, which relieved the ERK-dependent suppression of Sp1 activation and induced Sp1-dependent p27 gene transcription and protein stability. The

cyclin-dependent kinase inhibitor p27 then blocked Cdk2 activity and subsequent G₁/S cell cycle progression, which ultimately led to growth inhibition¹²⁹.

This study presents a new and exceptionally well-defined mechanism of growth inhibition induced by the specific interaction of a galectin-1 on the cell surface. This was triggered after the key interaction of galectins and integrins. In addition to their adhesive function, integrins also initiate and modulate signal transduction cascades. Both ligand occupancy and integrin clustering are critical for the activation of integrins and trigger intracellular signaling cascades¹³¹. The proto-type galectins-1, -2 and -7 with their dimeric character have the potential to modulate the ligand occupancy and clustering of integrins. Changing the point of view, the accessibility, composition and conformation of the glycan chains attached to the integrins in the molecular (glyco-)environment on the cell surface can be adjusted. These parameters have the capability of influencing galectin binding and therefore control galectin-responsiveness. And indeed this is not only hypothetical as there are data providing evidence for variant glycosylation as a regulatory mechanism for β 1 integrins¹³². Further research is certainly necessary to infer in which way galectins fit into this compelling regulatory network.

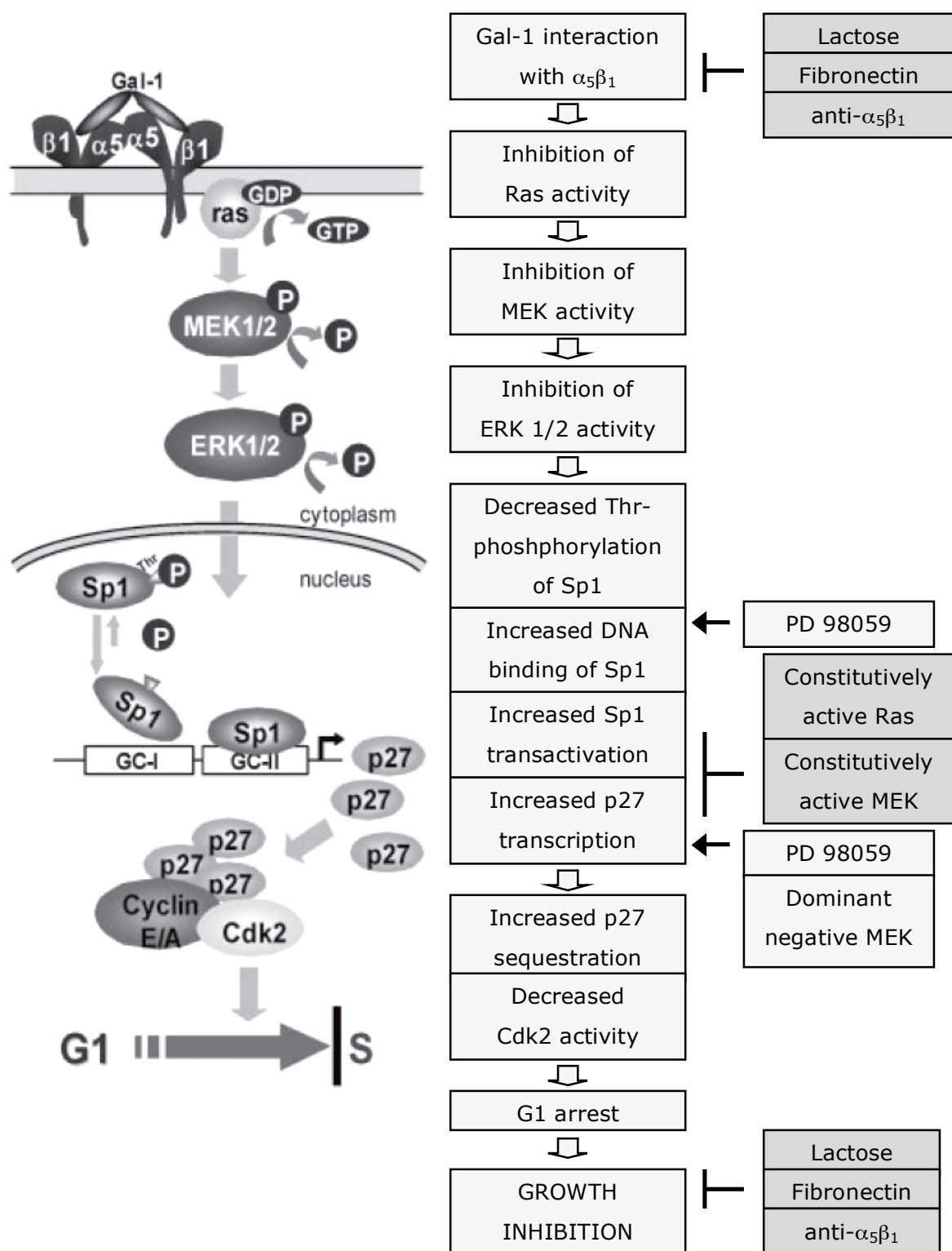


Figure 24. Scheme of galectin-1 mediated growth inhibition via transcriptional induction of the p27 gene promoter. Functional interaction of galectin-1 with fibronectin receptor $\alpha_5\beta_1$ inhibits the Ras-MEK-ERK signaling pathway resulting in reduced threonine-phosphorylation of Sp1, increased Sp1 transactivation and DNA binding and consecutive induction of p27 gene transcription. Accumulation of p27 inhibits Cdk2 activity and ultimately results in G₁ cell cycle arrest and growth inhibition. Galectin-1-mediated effects on most steps within the cascade can be either blocked (—) or mimicked (←) as indicated. For reasons of simplicity, galectin-1-induced p21 transcription is not included in the scheme. From Fischer et. al. (2005)¹²⁹.

Noteworthy for the present study and as mentioned above, Sturm et al. inferred cell lines of different origin to be responsive to the growth-inhibitory effect of galectin-1, underlining the importance of the described results⁷⁸. The two out of eight cell lines that did not react in the same manner were the colonic carcinoma cell lines included in the assay. Differences in the experimental conditions, i.e. the exogenous addition of galectin-1 to the medium as opposed to the ectopic overexpression, constitute unbridgeable gaps that prohibit extrapolations to the present study. Still, data gained in FACScan analysis (see 4.1.5) demonstrated the transport of galectin-1 to the cell surface, where functional cis- or trans- interactions with glycan chains are plausible. Therefore, comparison between the two studies is justified. It is appealing to correlate the lack of responsiveness to galectins-1, -2 or -7 of the colonic carcinoma HCT-15 cells with the absence of regulatory integrins, as described above for the cell lines HT-29 and Caco-2 that are of the same origin. Indeed, loss of either galectin-1 or $\alpha_5\beta_1$ integrin expression, which have been described during the process of malignant transformation in a variety of tissues^{133, 134}, would relieve galectin-1 restriction of cell cycle progression and thereby favor epithelial tumor cell growth. Further experiments evaluating the integrin profile of the HCT-15 cells could contribute to the understanding of sensitivity and resistance to growth-regulatory mechanisms and be of significant clinical relevance.

Having documented cell proliferation by manually counting cells, another method was chosen characterizing anchorage-dependent growth. To allow a large number of assays to be processed, a further system meeting this requirement was applied. In detail, this method will be introduced at the beginning of the next section.

4.2.3 MTT ASSAY

The MTT assay is a versatile method to analyze cell growth characteristics satisfying the requirements given above. Anchorage-dependent growth was evaluated under different experimental conditions with varying serum content of the medium. The experimental series began with measuring the response of the cells kept under the standard cell culture conditions as described in 3.3.2, regarded to be optimal for cell growth.

4.2.3.1 CELL GROWTH AFTER FOUR DAYS

Growth characteristics of HCT-15 cells were measured after seeding 2,000 cells into the wells - five for each cell clone - of a 96-well plate, which was incubated for 4 days at 37 °C. Then, the concentration of dye produced by viable cells after 4 hours of incubation with an MTT solution was photometrically measured in an ELISA minireader. The data in figure 25

represent means of six independent experiments with mock-transfected, WT cells, the galectin-1-cDNA-transfected clone 72s, the galectin-2-cDNA-transfected clone 18s and the galectin-7-cDNA-transfected clone 2s including the respective levels of standard deviation. The galectin-1-cDNA-transfected clones 17w and 35m were included in the last two experiments in order to illustrate any quantity-dependent effects of galectin-1 in the cells. The data of these two clones shown in figure 25 represent average values of two experiments \pm SD.

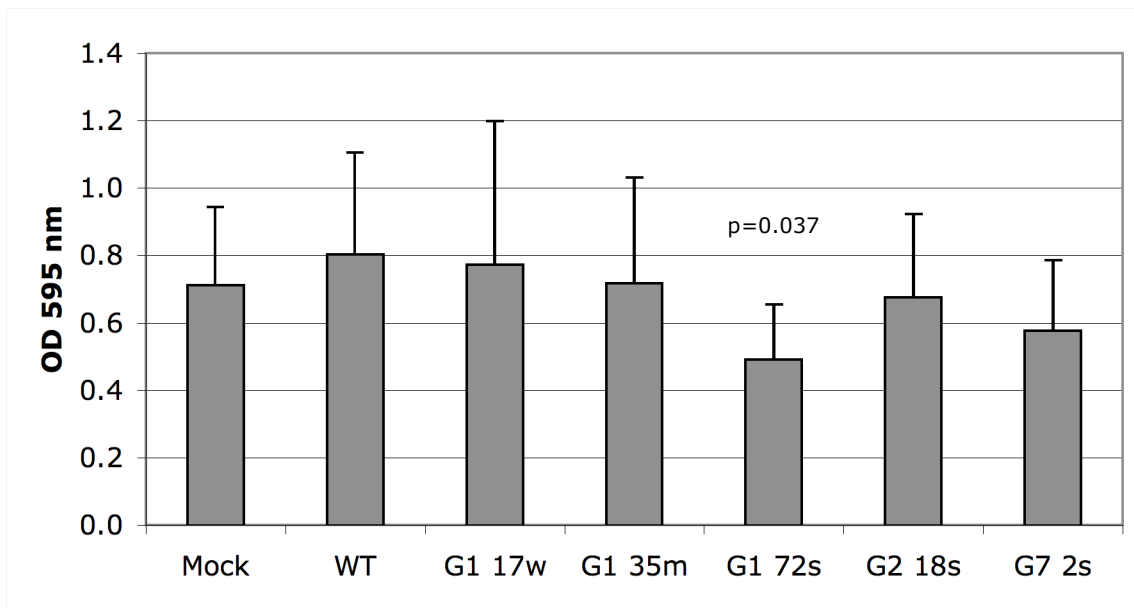


Figure 25. MTT assay 4 days after seeding. Response of HCT-15 mock-transfected cells (**Mock**) was compared with that of WT cells (**WT**), gal-1-cDNA-transfected clones 17w (**G1 17w**), 35m (**G1 35m**) and 72s (**G1 72s**), gal-2-cDNA-transfected clone 18s (**G2 18s**) and gal-7-cDNA-transfected clone 2s (**G7 2s**). The p-values ≤ 0.05 are displayed above the respective column. Numbers represent means \pm SD of six (Mock, WT, G1 72s, G2 18s, G7 2s) or two (G1 17w, G1 35m) independent experiments.

Differences were seen by comparing data of the mock-transfected clone with values obtained from the WT cells and from each of the other clones. The response of the galectin-1-overexpressing clone 72s was less than that of the mock-transfected clone in nearly every experiment. The differences were significant with a p-value of 0.037. The galectin-7-overexpressing clone 2s also had lower values than cells after mock treatment. The p-value resulting from the comparison of data from this clone with the data obtained from the mock-transfected cells was close to the level of significance ($p = 0.0559$). The reactivity of the WT

cells and the galectin-2-cDNA-transfected clone 18s was comparable to that of the mock-transfected cells. Their p-values were 0.427 and 0.715, respectively.

Overexpression of galectin-1 appeared to have an effect on the response of this assay. This will be substantiated if other galectin-1-overexpressing clones behave similarly. Therefore, clone 17w and clone 35m that had a “weak” and “medium” response in the ECL blots evaluating the galectin-1 content, respectively, were included in the assay. Neither was significantly different than the mock-transfected cells. But, as shown in figure 25, the reduction of the signal intensity relative to the mock-transfected cells corresponded directly with the protein content of the clones assayed in the ECL blots. This result is an indication for a quantity-dependent effect of galectin-1.

There are three possibilities to explain the obtained results. These are a.) retardation of cell growth, b.) cell death, or c.) a combination of both reactions. These two separate processes have already been related to galectin-dependent effects after addition of the lectin to the medium of cells in other cases. Kopitz et al. observed decreased neuroblastoma cell growth as an effect of carbohydrate-dependent cell surface binding of galectin-1⁷⁷. The increase of cell density of the cultured neuroblastoma cells (SK-N-MC) went along with an increase of the cell surface ganglioside sialidase activity. This sialidase is responsible for a shift from higher gangliosides toward GM₁ - the preferential ligand of galectin-1⁷⁶. Noteworthy for a comparison to the present study, the increase of cell surface ganglioside sialidase activity also coincided with a higher amount of galectin-1 cell surface expression. Maximum levels were reached when the growth kinetics of the cell population normally underwent the transition to density-dependent inhibition of proliferation. When galectin-1 was exogenously added to the medium and incubated with the cells for 48 hours, the cell number decreased in a concentration dependent manner. The data thus indicate that galectin-1 is an effector in the sialidase-dependent growth control in this system. Neither was the reduction of cell proliferation influenced by caspase inhibitors, nor was DNA fragmentation detected, making it unlikely that galectin-1 exerted its effects by acting as a classical proapoptotic factor on these cells. Interestingly, galectin-7 triggered identical responses in following comparative studies, in which the effects of exogenously added galectin-7 were evaluated in this experimental system¹³⁵. Again, the sugar chain of the ganglioside GM₁ was identified as a ligand for galectin-7. Similarity in ligand selection between galectins-1 and -7 should be reflected on a structural level. Indeed, Leonidas et al. analyzed the crystal structure of galectin-7 in free and carbohydrate-bound forms⁹¹. Their data showed that although the architecture of the carbohydrate recognition domain and the lengths and conformation of loop

regions differed relative to galectins-1 and -2, this factor will not markedly alter the specificity. Fittingly, Ahmad et al. showed rather similar binding data for *N*-acetylglucosamine for galectins-1 and -7 by isothermal titration calorimetry¹³⁶. Regarding the glycolipid, affinities of galectins-7 and -1 to the sugar chain of the ganglioside GM₁ were similar¹³⁵. As a consequence, binding parameters of galectin-7 to the neuroblastoma cell surface was indistinguishable from that of galectin-1. Incubating neuroblastoma cells with galectin-7 added to the medium led to inhibition of the proliferation of the cells¹³⁵. This occurred without signs of classical apoptosis such as caspase activation or DNA fragmentation.

Comparing the described results with the data presented in this work, it must be pointed out that these effects were evaluated after addition of exogenously added galectins to the medium. However, as described in the example of galectin-1 inhibiting neuroblastoma cell growth, the data are conclusive that the triggered reaction is responsible for cell density dependent growth arrest. This involves the interaction of galectin-1 and the sugar chain of ganglioside GM₁ (for details of interaction, please see¹³⁷). Notably, the cell surface presentation of both binding partners is upregulated during differentiation. As shown in FACSscan analysis in the present study, overexpression of galectin-1 and galectin-7 resulted in cell surface presentation of the respective galectins. It is therefore interesting to compare the data from the present study evaluating cell growth after 4 days to the results of the experiments by Kopitz et al. evaluating the growth inhibition properties of galectins-1 and -7. Nonetheless, the differences in the experimental conditions using a.) ectopic overexpression, b.) exogenous addition of galectins to the medium and c.) different cell lines constitute substantial variations. Therefore, any extrapolations between the systems are not *a priori* valid.

As mentioned above, the observed results of the MTT assay after 4 days can also be explained by an increased rate of cell death or a combination of cell death and growth retardation. Of particular interest in this respect, Sturm et al. describe comparative assays of the effects of exogenous galectins-1, -2 and -7 on activated T cells⁷⁸. Strikingly, definition of the binding partners of the respective galectins revealed distinct behavior. Despite the abundance of β -galactosides on the cell surface, galectins-1 and -2 not only targeted specific epitopes, but the two lectins actually did this in a qualitatively distinct manner. In contrast to galectin-1, the glycoproteins CD3 and CD7 were not ligands of galectin-2 on blots, while both lectins shared affinity to β_1 integrin (CD29). This differential selection of binding partners is all the more noteworthy, regarding the very similar amino acid sequences of these closely related galectins, especially around the carbohydrate recognition domain with its central tryptophan residue and conservation of the set of essential residues^{67,90}. Apparently, β -galactoside

derivatives with substitutions at the core lactose influence galectin selection of endogenous binding partners. This question was handled with by Ahmad et al. as already referred to above. In detail, they performed thermodynamic binding studies of cell surface carbohydrate epitopes to galectins-1, -3, and -7¹³⁶. Results showed that naturally occurring oligosaccharides can differ to a certain extent in ligand capacity for human galectins, as evaluated by isothermal titration calorimetry. Siebert et al. approached this question from a different angle, using a combined nuclear magnetic resonance-spectroscopical and computational study¹³⁷. Their aim was to illuminate the sites for binding of galectin-1 to a complex ligand by structural analysis of the two binding partners. They discovered that the pentasaccharide of ganglioside GM₁ makes contacts to the binding pocket of galectin-1 beyond the primary site accommodating the galactose moiety. This extended binding site is a probable explanation for the restricted binding of galectin-1 to a limited and specific set of interaction partners. As mentioned above, galectins-1 and -2 homed in on a specific and distinct set of targets on the cell surface of activated T cells. The result of this carbohydrate-dependent interaction of galectin-2 was the induction of apoptosis⁷⁸. This involved activity of caspases-3 and -9 as determined by fluorogenic substrate and inhibitor assays. Surveying key checkpoints of the apoptotic pathway revealed cleavage of the DNA fragmentation factor, enhanced cytochrome c release, disruption of the mitochondrial membrane potential and an increase of the Bax/Bcl-2 ratio by opposite regulation of expression of both proteins. The investigations proved that cell death was triggered by the intrinsic apoptotic pathway. Monitoring of cell cycle phases by measurement of the DNA content revealed no differences induced by the interaction of galectin-2. Protein expression of key cell cycle regulators was measured by Western blotting and also showed no alteration prompted by exogenous galectin-2. Comparative evaluation of the effects of galectins-1 and -7 binding to the cell surface of activated T cells revealed remarkable deviations from the reactions caused by galectin-2. Both galectins-1 and -7 had proapoptotic effects, but this involved distinct profiles of caspase activation. Galectin-1 induced the caspases-3, -8 and -9, while galectin-7 binding resulted in the activation of caspases-1, -3 and -8. In other words, while apoptosis induced by galectins-1 and -7 involved caspase-8, this was clearly not the case after the interaction of galectin-2 with the T cell surface ligands. An additional significant difference in the reactions caused by the three proto-type galectins was revealed by analyzing cell cycle parameters. Flow cytometric analysis of the expression of cyclin B₁ was performed because of its important role as an effector of cell cycle progression. Increasing concentrations of exogenous galectin-2 had no effect of this parameter in activated T cells. Galectins-1 and -7, however,

evoked a concentration dependent decrease of cyclin B₁ expression, inhibiting cell cycle phase progression. Summing up the results of this part of the study, this is an intriguing example of differential binding patterns and distinct responses of proto-type galectins in the same experimental system. As mentioned above, a decrease of the response of the MTT assay after 4 days of cell growth in the present study can be a result of growth retardation, increased cell death or a combination of both processes. Interestingly, the reactions after cell surface binding of proto-type galectins as described by Sturm et al.⁷⁸ include examples of the induction of apoptosis by itself and also in combination with the inhibition of cell cycle progression. In the model colon cancer cells, further experiments with the HCT-15 transfectants are necessary to assess cell cycle and apoptosis parameters in order to explain the molecular mechanisms of the measured effects. After assessment of growth behavior under optimal growth conditions, the question was addressed as to whether the reduction of supplied nutrients served as challenge to evoke galectin-specific reactions.

4.2.3.2 RESISTANCE TO FCS DEPRIVATION

The MTT assay was modified to observe how the cells reacted to different growth conditions, specifically to see their susceptibility to suboptimal parameters. Two thousand cells were seeded into each of the wells of a 96-well plate and cultivated over a period of 10 days in medium that contained 10 %, 3 %, 2 % or 1 % FCS (v/v). The amount of viable cells was assessed on day 1, 3, 6, 8 and 10. The medium was not exchanged until the day of measurement, when the cells were incubated with the MTT solution for 2 hours at 37 °C. The HCT-15 WT, mock-transfected cells, galectin-1-cDNA-transfected clones 17w and 72s, galectin-2-cDNA-transfected clone 18s and the galectin-7-cDNA-transfected clone 2s were included in the assay. Three independent experiments were performed in the assays with 1 %, 2 %, and 3 % FCS (v/v) in the medium. Four independent experiments were performed with 10 % FCS (v/v) in the medium. The mean values of the experiments are illustrated as median growth curves in figures 26 to 29.

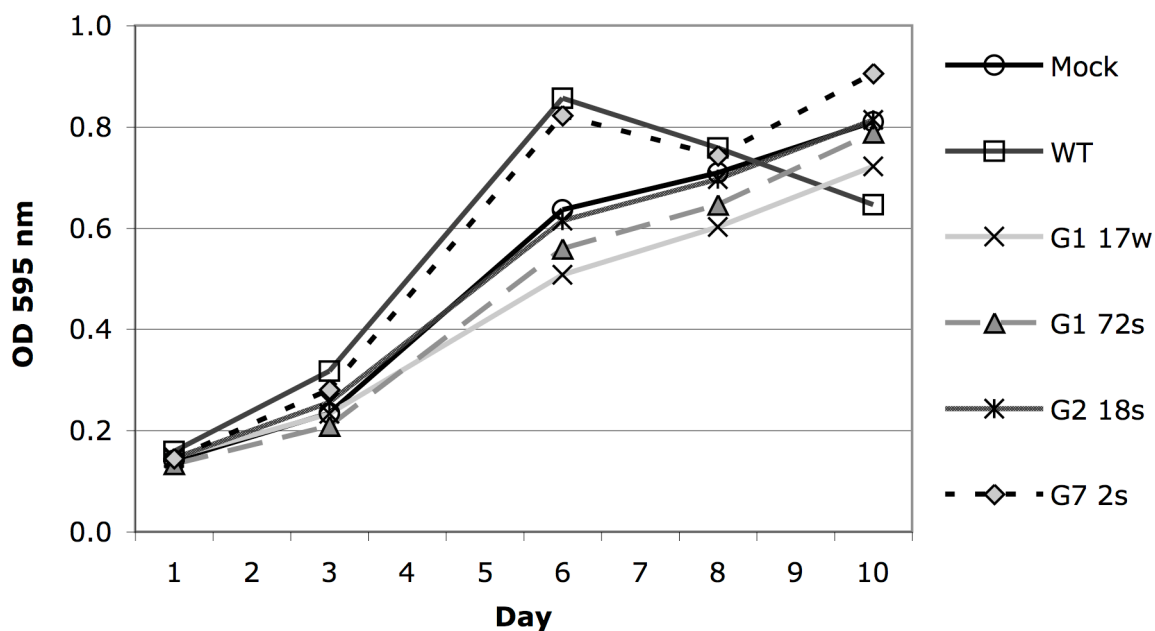


Figure 26. Growth curves of HCT-15 cells grown in medium with 10 % FCS (v/v). MTT assay of mock-transfected (**Mock**), WT (**WT**) cells, galectin-1-cDNA-transfected clone 17w (**G1 17w**) and clone 72s (**G1 72s**), galectin-2-cDNA-transfected clone 18s (**G2 18s**) and galectin-7-cDNA-transfected clone 2s (**G7 2s**). Data represents means of four independent experiments.

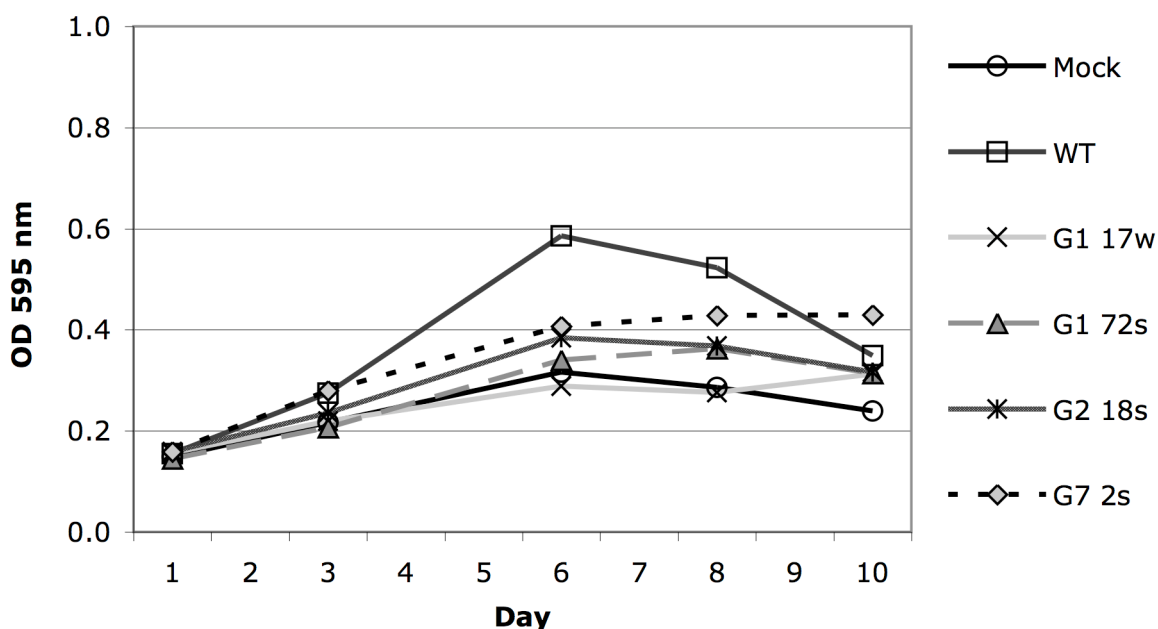


Figure 27. Growth curves of HCT-15 cells grown in medium with 3 % FCS (v/v). MTT assay of mock-transfected (**Mock**), WT (**WT**) cells, galectin-1-cDNA-transfected clone 17w (**G1 17w**) and clone 72s (**G1 72s**), galectin-2-cDNA-transfected clone 18s (**G2 18s**) and galectin-7-cDNA-transfected clone 2s (**G7 2s**). Data represents means of three independent experiments.

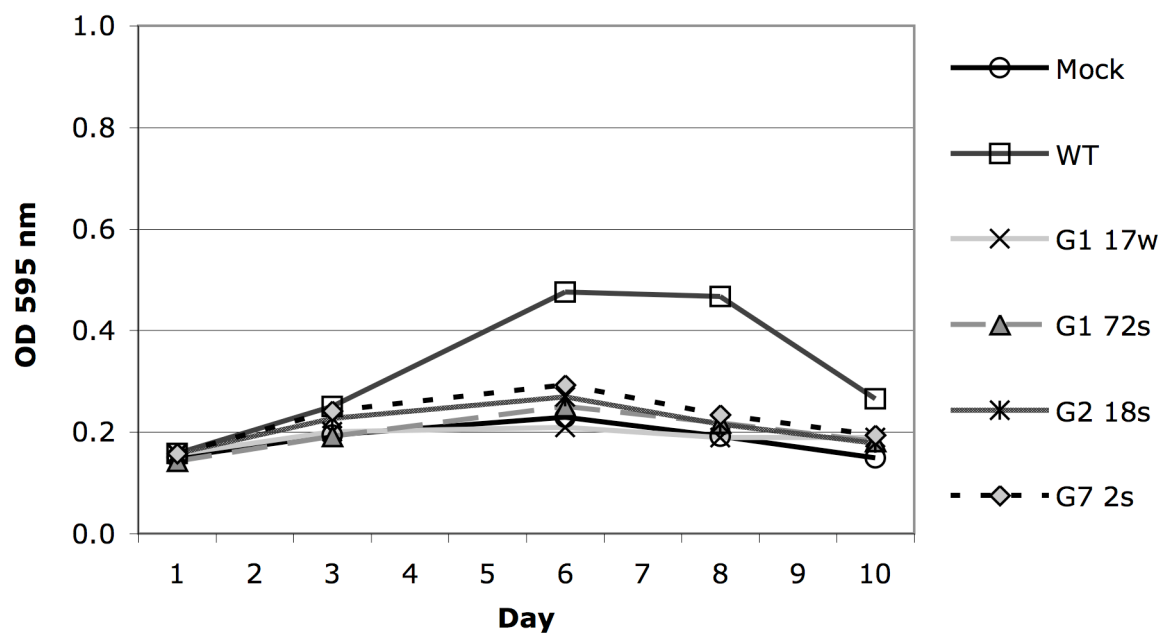


Figure 28. Growth curves of HCT-15 cells grown in medium with 2 % FCS (v/v). MTT assay of mock-transfected (**Mock**), WT (**WT**) cells, galectin-1-cDNA-transfected clone 17w (**G1 17w**) and clone 72s (**G1 72s**), galectin-2-cDNA-transfected clone 18s (**G2 18s**) and galectin-7-cDNA-transfected clone 2s (**G7 2s**). Data represents means of three independent experiments.

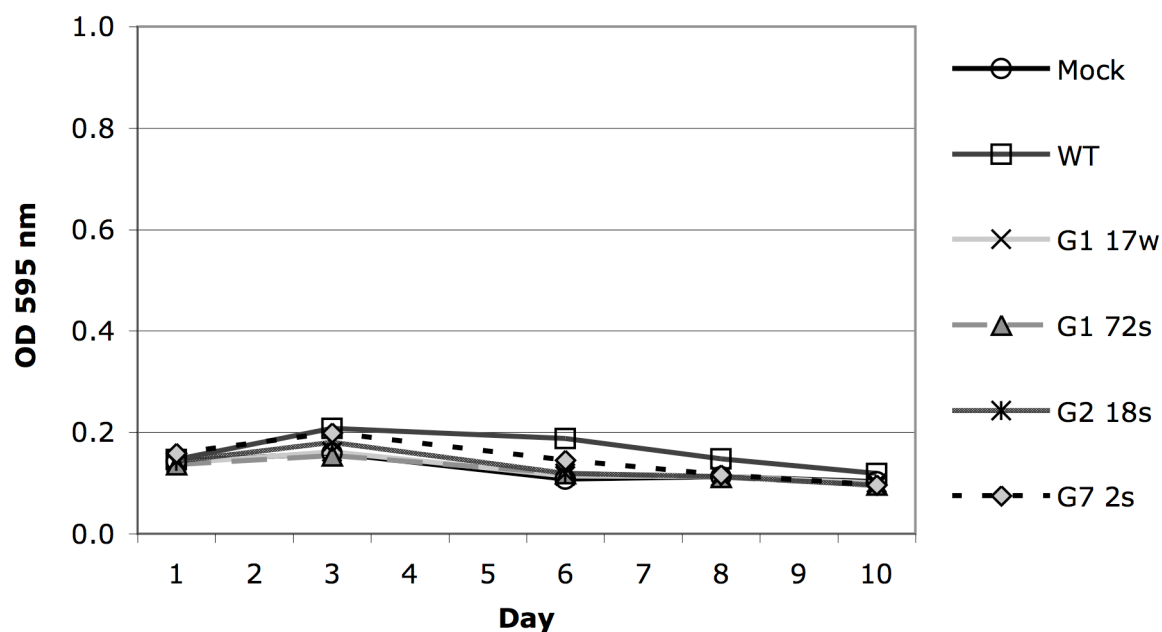


Figure 29. Growth curves of HCT-15 cells grown in medium with 1 % FCS (v/v). MTT assay of mock-transfected (**Mock**), WT (**WT**) cells, galectin-1-cDNA-transfected clone 17w (**G1 17w**) and clone 72s (**G1 72s**), galectin-2-cDNA-transfected clone 18s (**G2 18s**) and galectin-7-cDNA-transfected clone 2s (**G7 2s**). Data represents means of three independent experiments.

A general tendency of the WT cells in all four FCS concentrations was that they apparently grew faster than the transfected cells during the first days of the assay. The median growth curves peaked at the time around day 6, after which the number of viable cells decreased during the further duration of the assay. Comparing the median growth curves of the transfected cells, the galectin-7-overexpressing cells had the highest amount of viable cells of all transfectants in nearly every day of analysis. In contrast, the galectin-1-cDNA-transfected clone 17s often had the lowest response in the MTT assay.

The influence of FCS content was tested and proved to have a strong influence on cell growth and viability. In 10 % FCS (v/v), the response of the WT cells was considerably stronger than the mock-, galectin-1-cDNA- and galectin-2-cDNA-transfected cells during the first 6 days of the assay. The largest contrast to these cells was on day 6 of evaluation, after which the number of viable WT cells continuously decreased until the response was lowest of all evaluated cells on day 10. The galectin-7-overexpressing clone 2 initially reacted very similar to the WT cells and produced a stronger response than all other transfectants, but unlike the WT cells, the response remained highest among the transfectants until finishing the assay.

The curve representing data on viability of WT cells in 3 % FCS (v/v) clearly separated itself from the others by ascending at a higher angle. This continued until after day 6, when the response lessened and the curve converged towards those of the transfectants. The amount of viable cells was highest for galectin-7-overexpressing cells among all transfectants, although the absolute difference was not as substantial as in the assay with 10 % FCS (v/v). When the FCS concentration was lowered even further to 2 % and 1 % FCS (v/v) there was no considerable increase in viable transfected cells throughout the period of evaluation. The reaction of the WT cells in the MTT assay, however, did rise in 2 % FCS (v/v) during the first 8 days of the assay. In 1 % FCS (v/v), the response of WT cells was similarly low as the other cells assayed.

The values registered by examining the properties of cells grown in 10 % FCS are displayed as bar charts in figure 30 and represent the average means of four independent experiments \pm SD. The response of mock-transfected cells was compared with that of other cells analyzed under identical conditions. The calculated p-value is written above the respective bar when $p \leq 0.05$. On day 6 and day 10, the p-values of the data from the galectin-7-overexpressing clone 2 compared with that of the mock transfectant were low, but exceeded the limit of defining the differences as significant. They were $p = 0.069$ and $p = 0.068$, on day 6 and 10 respectively.

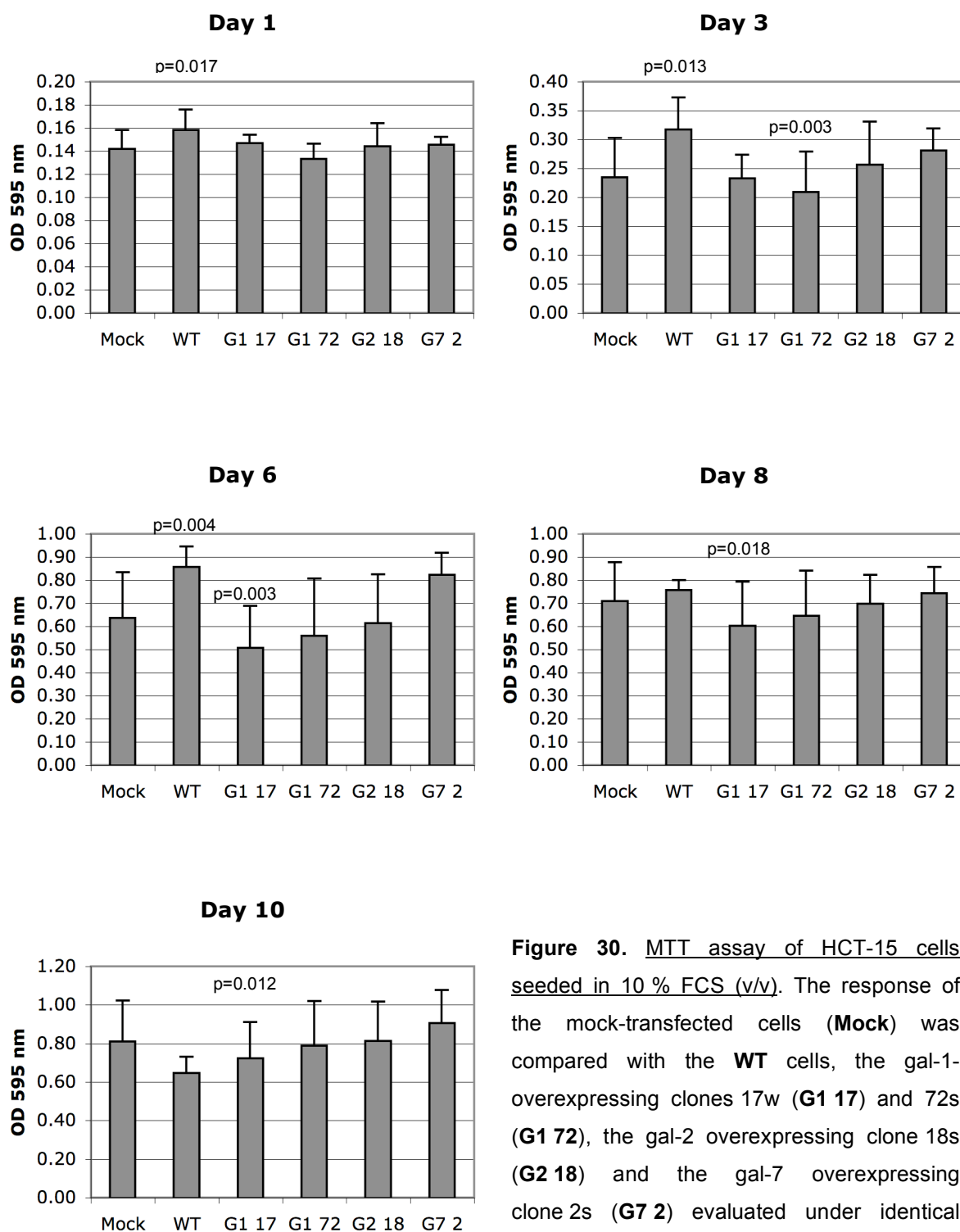


Figure 30. MTT assay of HCT-15 cells seeded in 10 % FCS (v/v). The response of the mock-transfected cells (**Mock**) was compared with the **WT** cells, the gal-1-overexpressing clones 17w (**G1 17**) and 72s (**G1 72**), the gal-2 overexpressing clone 18s (**G2 18**) and the gal-7 overexpressing clone 2s (**G7 2**) evaluated under identical conditions. The calculated p-value is written above the respective bar when $p \leq 0.05$.

Statistical analyses of the data gained from seeding the cells in medium with 3 % FCS (v/v) revealed significant differences of WT cells and the galectin-7-overexpressing cells when compared to the values of mock-transfected cells. These were seen on day 8 and day 10. The results of these assays is displayed in figure 31 representing the average means \pm SD of three independent experiments. The calculated p-value is given above the respective bar when $p \leq 0.05$.

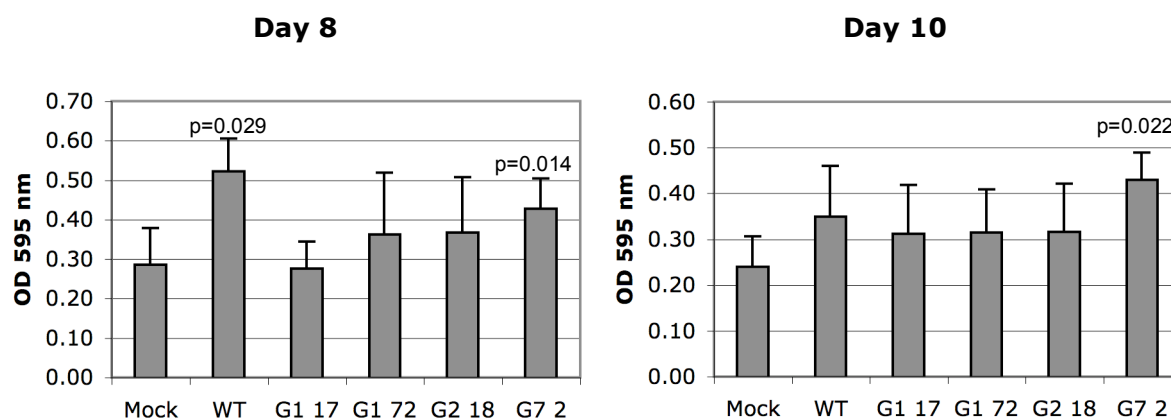


Figure 31. MTT assay of HCT-15 cells seeded in 3 % FCS (v/v). The response of the mock-transfected cells (**Mock**) was compared with the **WT** cells, the gal-1-overexpressing clones 17w (**G1 17**) and 72s (**G1 72**), the gal-2 overexpressing clone 18s (**G2 18**) and the gal-7 overexpressing clone 2s (**G7 2**) evaluated under identical conditions. The calculated p-value is written above the respective bar when $p \leq 0.05$.

On day 3 of the assay with 1 % FCS (v/v), the galectin-2-overexpressing cells behaved significantly different to the mock-transfected cells. The calculated p-value of this comparison was 0.001. The average mean values \pm SD are illustrated in figure 32.

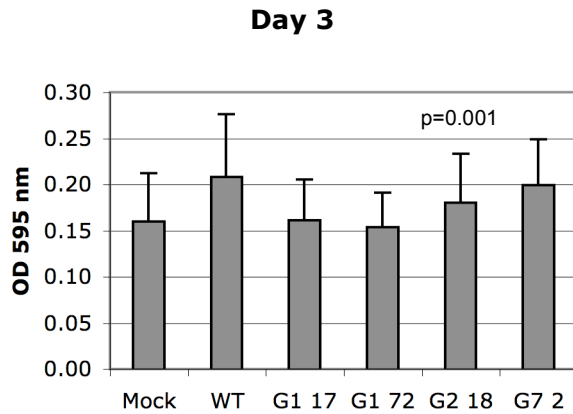


Figure 32. MTT assay of HCT-15 cells seeded in 1 % FCS (v/v). The response of the mock-transfected cells (**Mock**) was compared with the **WT** cells, the gal-1-overexpressing clones 17w (**G1 17**) and 72s (**G1 72**), the gal-2 overexpressing clone 18s (**G2 18**) and the gal-7 overexpressing clone 2s (**G7 2**) evaluated under identical conditions. The calculated p-value is written above the respective bar when $p \leq 0.05$.

The primary model object of research was the HCT-15 colon carcinoma cell line. One question to be addressed was whether effects seen in this system were unique or could be valid for other colon carcinoma cell lines as well. One step in answering this question was made by using the DLD-1 cell line and previously established clones overexpressing galectin-1 and galectin-7, which had been transfected in the same manner as the HCT-15 cells. Cells of the DLD-1 cell line were assayed under identical conditions as the HCT-15 cells. Specifically, these were DLD-1 WT, mock-transfected cells, the galectin-1-cDNA-transfected clone 15 and the galectin-7-cDNA-transfected clone 20. The mean values of three individual experiments is illustrated as median growth curves in figures 33 to 36.

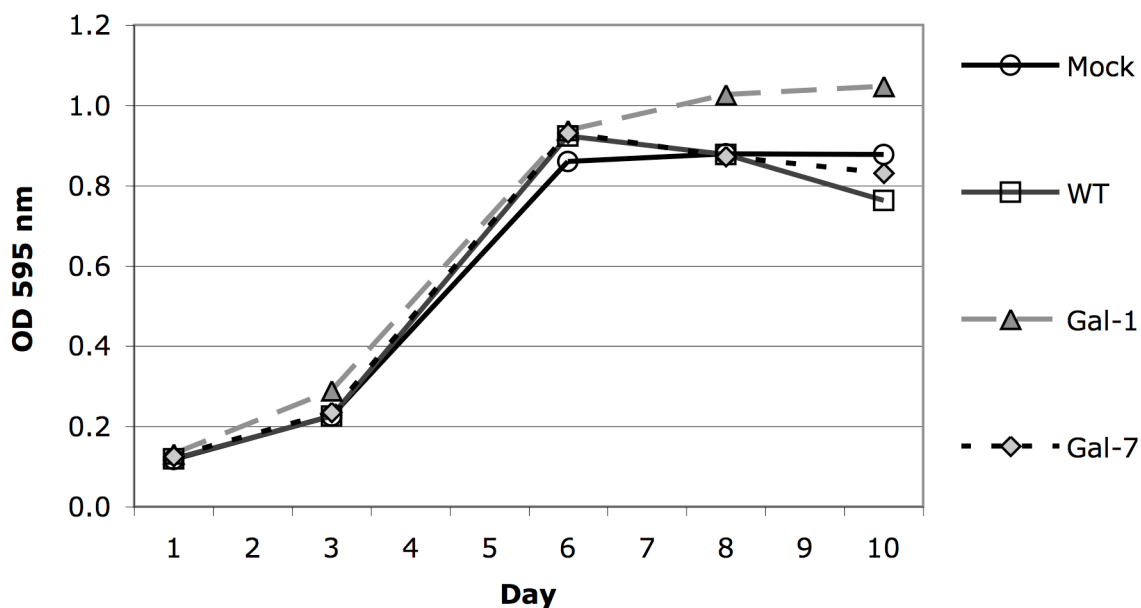


Figure 33. Growth curves of DLD-1 cells grown in medium with 10 % FCS (v/v). MTT assay of mock-transfected (**Mock**), WT (**WT**) cells, galectin-1-cDNA-transfected clone 15 (**Gal-1**) and galectin-7-cDNA-transfected clone 20 (**Gal-7**). Data represent means of three independent experiments.

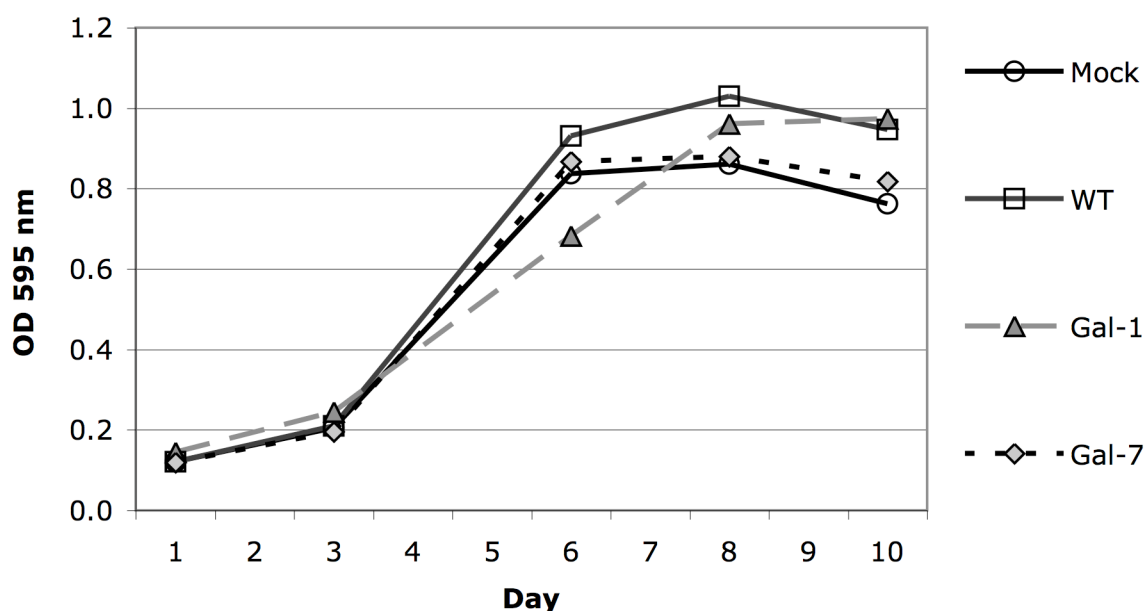


Figure 34. Growth curves of DLD-1 cells grown in medium with 3 % FCS (v/v). MTT assay of mock-transfected (**Mock**), WT (**WT**) cells, galectin-1-cDNA-transfected clone 15 (**Gal-1**) and galectin-7-cDNA-transfected clone 20 (**Gal-7**). Data represent means of three independent experiments.

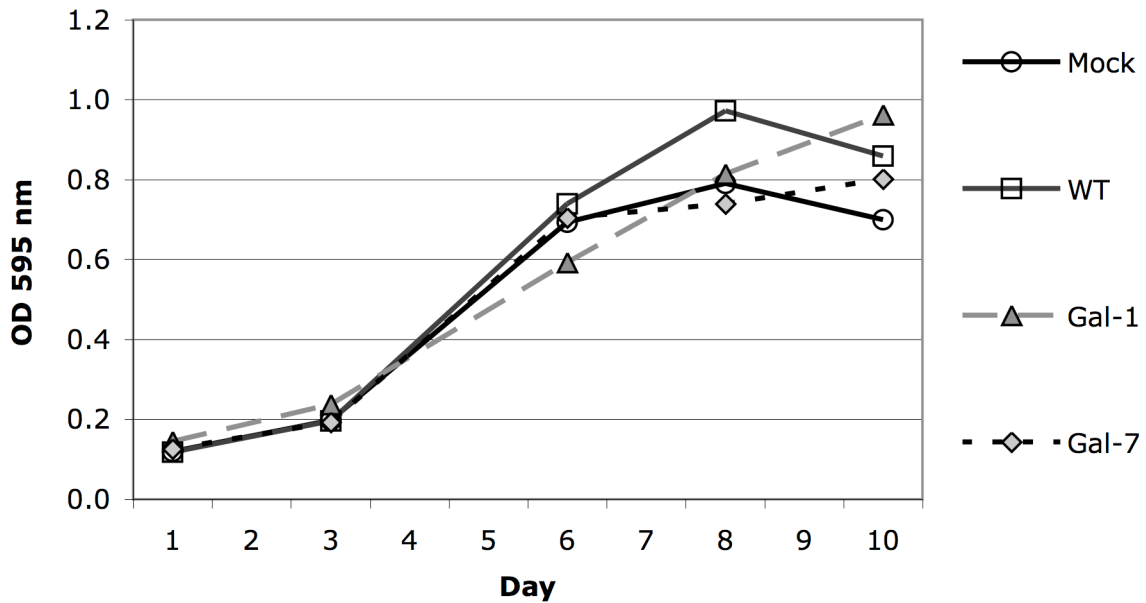


Figure 35. Growth curves of DLD-1 cells grown in medium with 2 % FCS (v/v). MTT assay of mock-transfected (**Mock**), WT (**WT**) cells, galectin-1-cDNA-transfected clone 15 (**Gal-1**) and galectin-7-cDNA-transfected clone 20 (**Gal-7**). Data represent means of three independent experiments.

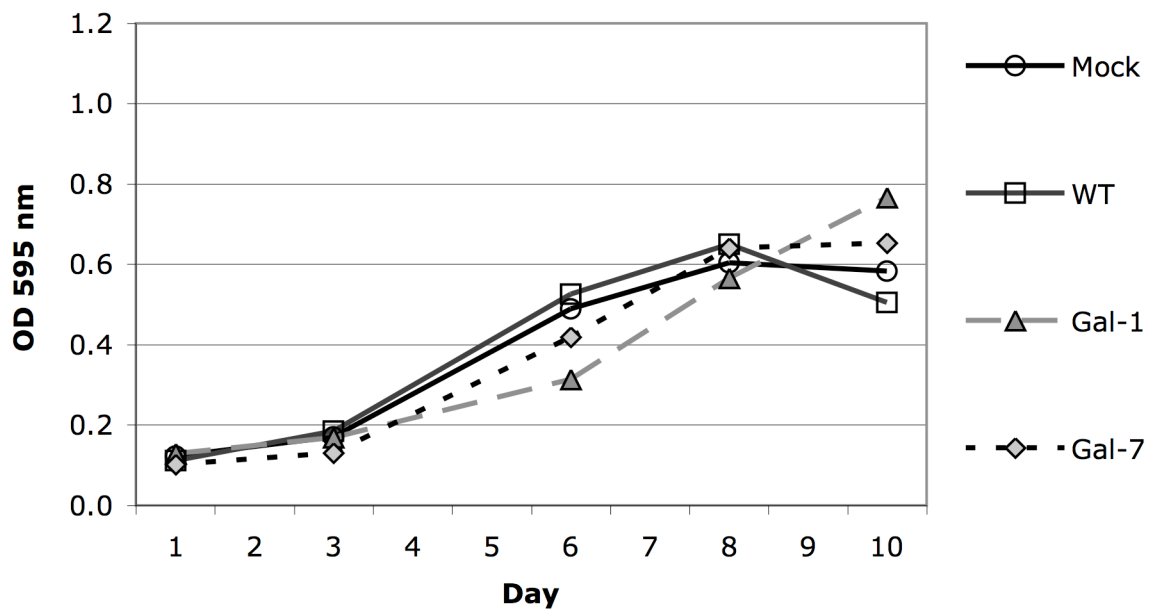


Figure 36. Growth curves of DLD-1 cells grown in medium with 1 % FCS (v/v). MTT assay of mock-transfected (**Mock**), WT (**WT**) cells, galectin-1-cDNA-transfected clone 15 (**Gal-1**) and galectin-7-cDNA-transfected clone 20 (**Gal-7**). Data represent means of three independent experiments.

The analyzed DLD-1 cells were much less sensitive to the reduction of FCS compared with the HCT-15 cells. The overall magnitude of the responses were similar even between the assays in 10 % and in 3 % FCS (v/v). Cell growth only gradually lessened in 2 % and 1 % FCS (v/v).

There were noteworthy overall tendencies seen in these growth curves that were valid for the data gained from the four different FCS concentrations. The median values of the WT cells were often in a slightly higher range of optical density than the other growth curves during the first 6 to 8 days of analysis. The curves then slanted downward until they reached or went below the values of the other cells. The behavior of the galectin-1-overexpressing cells was almost completely the opposite. In the assays with 1 %, 2 % and 3 % FCS (v/v), the amount of viable cells of galectin-1-cDNA-transfected clone 15 did not increase as quickly as the other cells, resulting in the lowest amount of viable cells among all that were examined on day 6. However, this cell clone had the highest OD values in the MTT assay at the end of assay, regardless of the added amount of FCS in the medium.

There were no large differences between the curves monitoring the cell viability of mock- and galectin-7-cDNA transfected cells in all of the assays. In general, they reached their highest values on day 6 and maintained these levels on the following days.

Next, behavior specific to each FCS concentration was analyzed. In the assay in which the cells were seeded in 10 % FCS (v/v), the responses of the analyzed cells were all very similar until day 6. The curve of the galectin-1-overexpressing cells then separated itself from the rest and continued to rise while the others remained the same or decreased.

In medium supplemented with 3 % FCS (v/v), the number of galectin-1-overexpressing cells increased at a slower rate than the other cells, but ended with the highest response on day 10. As was mentioned above, this behavior was also seen in 2 % and 1 % FCS (v/v). The curves of mock- and galectin-7-cDNA-transfected cells were almost identical in 3 % FCS (v/v). They increased until day 6, nearly remained at the same level on day 8 and then slightly descended until day 10 - the mock-transfected cells ending just below the galectin-7-overexpressing cells. The MTT response of the WT cells rose to an amount that was highest of the four cell types on day 6 and day 8, but then decreased to a level that was just below that of the galectin-1 overexpressing cells. This behavior of the WT cells was also seen in the assay in which the cells were seeded in 2 % FCS (v/v).

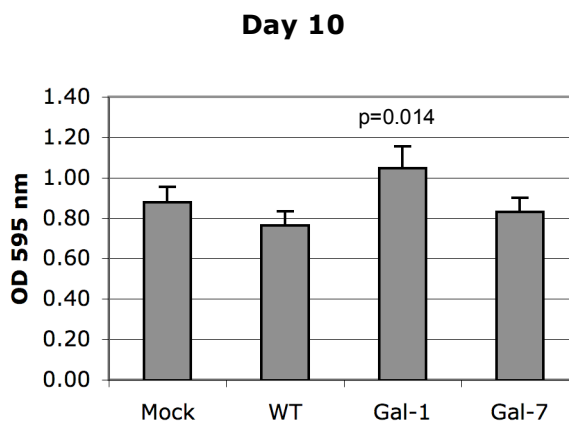
In the assays, in which the FCS content of the medium was reduced to 2 % FCS (v/v), the curves of the mock- and galectin-7-cDNA-transfected cells were indistinguishable until day 6. The galectin-7-overexpressing cells then had a slightly lower response on day 8, but this

continued to rise on day 10, whereas the mock-transfected cells produced a response that was lowest of all other cell types analyzed.

When the FCS content was decreased to 1 % (v/v) in the medium, it caused an evident reduction of the response. The illustrated curves ascended at a lower angle than in the previously described experiments. The signal of mock, WT and galectin-7-overexpressing cells rose until day 8. The response of mock- and galectin-7-cDNA-transfected cells on day 10 was almost identical to the values that had been evaluated from the respective cells on day 8. The signal of the WT cells, which to this point had been responsible for the highest values under these conditions, then produced a response that was markedly less than on day 8, lower than that of the other cells on that day of evaluation in the assay. As mentioned above, the response of the galectin-1-cDNA-transfected clone increased at a slower rate compared to the other cells, but ultimately surpassed that of all the other cells in the assay.

Statistical analyses showed most significant differences of the cells compared to the mock-transfected cells to appear on the last day of evaluation. On day 10 of the assay with 10 % FCS (v/v), the galectin-1-overexpressing cell clone had a significantly higher response than the mock-transfected cells, as illustrated in figure 37.

Figure 37. MTT assay of DLD-1 cells seeded in 10 % FCS (v/v). The response of the mock-transfected cells was compared with the other cells evaluated under identical conditions. The calculated p-value is written above the respective bar when $p \leq 0.05$.



In 3 % FCS (v/v), significant differences were seen on day 8 and day 10 in the WT and galectin-1-overexpressing cells. This is demonstrated in figure 38.

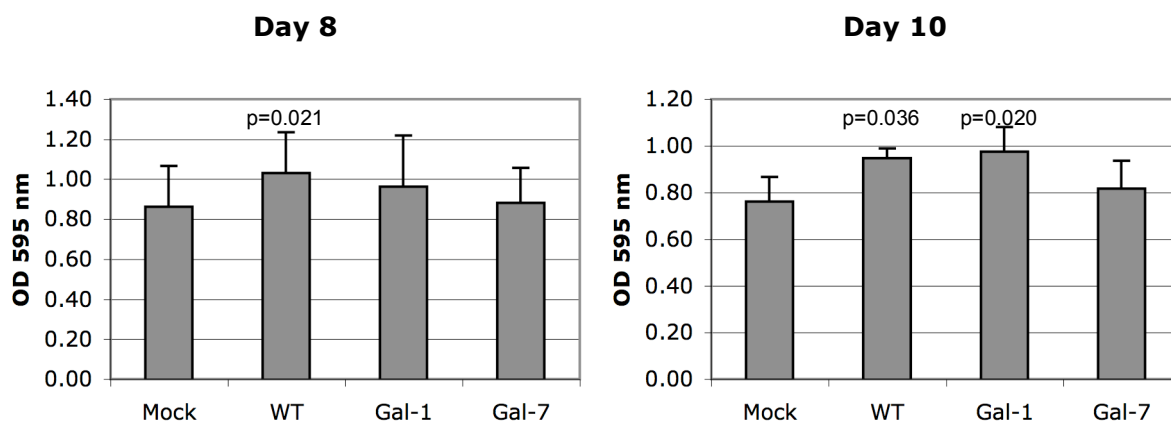


Figure 38. MTT assay of DLD-1 cells seeded in 3 % FCS (v/v). The response of the mock-transfected cells was compared with the other cells evaluated under identical conditions. The calculated p-value is written above the respective bar when $p \leq 0.05$

Most differences in group behavior were seen analyzing the data of the DLD-1 cells seeded in medium with 2 % FCS (v/v). These are displayed in figure 39.

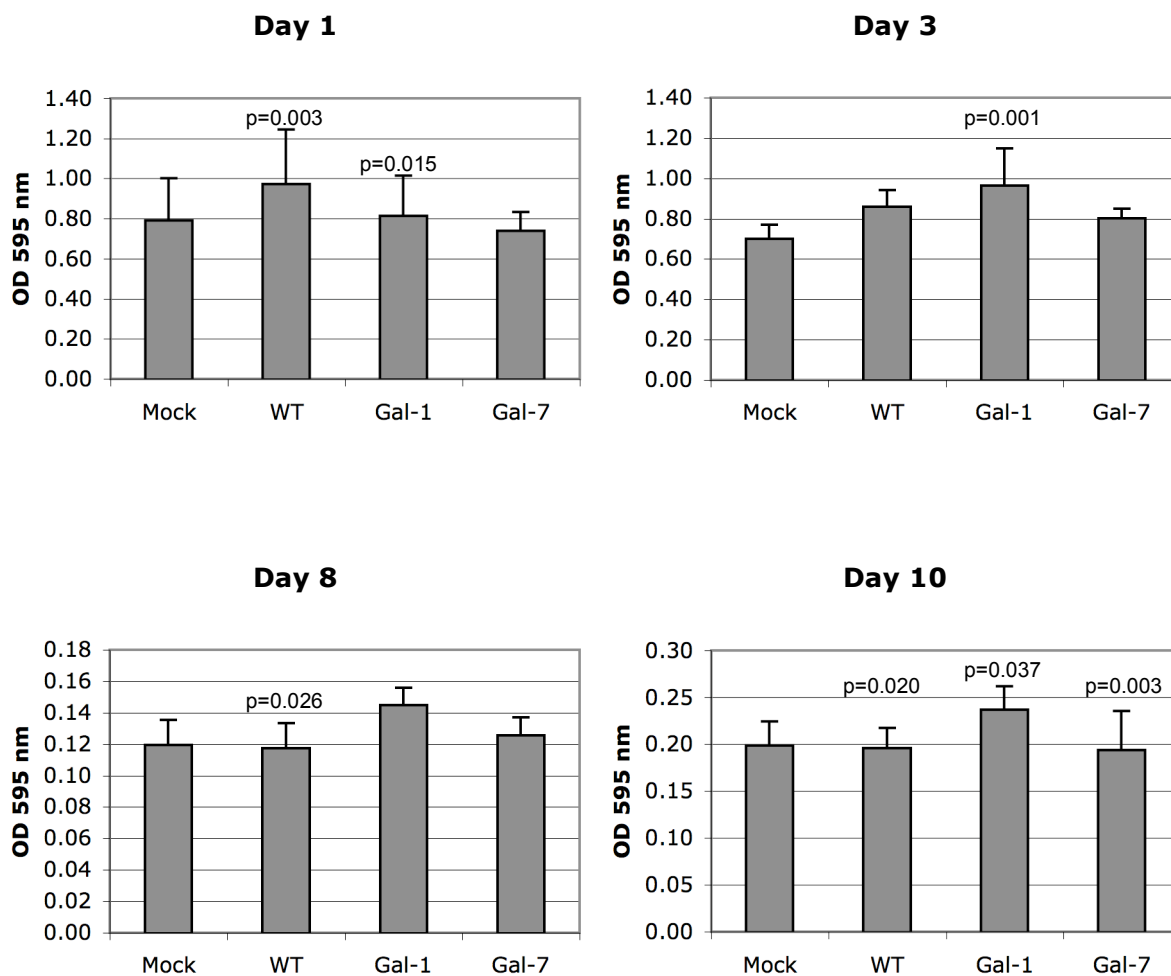


Figure 39. MTT assay of DLD-1 cells seeded in 2 % FCS. The response of the mock-transfected cells was compared with the other cells evaluated under identical conditions. The calculated p-value is written above the respective bar when $p \leq 0.05$

In 1 % FCS (v/v), only the data on cell population from the WT cells were distinct enough from that of the mock-transfected cells for differences to be significant. These were from measurements on day 1, 3 and 10 and are demonstrated in figure 40.

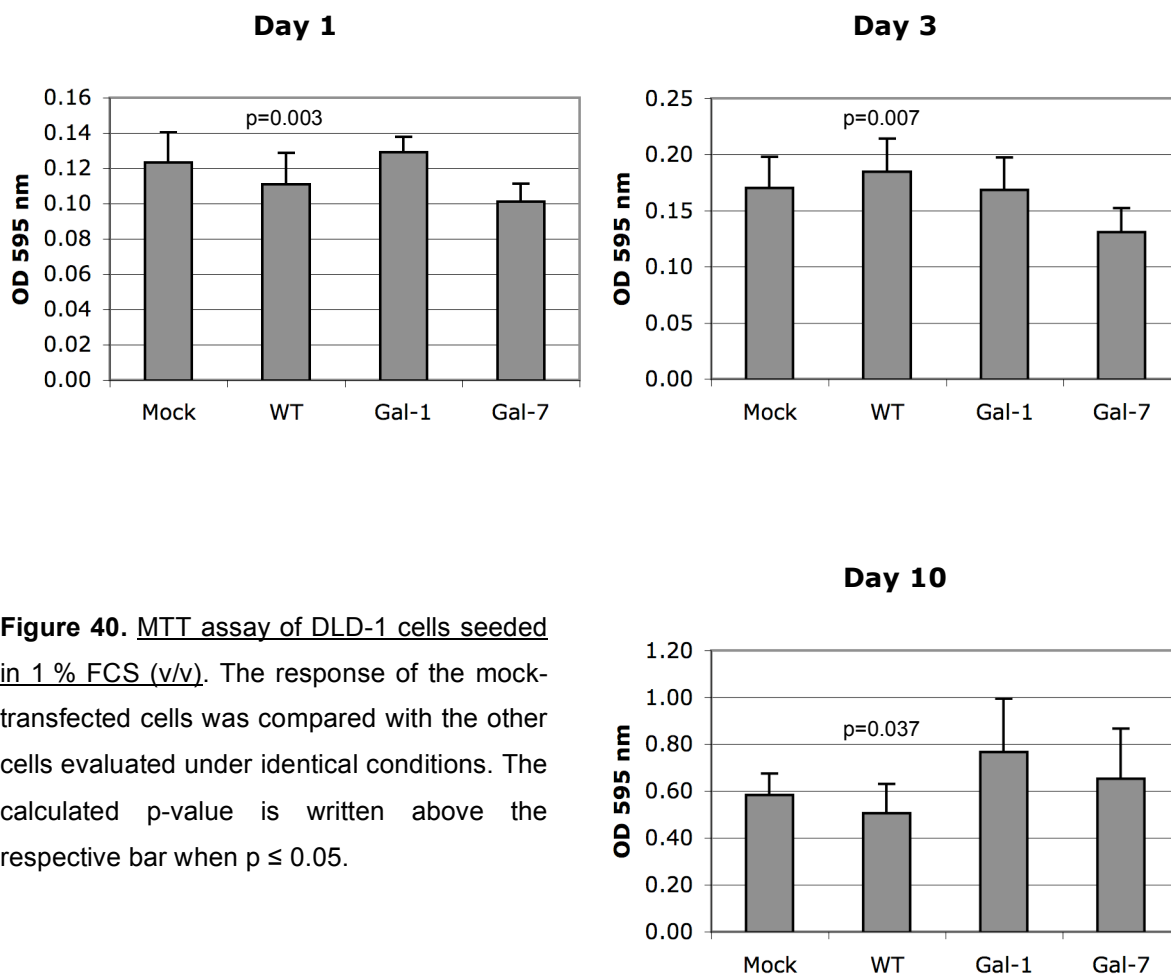


Figure 40. MTT assay of DLD-1 cells seeded in 1 % FCS (v/v). The response of the mock-transfected cells was compared with the other cells evaluated under identical conditions. The calculated p-value is written above the respective bar when $p \leq 0.05$.

Despite the described efforts to infer a correlation between reduction in nutrient supply and galectin overexpression by systematic analyses, there is no obvious indication that galectin overexpression might have a compensatory role in this experimental system. It is clear that the overexpression of these galectins will not confer a marked growth advantage to the tumor cells under the unfavorable conditions defined in this assay. Galectins have demonstrated to not readily reveal specific effects such as a higher sensitivity to apoptosis-inducing agents¹³⁸. FCS deprivation was one stimulus to provoke galectin-specific effects. A possibility to take this one step further would be to assess cell viability under the influence of cell death inducing drugs. This was the next aim of this study.

4.2.4 MTT ASSAY WITH CYTOTOXIC DRUGS ADDED TO THE MEDIUM

Galectins are known to have an acting spectrum that can either inhibit^{139, 140, 141} or enhance cell death^{78, 100}. Heterogeneous tumors are made up of cells with different levels of galectin content. This could lead to a varying degree of susceptibility to cancer treatment with cell

death inducing chemotherapeutical agents. The possible relationship of cellular galectin content and resistance to cytotoxic drugs was analyzed. HCT-15 colon carcinoma cells overexpressing galectins-1, -2 and -7 were incubated with oncologically relevant cytostatics. Oxaliplatin is a platinum-based drug commonly used in the treatment of colorectal carcinoma. The exact mechanism by which this drug is toxic to cancer cells is still being investigated, but broadly speaking, these molecules form adducts with cellular DNA. This process inhibits DNA replication and transcription, leading to apoptosis^{142, 143, 144}. Irinotecan and SN38 (a potent metabolite of irinotecan) are chemotherapeutical agents belonging to the group of topoisomerase I inhibitors. Topoisomerase I inhibitor-related cytotoxicity appears to be correlated to the induction of drug-stabilized complexes, which interfere with replication forks, leading to replication arrest and fork disassembly¹⁴⁵.

In the assay, HCT-15 WT, mock-transfected cells, galectin-1-cDNA-transfected clone 72s, galectin-2-cDNA-transfected clone 18s and galectin-7-cDNA-transfected clone 2s were treated with four increasing concentrations of the respective cytotoxic agent for 72 hours. The effects were evaluated by measuring cell viability compared to a control value of the cells without addition of the cytostatic. Cell viability was assessed by incubation of the cells with the MTT solution for 4 hours at 37 °C and subsequent photometric measurement. The percentage of the measured optical density compared to that of the control was determined. This value could then be displayed in a diagram in relation to the used concentrations of the cytotoxic agent on a logarithmic scale. The effect of the agent was described as the concentration responsible for 50 % inhibition of cell viability compared to the control value (IC₅₀).

The inhibition of cell viability by the chemotherapeutical agents is illustrated in figures 41 to 43. The curves represent the average values of data from four independent experiments. The IC₅₀ was determined using the curve of each individual experiment. The mean values of the IC₅₀ ± SD are displayed in figure 44. The p-values ≤ 0.05 are displayed above the respective bar.

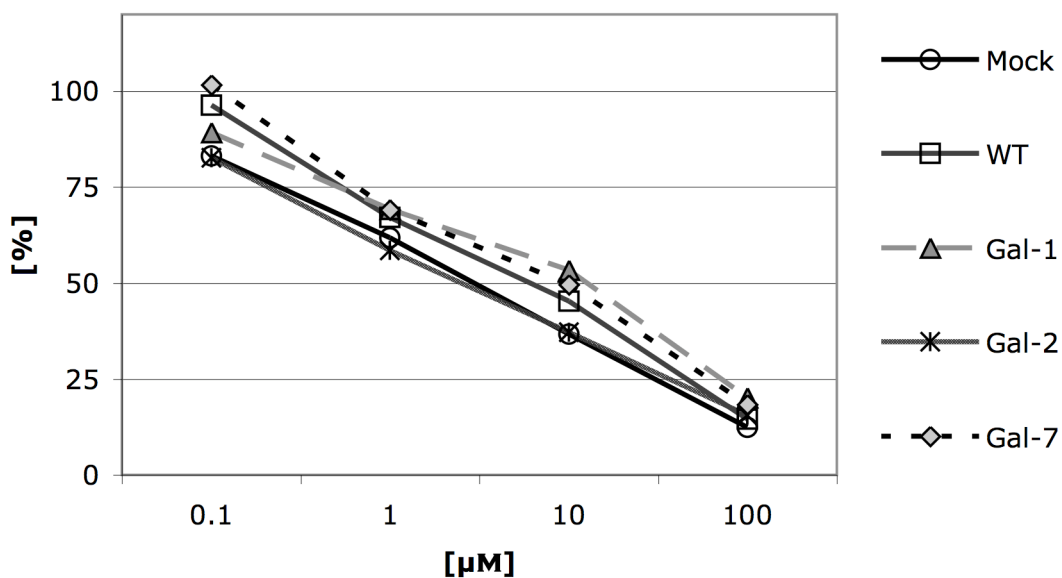


Figure 41. Inhibition of cell viability of HCT-15 WT, mock, galectins-1, -2- and -7-overexpressing cells by oxaliplatin. The x-axis describes the concentration of oxaliplatin [μM] on a logarithmic scale. The y-axis documents the average response of the MTT assay compared to the control value of the cells, incubated in the absence of the cytotoxic agent (n = 4).

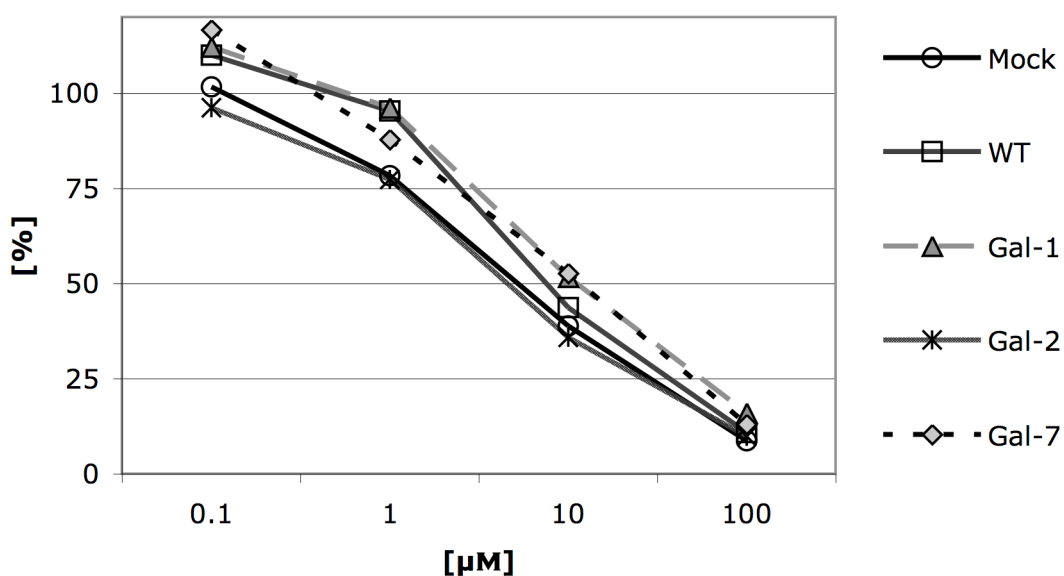


Figure 42. Inhibition of cell viability of HCT-15 WT, mock, galectins-1, -2- and -7-overexpressing cells by irinotecan. The x-axis describes the concentration of irinotecan [μM] on a logarithmic scale. The y-axis documents the average response of the MTT assay compared to the control value of the cells, incubated in absence of the cytotoxic agent (n = 4).

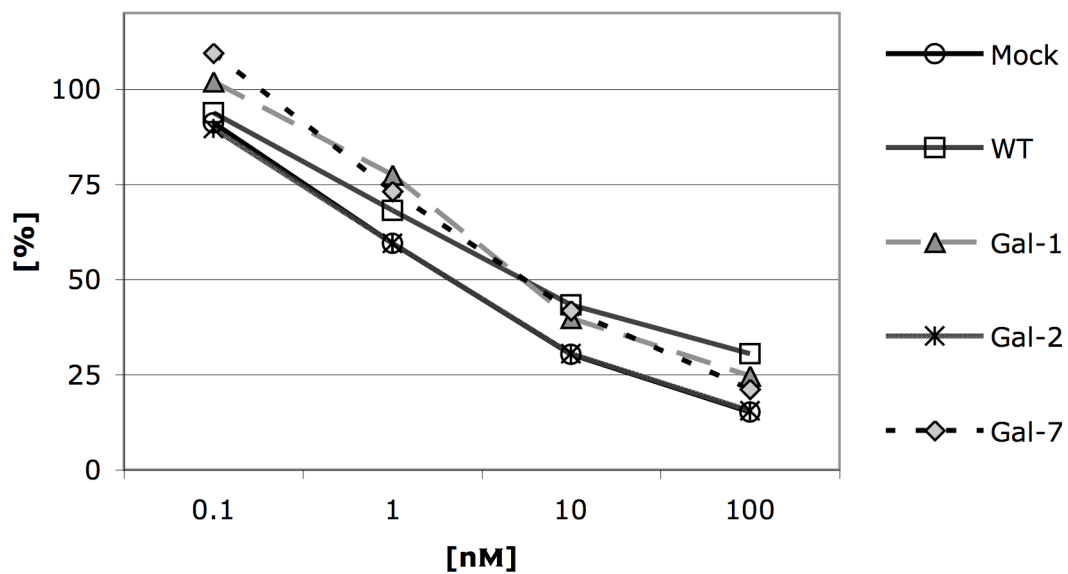


Figure 43. Inhibition of cell viability of HCT-15 WT, mock, galectins-1, -2- and -7-overexpressing cells by SN38. The x-axis describes the concentration of SN38 [nM] on a logarithmic scale. The y-axis documents the average response of the MTT assay compared to the control value of the cells, incubated in absence of the cytotoxic agent (n = 4).

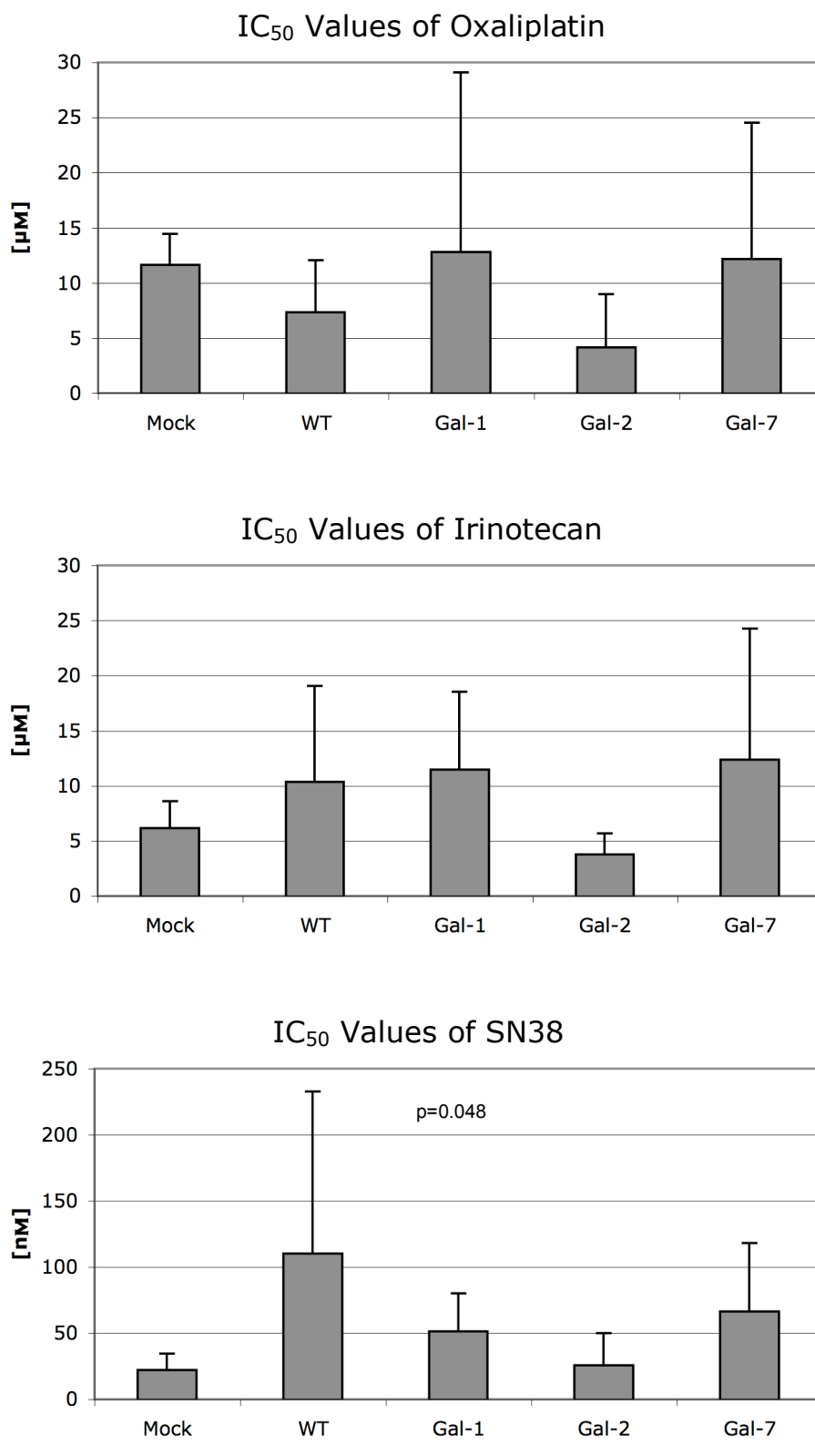


Figure 44. IC₅₀ values of oxaliplatin (**top**), irinotecan (**middle**) and SN38 (**bottom**). HCT-15 WT, mock-, galectin-1-cDNA, galectin-2-cDNA and galectin-7-cDNA-transfected cells were assayed. Bars represent means ± SD of four independent experiments. p-values ≤ 0.05 are displayed above the respective bar.

One unfavorable factor not to be ignored for the interpretation of the results of the assay was the relatively large standard deviation seen when evaluating the data. When the cells were incubated with oxaliplatin, the galectin-2-overexpressing cells showed a high sensitivity to the treatment of the cytostatic relative to the other cell types in the assay. The WT cells also had a comparatively low IC₅₀ concentration, while the other examined cell types had similar average values. Statistically, the data sets were not significantly different to the data obtained with mock-transfected cells.

Irinotecan was most effective in inducing cell death in galectin-2-cDNA-transfected cells. Mock-transfected cells were similarly sensitive, while higher concentrations were necessary to achieve the same effects on cell viability in WT, galectin-1- and galectin-7-cDNA-transfected cells. The differences of the values to those gained from the mock-transfected cells were not high enough to be defined as significant.

When SN38 was added to the medium, the reaction of the mock- and galectin-2-cDNA-transfected cells was very similar. Observation of the behavior relative to the other cell types showed the WT, galectin-1- and galectin-7-overexpressing cells to be less sensitive to the influence of SN38. The data of the galectin-1-cDNA-transfected cells passed the level of significance when set into relation to those of the mock-transfected cells (p -value = 0.048).

To date, no evidence has been presented directly linking galectin-specific effects of the proto-type family members with drug resistance of cancer cells to chemotherapeutical agents. In the present study, no irrefutable proof of such an effect could be observed. However, interesting results are seen in literature, which are encouraging that such a correlation could be discovered in the near future. Nagy et al. have associated a significant prognostic value of galectin-1 with colon tumors, which had been classified as Dukes A and B tumors⁹⁶. High levels of galectin-1 correlated with lower survival periods. Despite its known effects as a proapoptotic factor, high levels of galectin-7 has recently been related by Saussez et al. to a high recurrence rate and poor prognosis of stage IV hypopharyngeal cancer¹⁰¹.

Associations have also been made between tumor prognosis and glycostructures with potential impact on the galectin regulatory network. Modulation of expression of ABH histo-blood group antigens on tumor cells had first been described in gastric cancer by Masamune et al.¹⁴⁶. In this study, the level of expression of histo-blood group A or B epitopes were reduced in tumors of patients with histo-blood group A or B status. Interestingly, invasive and metastatic properties have been correlated with the degree of A/B deletion in cervical, lung, oral and bladder cancer^{147, 148, 149, 150}. A likely explanation for the increase in invasive and metastatic properties was presented in a study by Ichikawa et al.¹⁵¹. The

experiments were performed with the gastric carcinoma cell line MKN74 and the colonic cancer cell line HRT18. The H-antigenic determinant in A- and B-negative/H-positive parental cell lines was glycosylated after transfection with the cDNA encoding A or B transferases. This resulted in acquisition of the A- or B-positive/H-negative phenotype. Comparison of the transfectants with the parental cells revealed that the haptotactic motility was significantly reduced in the A-positive or B-positive/H-negative cells. Motility assays were also performed with integrin-specific monoclonal antibodies, each specific for $\alpha 3$, $\alpha 6$ or $\beta 1$ integrin, on H-positive parental cells. These were less motile, the responses in the assay being similar to the effect of the altered glycosylation after A or B transfection. This revealed the modulated H versus A/B glycosylation of $\alpha 3$ or $\alpha 6/\beta 1$ integrin receptor to be responsible for the differences in motility. This behavior was also observed in another experiment with the colonic carcinoma cell lines SW480 and HT29¹⁵². A-positive and A-negative subpopulations, which derived from originally A-positive tumor cell lines by spontaneous alterations of the phenotype, were selected for these investigations. These spontaneous changes are a more suitable model of physiological processes than modifications induced by transfections. Compared to the A-positive cells, A-negative populations were characterized by greatly enhanced haptotactic motility associated with reduced or deleted A expression at $\alpha 3$, $\alpha 6$ and $\beta 1$ integrin receptors.

Changes in expression of ABH and Lewis-related histo-blood group antigens are among the most frequent alterations in human colon cancer¹⁵³. Accumulation of $\alpha 1,2$ -fucosylated antigens including Le^b and H type 2 in colorectal carcinoma has been characterized by Yazawa et al.¹⁵⁴. This investigation also implied a correlation of the expression of $\alpha 1,2$ -fucosylated antigens with survival among patients with primary colorectal cancer. Of particular interest for the present study, $\alpha 1,2$ -fucosylated glycan structures on colon cancer cells have been implicated to influence resistance to chemotherapy. Cordel et al. performed assays with rat colon carcinoma cells and determined molecular aspects of their acquired resistance to 5-fluorouracil (5-FU), which is a drug of standard use in chemotherapy of colon carcinoma¹⁵⁵. Cells resistant to 5-FU were generated by continuous exposure to the drug over several months. To investigate whether resistance to 5-FU was associated with a particular carbohydrate cell-surface phenotype, cells were processed with a panel of monoclonal antibodies and lectins, each specific for distinct tumor-associated carbohydrate antigens. This procedure revealed the antigen H type 2 to be increased. This enhanced expression was also accompanied by an increase in $\alpha 1,2$ -fucosyltransferase activity, the key enzyme involved in the synthesis of H antigens. To test the relevance of this observation, cells devoid of this

enzymatic activity were transfected by an α 1,2-fucosyltransferase-cDNA, which resulted in expression of H type 2 antigen. As a result, these cells demonstrated an increased resistance to 5-FU. This relationship was further substantiated by a negative control. Cells that possessed enzymatic activity were transfected by a cDNA of α 1,2-fucosyltransferase in anti-sense orientation. Consequently, both H type 2 cell-surface antigen and resistance to the drug was reduced. The intriguing relationship between carbohydrate cell-surface phenotype and resistance to chemotherapy was also confirmed in the human colonic cancer cell line DLD-1 by Yazawa et al.¹⁵⁶. DLD-1/5-FU-resistant cells were established by repeating continuous exposure of the cells to 5-FU with stepwise increases of concentration of the chemotherapeutic agent. Elevated expression of fucosylated antigens was found in the resistant cells compared to parental DLD-1 cells. Likewise, marked increases of α 1,2- and α 1,3-fucosyltransferase activities were also determined in the resistant cells. In contrast, α 1,4-fucosyltransferase activity was found to be reduced in these cells. An interesting approach to modify the cell-surface glycans was chosen. Sugar acceptors for α 1,2-fucosyltransferase - particularly β -galactosyl derivatives with hydrophobic aglycones - were added to the medium. This resulted in suppression of α 1,2-fucosylated antigen expression on the tumor cells and increased susceptibility to anticancer treatment.

The mechanisms by which this modification of glycan structures on the cell surface influences drug resistance are presently unclear. Fucosylation might modify the glycan chains of receptors, which promote or counteract cell death mechanisms. As demonstrated by Ichikawa et al.¹⁵¹, changes in the sugar structures of receptors have the potential to modify their function. Alternatively, the sugar can serve as ligand for endogenous lectins eliciting signaling pathways with impact for growth control. Indeed, the study of Fischer et al.¹²⁹ cited above gives an example for distinct glycosylation and growth control via galectins. Regulation of immunological functions by cell-type and activation-dependent glycosylation in the interplay with selectins or the C-type lectin DC-SIGN provide further important examples for a role beyond tumor biology⁵⁶.

5 SUMMARY

Galectins are a family of endogenous sugar-epitope-specific receptors (lectins). They influence adhesion, growth and invasion in cancer. The clinical relevance of these important parameters prompts the question, whether expression profiles of galectins will correlate with distinct cell properties. Noteworthy in this respect, homodimeric proto-type galectins regulate e.g. neuroblastoma cell growth, and the expression of one of these galectins (galectin-7) is enhanced upon p53-induced apoptosis. These facts explain the given focus on the proto-type galectins-1, -2 and -7. Their effects are known to overlap (galectins-1, -2 and -7 in neuroblastoma cell growth) or be functionally distinct (induction of apoptosis by galectins-1, -2 and -7 in activated T cells). As a key step towards answering the given question, establishment of genetically engineered variants of cell lines with ectopic expression of these lectins is mandatory. Their availability will then allow evaluating whether and to what extent these homologous galectins can contribute to the malignant phenotype in colon cancer. Therefore, galectin-specific cDNA was inserted into a vector (pcDNA3.1), which was then stably incorporated into the genome of cells of established colon carcinoma cell lines (HCT-15, DLD-1). This was verified by PCR analysis on genomic DNA. Subclones with different extent of galectin expression were selected to probe for dose dependence of potential effects. Systematic measurements of mRNA and protein ascertained gene activity and differing levels of galectin synthesis. Their presence was identified on the cell surface as well as in cytoplasm and nuclei by fluorescence-activated cell sorting and immunocytochemical analysis, respectively. These results provide first evidence for nuclear presence of galectins-2 and -7 in colon cancer cells. Morphological appearance was not significantly affected. Moreover, the doubling time was determined and cell growth was assayed under different conditions, i.e. cultivating the cells without/with anchorage, under conditions of reduced supply of nutrients, and in the presence of chemotherapeutics (oxaliplatin, irinotecan, SN-38). A marked correlation between galectin expression and proliferation was not detectable. No pronounced differences were obtained when comparing data sets of the three proto-type galectins. Overall, the successfully generated clones with stable ectopic lectin expression are valuable tools for further examining the correlation between galectins and tumor biologically relevant parameters. Future analyses will also include histopathologic monitoring.

6 BIBLIOGRAPHY

- ¹ Lodish H, Berk A, Matsudaira P, Kaiser CA, Krieger M, Scott MP, Zipursky SL, Darnell J (2004) *Molecular Cell Biology*. 5th Ed. New York: W.H. Freeman and Company, p. 1
- ² Gabius HJ (2000) Biological information transfer beyond the genetic code: the sugar code. *Naturwissenschaften* **87**, 108-121
- ³ Gabius HJ, André S, Kaltner H, Siebert HC (2002) The sugar code: functional lectinomics. *Biochim. Biophys. Acta.* **1572**, 165-77
- ⁴ Hirabayashi J, Kasai K-i (2000) Glycomics, coming of age! *Trends Glycosci. Glycotechnol.* **12**, 1-5
- ⁵ Dwek RA, Edge CJ, Harvey DJ, Wormald MR, Parekh RB (1993) Analysis of glycoprotein-associated oligosaccharides. *Annu. Rev. Biochem.* **62**, 65-100
- ⁶ Hounsell EF (1997) Methods of glycoconjugate analysis. In: *Gabius HJ, Gabius S (Eds.) Glycosciences: Status and Perspectives*. London: *Chapman & Hall*, pp. 15-29
- ⁷ Geyer H, Geyer R (1998) Strategies for glycoconjugate analysis. *Acta Anat.* **161**, 18-35
- ⁸ Lemieux RU (1989) The origin of the specificity in the recognition of oligosaccharides by proteins. *Chem. Soc. Rev.* **18**, 347-374
- ⁹ Lemieux RU (1996) How water provides the impetus for molecular recognition in aqueous solution. *Acc. Chem. Res.* **29**, 373-380
- ¹⁰ Gabius HJ (1998) The how and why of protein-carbohydrate interaction: a primer to the theoretical concept and a guide to application in drug design. *Pharm. Res.* **15**, 23-30
- ¹¹ Habuchi H, Habuchi O, Kimata K (1998) Biosynthesis of heparan sulfate and heparin: how are multifunctional glycosaminoglycans built up? *Trends Glycosci. Glycotechnol.* **10**, 65-80
- ¹² Laine RA (1997) The information-storing potential of the sugar code. In: *Gabius HJ, Gabius S (Eds.) Glycosciences: Status and Perspectives*. London (UK)/Weinheim (Germany): *Chapman & Hall*, pp. 1-14
- ¹³ Wormald MR, Dwek RA (1999) Glycoproteins: glycan presentation and protein-fold stability. *Structure* **7**, R155-R160
- ¹⁴ Kornfeld R, Kornfeld S (1985) Assembly of asparagine-linked oligosaccharides. *Annu. Rev. Biochem.* **54**, 631-664

-
- ¹⁵ Kobata A (1992) Structures and functions of the sugar chains of glycoproteins. *Eur. J. Biochem.* **209**, 483-501
- ¹⁶ Sharon N, Lis H (1997) Glycoproteins: structure and function. In: *Gabius HJ, Gabius S (Eds.) Glycosciences: Status and Perspectives*. London (UK)/Weinheim (Germany): Chapman & Hall, pp. 133-162
- ¹⁷ Reuter G, Gabius HJ (1999) Eukaryotic glycosylation - whim of nature or multipurpose tool? *Cell Mol. Life Sci.* **55**, 368-422
- ¹⁸ Spiro RG (2002) Protein glycosylation: nature, distribution, enzymatic formation, and disease implications of glycopeptide bonds. *Glycobiology* **12**, 43R-56R
- ¹⁹ Amado M, Almeida R, Schwientek T, Clausen H (1999) Identification and characterization of large galactosyltransferase gene families: galactosyltransferases for all functions. *Biochim. Biophys. Acta.* **1473**, 35-53
- ²⁰ Furukawa K, Sato T (1999) β 1,4-Galactosylation of N-glycans is a complex process. *Biochim. Biophys. Acta.* **1473**, 54-66
- ²¹ Gastinel LN (2001) Galactosyltransferases: a structural overview of their function and reaction mechanisms. *Trends Glycosci. Glycotechnol.* **13**, 131-145
- ²² Harduin-Lepers A, Vallejo-Ruiz V, Krzewinski-Recchi MA, Samyn-Petit B, Julien S, Delannoy P (2001) The human sialyltransferase family. *Biochimie* **83**, 727-737
- ²³ Habuchi H, Habuchi O, Kimata K (1998) Biosynthesis of heparan sulfate and heparin: how are the multifunctional glycosaminoglycans built up? *Trends Glycosci. Glycotechnol.* **10**, 65-80
- ²⁴ Bowman KG, Bertozzi CR (1999) Carbohydrate sulfotransferases: mediators of extracellular communication. *Chem. Biol.* **6**, R9-R22
- ²⁵ Fukuda M, Hiraoka N, Akama TO, Fukuda MN (2001) Carbohydrate-modifying sulfotransferases: structure, function, and pathophysiology. *J. Biol. Chem.* **276**, 47747-47750
- ²⁶ Negishi M, Pedersen LG, Petrotchenko E, Shevtsov S, Gorokhov A, Kakuta Y, Pedersen LC (2001) Structure and function of sulfotransferases. *Arch. Biochem. Biophys.* **390**, 149-157
- ²⁷ Damjanov I (1987) Lectin cytochemistry and histochemistry. *Lab. Invest.* **57**, 5-20
- ²⁸ Spicer SS, Schulte BA (1988) Detection and differentiation of glycoconjugates in various cell types by lectin histochemistry. *Basic Appl. Histochem.* **32**, 307-320

-
- ²⁹ Bourrillon R, Aubery M (1989) Cell surface glycoproteins in embryonic development. *Int. Rev. Cytol.* **116**, 257-338
- ³⁰ Mann PL (1988) Membrane oligosaccharides: structure and function during differentiation. *Int. Rev. Cytol.* **112**, 67-96
- ³¹ Varki A, Marth J (1995) Oligosaccharides in vertebrate development. *Semin. Dev. Biol.* **6**, 127-138
- ³² Muramatsu T (2000) Protein-bound carbohydrates on cell-surface as targets of recognition: an odyssey in understanding them. *Glycoconj. J.* **17**, 577-595
- ³³ Manning JC, Seyrek K, Kaltner H, André S, Sinowatz F, Gabius HJ (2004) Glycomic profiling of developmental changes in bovine testis by lectin histochemistry and further analysis of the most prominent alteration on the level of the glycoproteome by lectin blotting and lectin affinity chromatography. *Histol. Histopathol.* **19**, 1043-1060
- ³⁴ Caselitz J. (1987) Lectins and blood group substances as "tumor markers". *Curr. Top. Pathol.* **77**, 245-277
- ³⁵ Alhadeff JA (1989) Malignant cell glycoproteins and glycolipids. *Crit. Rev. Oncol. Hematol.* **9**, 37-107
- ³⁶ Gabius HJ (1997) Concepts of tumor lectinology. *Cancer Investig.* **15**, 454-464
- ³⁷ Brockhausen I, Schutzbach J, Kuhns W (1998) Glycoproteins and their relationship to human disease. *Acta Anat.* **161**, 36-78
- ³⁸ Hakomori S (1998) Cancer-associated glycosphingolipid antigens: their structure, organization, and function. *Acta Anat.* **161**, 79-90
- ³⁹ Listinsky JJ, Siegal GP, Listinsky CM (1998) α -L-fucose: a potentially critical molecule in pathologic processes including neoplasia. *Am. J. Clin. Pathol.* **110**, 425-440
- ⁴⁰ Etzioni A, Tonetti M (2000) Leukocyte adhesion deficiency II - from A to almost Z. *Immunol. Rev.* **178**, 138-147
- ⁴¹ Hirschberg CB (2001) Golgi nucleotide sugar transport and leukocyte adhesion deficiency II. *J. Clin. Invest.* **108**, 3-6
- ⁴² Kaltner H, Stierstorfer B (1998) Animal lectins as cell adhesion molecules. *Acta Anat.* **161**, 162-179
- ⁴³ Fukuda M, Hiraoka N, Yeh JC (1999) C-type lectins and sialyl Lewis^x oligosaccharides: versatile roles in cell-cell interaction. *J. Cell Biol.* **147**, 467-470
- ⁴⁴ Dahms NM, Hancock MK (2002) P-type lectins. *Biochim. Biophys. Acta* **1572**, 317-340

-
- ⁴⁵ Sly WS (2000) The missing link in lysosomal enzyme targeting. *J. Clin. Invest.* **105**, 563-564
- ⁴⁶ Berg JM, Tymoczko JL, Stryer L (2002) Biochemistry. 5th Ed. New York: W.H. Freeman and Company, p. 310
- ⁴⁷ Mitchell SW (1860) Researches upon the venom of the rattlesnake. *Smithson. Contrib. Knowl.* **XII**, 89-90
- ⁴⁸ Mitchell SW, Reichert ET (1886) Researches upon the venoms of poisonous serpents. *Smithson. Contrib. Knowl.* **XXVI**, 155
- ⁴⁹ Sumner JB, Howell SF (1936) Identification of Hemagglutinin of Jack Bean with Concanavalin A. *J. Bacteriol.* **32**, 227-237
- ⁵⁰ Boyd WC, Reguera RM (1944) Haemagglutinating substances for human cells in various plants. *J. Immunol.* **62**, 333-339
- ⁵¹ Renkonen KO (1948) Studies on the nature of hemagglutinins present in seeds of some representatives of the family of leguminosae. *Ann. Med. Exp. Biol. Fenn.* **26**, 66-72
- ⁵² Watkins WM, Morgan WTJ (1952) Neutralization of the anti-H agglutinin in eel serum by simple sugars. *Nature* **169**, 825-826
- ⁵³ Watkins WM (1999) A half century of blood-group antigen research: some personal recollections. *Trends Glycosci. Glycotechnol.* **11**, 391-411
- ⁵⁴ Boyd WC (1954) The proteins of immune reactions. In: *Neurath H, Bailey K (Eds.) The Proteins*. New York: Academic Press, **Vol. 2**, Part 2, pp. 756-844
- ⁵⁵ Gabius HJ, Siebert HC, André S, Jiménez-Barbero J, Rüdiger H (2004) Chemical biology of the sugar code. *ChemBioChem* **5**, 740-764
- ⁵⁶ Gabius HJ (1997) Animal lectins. *Eur. J. Biochem.* **243**, 543-576
- ⁵⁷ Kocourek J, Horejsi V (1983) A note on the recent discussion on definition of the term "lectin". In: *Bog-Hansen TC, Spengler GA (Eds.) Lectins: Biology, Biochemistry, Clinical Biochemistry*. Berlin: Walter de Gruyter, **Vol. 3**, pp. 3-6
- ⁵⁸ Barondes SH (1988) Bifunctional properties of lectins: lectins redefined. *Trends Biochem. Sci.* **13**, 480-482
- ⁵⁹ Kilpatrick DC (2000) Handbook of Animal Lectins. Wiley, Chichester
- ⁶⁰ Gabius HJ (2001) Glycohistochemistry: the how and why of detection and localization of endogenous lectins. *Anat. Histol. Embryol.* **30**, 3-31

-
- ⁶¹ Gabius HJ (2006) Cell surface glycans: the why and how of their functionality as biochemical signals in lectin-mediated information transfer. *Crit. Rev. Immunol.* **26**, 43-80
- ⁶² Brewer CF (2002) Binding and cross-linking properties of galectins. *Biochim. Biophys. Acta* **1572**, 255-262
- ⁶³ Liu FT, Patterson RJ, Wang JL (2002) Intracellular functions of galectins. *Biochim. Biophys. Acta* **1572**, 263-273
- ⁶⁴ Rabinovich GA, Rubinstein N, Toscano M (2002) Role of galectins in inflammatory and immunomodulatory processes. *Biochim. Biophys. Acta* **1572**, 274-284
- ⁶⁵ Danguy A, Camby I, Kiss R (2002) Galectins and cancer. *Biochim. Biophys. Acta* **1572**, 285-293
- ⁶⁶ Gabius HJ, Brehler R, Schauer A, Cramer F (1986) Localization of endogenous lectins in normal human breast, benign breast lesions and mammary carcinomas. *Virchows Arch. B Cell Pathol Incl. Mol. Pathol.* **52**, 107-115
- ⁶⁷ Lobsanov YD, Gitt MA, Leffler H, Barondes SH, Rini JM (1993) X-ray crystal structure of the human dimeric S-Lac lectin, L-14-II, in complex with lactose at 2.9-Å resolution. *J. Biol. Chem.* **268**, 27034-27038
- ⁶⁸ Loris R (2002) Principles of structures of animal and plant lectins. *Biochim. Biophys. Acta* **1572**, 198-208
- ⁶⁹ Kilpatrick DC (2002) Animal lectins: a historical introduction and overview. *Biochim. Biophys. Acta* **1572**, 187-197
- ⁷⁰ Hirabayashi J, Hashidate T, Nishi N, Nakamura T, Hirashima M, Urashima T, Oka T, Futai M, Müller WEG, Yagi F, Kasai K-i (2002) Oligosaccharide specificity of galectins: a search by frontal affinity chromatography. *Biochim. Biophys. Acta* **1572**, 232-254
- ⁷¹ Hirabayashi J, Arata Y, Hyama K, Kasai K-i (2001) Galectins from the nematode *Caenorhabditis elegans* and the glycome project. *Trends Glycosci. Glycotechnol.* **13**, 533-549
- ⁷² Solís D, Romero A, Kaltner H, Gabius HJ, Díaz-Mauriño (1996) Different architecture of the combining sites of two chicken galectins revealed by chemical-mapping studies with synthetic ligand derivatives. *J. Biol. Chem.* **271**, 12744-12748
- ⁷³ Wu AM, Wu JH, Tsai MS, Kaltner H, Gabius HJ (2001) Carbohydrate specificity of a galectin from chicken liver (CG-16). *Biochem. J.* **358**, 529-538

-
- ⁷⁴ André S, Pieters RJ, Vrasidas I, Kaltner H, Kuwabara I, Liu FT, Liskamp RMJ, Gabius HJ (2001) Wedgelike glycodendrimers as inhibitors of binding of mammalian galectins to glycoproteins, lactose maxiclusters, and cell surface glycoconjugates. *ChemBioChem* **2**, 822-830
- ⁷⁵ Hirabayashi J, Kasai K-i (1993) The family of metazoan metal-independent β -galactoside-binding lectins: structure, function and molecular evolution. *Glycobiology* **3**, 297-304
- ⁷⁶ Kopitz J, von Reitzenstein C, Burchert M, Cantz M, Gabius HJ (1998) Galectin-1 is a major receptor for ganglioside GM₁, a product of the growth-controlling activity of a cell surface ganglioside sialidase, on human neuroblastoma cells in culture. *J. Biol. Chem.* **273**, 11205-11211
- ⁷⁷ Kopitz J, von Reitzenstein C, André S, Kaltner H, Uhl J, Ehemann V, Cantz M, Gabius HJ (2001) Negative regulation of neuroblastoma cell growth by carbohydrate-dependent surface binding of galectin-1 and functional divergence from galectin-3. *J. Biol. Chem.* **276**, 35917-35923
- ⁷⁸ Sturm A, Lensch M, André S, Kaltner H, Wiedenmann B, Rosewicz S, Dignass AU, Gabius HJ (2004) Human galectin-2: novel inducer of T cell apoptosis with distinct profile of caspase activation. *J. Immunol.* **173**, 3825-3837
- ⁷⁹ Liao DI, Kapadia G, Ahmed H, Vasta GR, Herzberg O (1994) Structure of S-lectin, a developmentally regulated vertebrate β -galactoside-binding protein. *Proc. Natl. Acad. Sci. USA* **91**, 1428-1432
- ⁸⁰ Oda Y, Herrmann J, Gitt MA, Turck CW, Burlingame AL, Barondes SH, Leffler H (1993) Soluble lactose-binding lectin from rat intestine with two different carbohydrate-binding domains in the same peptide chain. *J. Biol. Chem.* **268**, 5929-5939
- ⁸¹ Hsu DK, Zuberi RI, Liu FT (1992) Biochemical and biophysical characterization of human recombinant IgE-binding protein, an S-type animal lectin. *J. Biol. Chem.* **267**, 14167-14174
- ⁸² Massa SM, Cooper DN, Leffler H, Barondes SH (1993) L-29, an endogenous lectin, binds to glycoconjugate ligands with positive cooperativity. *Biochemistry* **32**, 260-267
- ⁸³ Ahmad N, Gabius HJ, André S, Kaltner H, Sabesan S, Roy R, Liu B, Macaluso F, Brewer CF (2004) Galectin-3 precipitates as a pentamer with synthetic multivalent carbohydrates and forms heterogeneous cross-linked complexes. *J. Biol. Chem.* **279**, 10841-10847

-
- ⁸⁴ Barondes SH (1984) Soluble lectins: a new class of extracellular proteins. *Science* **223**, 1259-1264
- ⁸⁵ Feizi T, Childs RA (1987) Growth regulating network? *Nature* **329**, 678
- ⁸⁶ Leffler H (1997) Introduction to galectins. *Trends Glycosci. Glycotechnol.* **9**, 9-19
- ⁸⁷ Park JW, Voss PG, Grabski S, Wang JL, Patterson RJ (2001) Association of galectin-1 and galectin-3 with Gemin4 in complexes containing the SMN protein. *Nucleic Acids Res.* **29**, 3595-3602
- ⁸⁸ Paz A, Haklai R, Elad-Sfadia G, Ballan E, Kloog Y (2001) Galectin-1 binds oncogenic H-Ras to mediate Ras membrane anchorage and cell transformation. *Oncogene* **20**, 7486-7493
- ⁸⁹ Rini JM, Lobsanov YD (1999) New animal lectin structures. *Curr. Opin. Struct. Biol.* **9**, 578-584
- ⁹⁰ López-Lucendo MF, Solís D, André S, Hirabayashi J, Kasai K-i, Kaltner H, Gabius HJ, Romero A (2004) Growth-regulatory human galectin-1: crystallographic characterisation of the structural changes induced by single-site mutations and their impact on the thermodynamics of ligand binding. *J. Mol. Biol.* **343**, 957-970
- ⁹¹ Leonidas DD, Vatzaki EH, Vorum H, Celis JE, Madsen P, Acharya KR (1998) Structural basis for the recognition of carbohydrates by human galectin-7. *Biochemistry* **37**, 13930-13940
- ⁹² Cohen AM, Minsky BD, Schilsky RL (1993) Colon cancer. In: *DeVita VT, Hellman S, Rosenberg SA (Eds.) Cancer: Principles & Practice of Oncology*. Philadelphia: J.B. Lippincott Co., p. 929-977
- ⁹³ Sharon MW (1994) Transforming growth factor β . The good, the bad and the ugly. *J. Exp. Med.* **180**, 1587-1590
- ⁹⁴ Lee EC, Woo HJ, Korzelius CA, Steele GE, Mercurio AM (1991) Carbohydrate-binding protein 35 is the major cell-surface laminin-binding protein in colon carcinoma. *Arch. Surg.* **126**, 1496-1502
- ⁹⁵ Sanjuan X, Fernandez PL, Castells A, Castronovo V, van den Brule F, Liu FT, Cardesa A, Campo E (1997) Differential expression of galectin 3 and galectin 1 in colorectal cancer progression. *Gastroenterology* **113**, 1906-1915

-
- ⁹⁶ Nagy N, Legendre H, Engels O, André S, Kaltner H, Wasano K, Zick Y, Pector JC, Decaestecker C, Gabius HJ, Salmon I, Kiss R (2003) Refined prognostic evaluation in colon carcinoma using immunohistochemical galectin fingerprinting. *Cancer* **97**, 1849-1858
- ⁹⁷ Berberat PO, Friess H, Wang L, Zhu Z, Bley T, Frigeri L, Zimmermann A, Buchler MW (2001) Comparative analysis of galectins in primary tumors and tumor metastasis in human pancreatic cancer. *J. Histochem. Cytochem.* **49**, 539-549
- ⁹⁸ Saal I, Nagy N, Lensch M, Lohr M, Manning JC, Decaestecker C, André S, Kiss R, Salmon I, Gabius HJ (2005) Human galectin-2: expression profiling by RT-PCR/immunohistochemistry and its introduction as a histochemical tool for ligand localization. *Histol. Histopathol.* **20**, 1191-1208
- ⁹⁹ Polyak K, Xia Y, Zweier JL, Kinzler KW, Vogelstein B (1997) A model for p53-induced apoptosis. *Nature* **389**, 300-305
- ¹⁰⁰ Kuwabara I, Kuwabara Y, Yang RY, Schuler M, Green DR, Zuraw BL, Hsu DK, Liu FT (2002) Galectin-7 (PIG1) exhibits pro-apoptotic function through JNK activation and mitochondrial cytochrome c release. *J. Biol. Chem.* **277**, 3487-3487
- ¹⁰¹ Saussez S, Cucu DR, Decaestecker C, Chevalier D, Kaltner H, André S, Wacreniez A, Toubeau G, Camby I, Gabius HJ, Kiss R: Galectin-7 (p53-induced gene-1): a new prognostic predictor of recurrence and survival in stage IV hypopharyngeal cancer. *Ann. Surg. Oncol.*, in press
- ¹⁰² Lahm H, André S, Höflich A, Fischer JR, Sordat B, Kaltner H, Wolf E, Gabius HJ (2001) Comprehensive galectin fingerprinting in a panel of 61 human tumor cell lines by RT-PCR and its implications for diagnostic and therapeutic procedures. *J. Cancer Res. Clin. Oncol.* **127**, 375-386
- ¹⁰³ Sambrook J, Fritsch EF, Maniatis T (1989) *Molecular Cloning: A Laboratory Manual*. 2nd Ed. Cold Spring Harbor, NY: Cold Spring Harbor Laboratory Press
- ¹⁰⁴ Ausubel FM, Brent R, Kingston RE, Moore DD, Seidman JG, Smith JA, Struhl K (Eds.) (1991) *Current Protocols in Molecular Biology*. New York: Wiley Interscience
- ¹⁰⁵ André S, Kaltner H, Furuie T, Nishimura S, Gabius HJ (2004) Persubstituted cyclodextrin-based glycoclusters as inhibitors of protein-carbohydrate recognition using purified plant and mammalian lectins and wild-type and lectin-gene-transfected tumor cells as targets. *Bioconjugate Chem.* **15**, 87-98

-
- ¹⁰⁶ Bradford MM (1976) A rapid and sensitive method for the quantitation of microgram quantities of protein utilizing the principle of protein-dye binding. *Anal. Biochem.* **72**, 248-254
- ¹⁰⁷ Redinbaugh MG, Campbell WH (1985) Adaptation of the dye-binding protein assay to microtiter plates. *Anal. Biochem.* **147**, 144-147
- ¹⁰⁸ Laemmli UK (1970) Cleavage of structural proteins during the assembly of the head of bacteriophage T4. *Nature* **227**, 680-685
- ¹⁰⁹ Towbin H, Staehelin T, Gordon J (1979) Electrophoretic transfer of proteins from polyacrylamide gels to nitrocellulose sheets: procedure and some applications. *Proc. Nat. Acad. Sci. USA* **76**, 4350-4354
- ¹¹⁰ Gabius HJ, Bodanowitz S, Schauer A (1988) Endogenous sugar-binding proteins in human breast tissue and benign and malignant breast lesions. *Cancer* **61**, 1125-1131
- ¹¹¹ Smetana K Jr, Dvořánková B, Chovanec M, Bouček J, Klíma J, Motlík J, Lensch M, Kaltner H, André S, Gabius HJ (2006) Nuclear presence of adhesion-/growth-regulatory galectins in normal/malignant cells of squamous epithelial origin. *Histochem. Cell Biol.* **125**, 171-182
- ¹¹² Hittélet A, Camby I, Nagy N, Legendre H, Bronckart Y, Decaestecker C, Kaltner H, Nifant'ev NE, Bovin NV, Pector JC, Salmon I, Gabius HJ, Kiss R, Yeaton P (2003) Binding sites for Lewis antigens are expressed by human colon cancer cells and negatively affect their migration. *Lab. Invest.* **83**, 777-787
- ¹¹³ Freedman UH, Shin S (1974) Cellular tumorigenicity in nude mice: correlation with cell growth in semi-solid medium. *Cell* **3**, 355-359
- ¹¹⁴ Mosmann T (1983) Rapid colorimetric assay for cellular growth and survival: application to proliferation and cytotoxicity assays. *J. Immunol. Methods* **65**, 55-63
- ¹¹⁵ Southern PJ, Berg P (1982) Transformation of mammalian cells to antibiotic resistance with a bacterial gene under control of the SV40 early region promoter. *J. Mol. Appl. Genet.* **1**, 327-341
- ¹¹⁶ Dam TK, Gabius HJ, André S, Kaltner H, Lensch M, Brewer CF (2005) Galectins bind to the multivalent glycoprotein asialofetuin with enhanced affinities and a gradient of decreasing binding constants. *Biochemistry* **44**, 12564-12571
- ¹¹⁷ Barondes SH, Cooper DN, Gitt MA, Leffler H (1994) Galectins. Structure and function of a large family of animal lectins. *J. Biol. Chem.* **269**, 20807-20810

-
- ¹¹⁸ Hughes RC (1999) Secretion of the galectin family of mammalian carbohydrate-binding proteins. *Biochim. Biophys. Acta* **1473**, 172-185
- ¹¹⁹ Gerdes J, Lemke H, Baisch H, Wacker HH, Schwab U, Stein H (1984) Cell cycle analysis of a cell proliferation-associated human nuclear antigen defined by the monoclonal antibody Ki-67. *J. Immunol.* **133**, 1710-1715
- ¹²⁰ Madsen P, Rasmussen HH, Flint T, Gromov P, Kruse TA, Honoré B, Vorum H, Celis JE (1995) Cloning, expression, and chromosome mapping of human galectin-7. *J. Biol. Chem.* **270**, 5823-5829
- ¹²¹ Ueda S, Kuwabara I, Liu FT (2004) Suppression of tumor growth by galectin-7 gene transfer. *Cancer Res.* **64**, 5672-5676
- ¹²² Zhao JJ, Gjoerup OV, Subramanian RR, Cheng Y, Chen W, Roberts TM, Hahn WC (2003) Human mammary epithelial cell transformation through the activation of phosphatidylinositol 3-kinase. *Cancer Cell* **3**, 483-495
- ¹²³ van Golen KL, WeiBao L, Pan Q, Miller FR, FenWu Z, Merajver SD (2002) Mitogen activated protein kinase pathway is involved in RhoC GTPase induced motility, invasion and angiogenesis in inflammatory breast cancer. *Clin. Exp. Metast.* **19**, 301-311
- ¹²⁴ Nakanishi K, Sakamoto M, Yasuda J, Takamura M, Fujita N, Tsuruo T, Todo S, Hirohashi S (2002) Critical involvement of the phosphatidylinositol 3-kinase/Akt pathway in anchorage-independent growth and hematogenous intrahepatic metastasis of liver cancer. *Cancer Res.* **62**, 2971-2975
- ¹²⁵ Elad-Sfadia G, Haklai R, Ballan E, Gabius H-J, Kloog Y (2002) Galectin-1 augments Ras activation and diverts Ras signals to Raf-1 at the expense of phosphoinositide 3-kinase. *J. Biol. Chem.* **277**, 37169-37175
- ¹²⁶ Rotblat B, Niv H, André S, Kaltner H, Gabius HJ, Kloog Y (2004) Galectin-1 (L11A) predicted from a computed galectin-1 farnesyl-binding pocket selectively inhibits Ras-GTP. *Cancer Res.* **64**, 3112-3118
- ¹²⁷ Lin HM, Pestell RG, Raz A, Kim HRC (2002) Galectin-3 enhances cyclin D1 promoter activity through SP1 and a cAMP-responsive element in human breast epithelial cells. *Oncogene* **21**, 8001-8010

-
- ¹²⁸ Sharma UC, Pokharel S, van Brakel TJ, van Berlo JH, Cleutjens JPM, Schroen B, André S, Crijns HJM, Gabius HJ, Maessen J, Pinto YM (2004) Galectin-3 marks activated macrophages in failure-prone hypertrophied hearts and contributes to cardiac dysfunction. *Circulation* **110**, 3121-3128
- ¹²⁹ Fischer C, Sanchez-Ruderisch H, Welzel M, Wiedenmann B, Sakai T, André S, Gabius HJ, Khachigian L, Detjen KM, Rosewicz S (2005) Galectin-1 interacts with the $\alpha 5\beta 1$ fibronectin receptor to restrict carcinoma cell growth via induction of p21 and p27. *J. Biol. Chem.* **280**, 37266-37277
- ¹³⁰ Hynes RO (2002) Integrins: bidirectional, allosteric signaling machines. *Cell* **110**, 673-687
- ¹³¹ Giancotti FG, Ruoslahti E (1997) Integrin signaling. *Science* **285**, 1028-1032
- ¹³² Bellis S (2004) Variant glycosylation: an underappreciated regulatory mechanism for $\beta 1$ integrins. *Biochim. Biophys. Acta* **1663**, 52-60
- ¹³³ Berberat PO, Friess H, Wang L, Zhu Z, Bley T, Frigeri L, Zimmermann A, Büchler MW (2001) Comparative analysis of galectins in primary tumors and tumor metastasis in human pancreatic cancer. *J. Histochem. Cytochem.* **49**, 539-549
- ¹³⁴ Plantefaber LC, Hynes RO (1989) Changes in integrin receptors on oncogenically transformed cells. *Cell* **56**, 281-290
- ¹³⁵ Kopitz J, André S, von Reitzenstein C, Versluis K, Kaltner H, Pieters RJ, Wasano K, Kuwabara I, Liu FT, Cantz M, Heck AJR, Gabius HJ (2003) Homodimeric galectin-7 (p53-induced gene 1) is a negative growth regulator for human neuroblastoma cells. *Oncogene* **22**, 6277-6288
- ¹³⁶ Ahmad N, Gabius HJ, Kaltner H, André S, Kuwabara I, Liu FT, Oscarson S, Norberg T, Brewer F (2002) Thermodynamic binding studies of cell surface carbohydrate epitopes to galectins-1, -3, and -7: evidence for differential binding specificities. *Can. J. Chem.* **80**, 1096-1104
- ¹³⁷ Siebert HC, André S, Lu SY, Frank M, Kaltner H, van Kuik JA, Korchagina EY, Bovin NV, Tajkhorshid E, Kaptein R, Vliegthart JFG, von der Lieth CW, Jiménez-Barbero J, Kopitz J, Gabius HJ (2003) Unique conformer selection of human growth-regulatory lectin galectin-1 for ganglioside GM₁ versus bacterial toxins. *Biochemistry* **42**, 14762-14773
- ¹³⁸ Bernerd F, Sarasin A, Magnaldo T (1999) Galectin-7 overexpression is associated with the apoptotic process in UVB-induced sunburn keratinocytes. *Proc. Natl. Acad. Sci. U.S.A.* **96**, 11329-11334

-
- ¹³⁹ Lin HM, Moon BK, Yu F, Kim HR (2000) Galectin-3 mediates genistein-induced G₂/M arrest and inhibits apoptosis. *Carcinogenesis* **21**, 1941-1945
- ¹⁴⁰ Kim HRC, Lin HM, Biliran H, Raz A (1999) Cell cycle arrest and inhibition of anoikis by galectin-3 in human breast epithelial cells. *Cancer Res.* **59**, 4148-4154
- ¹⁴¹ Yang RY, Hsu DK, Liu FT (1996) Expression of galectin-3 modulates T cell growth and apoptosis. *Proc. Natl. Acad. Sci. USA* **93**, 6737-6742
- ¹⁴² Jamieson ER, Lippard SJ (1999) Structure, recognition, and processing of cisplatin–DNA adducts. *Chem. Rev.* **99**, 2467-2498
- ¹⁴³ Di Francesco AM, Ruggiero A, Riccardi R (2002) Cellular and molecular aspects of drugs of the future: oxaliplatin. *Cell. Mol. Life Sci.* **59**, 1914-1927
- ¹⁴⁴ Raymond E, Faivre S, Woynarowski JM, Chaney SG (1998) Oxaliplatin: mechanism of action and antineoplastic activity. *Semin. Oncol.* **25**, 4-12
- ¹⁴⁵ Ryan AJ, Squires S, Strutt HL, Johnson RT (1991) Camptothecin cytotoxicity in mammalian cells is associated with the induction of persistent double strand breaks in replicating DNA. *Nucleic Acids Res.* **19**, 3295-3300
- ¹⁴⁶ Masamune H, Yosizawa Z, Oh-Uti K, Matuda Y, Masudawa A (1952) Biochemical studies on carbohydrates. CLVI. On the sugar components of the hexosamine-containing carbohydrates from gastric cancers, normal human gastric mucosa and human liver and of the glacial acetic acid-soluble proteins from those tissues as well as a metastasis in liver of gastric cancer. *Tohoku J. Exp. Med.* **56**, 37-42
- ¹⁴⁷ Davidsohn I, Kovarik S, Ni LY (1969) Isoantigens A, B, and H in benign and malignant lesions of the cervix. *Arch Pathol.* **87**, 306-314
- ¹⁴⁸ Davidsohn I, Ni LY (1969) Loss of isoantigens A, B, and H in carcinoma of the lung. *Am J Pathol.* **57**, 307-334
- ¹⁴⁹ Dabelsteen E, Roed-Petersen B, Pindbrog JJ (1975) Loss of epithelial blood group antigens A and B in oral premalignant lesions. *Acta Pathol. Microbiol. Scand.* **83**, 292-300
- ¹⁵⁰ Orntoft TF (1992) Carbohydrate changes in bladder carcinomas. *APMIS Suppl.* **27**, 181-187
- ¹⁵¹ Ichikawa D, Handa K, Withers DA, Hakomori S (1997) Histo-blood group A/B versus H status of human carcinoma cells as correlated with haptotactic cell motility: approach with A and B gene transfection. *Cancer Res.* **57**, 3092-3096

-
- ¹⁵² Ichikawa D, Handa K, Hakomori S (1998) Histo-blood group A/B antigen deletion/reduction vs. continuous expression in human tumor cells as correlated with their malignancy. *Int. J. Cancer* **76**, 284-289
- ¹⁵³ Itzkowitz S (1992) Carbohydrate changes in colon carcinoma. *APMIS Suppl.* **27**, 173-180
- ¹⁵⁴ Yazawa S, Akamatsu S, Tachikawa T, Naito H, Nakamura J, Asao T, Nagamachi Y, Nakajima T, Shin S, Chia D (1993) Development and characterization of a novel anti-fucosylated antigen monoclonal antibody YB-2 and its usefulness in the immunohistochemical diagnosis of colorectal cancer. *Jpn. J. Cancer Res.* **84**, 641-648
- ¹⁵⁵ Cordel S, Goupille C, Hallouin F, Meflah K, Le Pendu J (2000) Role for α 1,2-fucosyltransferase and histo-blood group antigen H type 2 in resistance of rat colon carcinoma cells to 5-fluorouracil. *Int. J. Cancer* **85**, 142-148
- ¹⁵⁶ Yazawa S, Nishimura T, Ide M, Asao T, Okamura A, Tanaka S, Takai I, Yagihashi Y, Saniabadi AR, Kochibe N (2002) Tumor-related expression of α 1,2-fucosylated antigens on colorectal carcinoma cells and its suppression by cell-mediated priming using sugar acceptors for α 1,2-fucosyltransferase. *Glycobiology* **12**, 545-553

7 DANKSAGUNG

Zuerst möchte ich mich ganz herzlich bei meiner Betreuerin Dr. Sabine André bedanken. Sie stand mir immer mit Rat und Tat zur Seite. Ihre Bereitschaft mir zu helfen war sehr viel höher, als man es allgemein erwarten könnte. Selbst zu unmenschlichen Zeiten morgens oder auch am Wochenende hat sie meine Arbeit mit herzlicher Freundlichkeit unterstützt. Ohne ihre Hilfe hätte die Dissertation nicht diese Form annehmen können.

Als nächstes will ich mich besonders bei Univ.-Prof. Dr. rer. nat. H.-J. Gabius bedanken. Vor allem seine konstruktive Kritik hat mir gezeigt, was Wissenschaft ist und wie man in der Wissenschaft arbeitet. Er hatte immer sofort Zeit für meine Probleme, auch wenn sich die Arbeit auf seinem Schreibtisch gestapelt hat. Desweiteren möchte ich mich für die Überlassung des sehr interessanten Themas und für die des Arbeitsplatzes bedanken.

Bei Prof. Dr. med. vet. Kaltner möchte ich mich herzlich für seine freundliche Unterstützung, die keine zeitlichen Begrenzungen kannte, bedanken.

Bei Frau Helfrich, Frau Hofer, Frau Mantel und bei meinen Kollegen in der Arbeit möchte ich mich für die große Hilfsbereitschaft und die herzliche Zusammenarbeit bedanken.

Bei meiner Freundin Dr. Antonia Hingerle will ich mich für ihre moralische Unterstützung ganz besonders bedanken. Sie hatte großes Verständnis für meine Probleme und hat mir immer geholfen.

Bei meiner Schwester Rayissa Armata, meinem Schwager Andrew Armata und meiner Nichte Clarissa Armata möchte ich mich für das Korrekturlesen und für die Aufmunterungen bedanken.

Last but definitely not least, möchte ich mich bei meinem Vater bedanken. Seine Unterstützung kannte keine Grenzen. Er ist ein Vorbild für mich.

8 CURRICULUM VITAE

Joachim Christian Reha Manning

geboren am 4. März 1977 in San Francisco, California, U.S.A.

SCHULE

1983 - 1989	Brookside Elementary School, CA, U.S.A. Ross Middle School, CA, U.S.A. Kent Middle School, CA, U.S.A.
1989 - 1990	Schottenstift Gymnasium, Wien, Österreich
1991 - 1995	Akademisches Gymnasium, Salzburg, Österreich
12. Juni 1995	Matura

STUDIUM

1995 - 2002	Studium der Tiermedizin an der Tiermedizinischen Fakultät der LMU München
12. Juli 2002	Abschluss des Tiermedizin Studiums
7. März 2005	Approbation als Tierarzt

PROMOTION

Seit Sept. '02	Angestellt als wissenschaftlicher Mitarbeiter am Lehrstuhl für Physiologische Chemie (Univ.-Prof. Dr. rer. nat. H.-J. Gabius)
----------------	---